QUARTERLY PROGRESS REPORT

July 1 to September 30, 2017

Florida International University's Continued Research Support for the Department of Energy's Office of Environmental Management

Principal Investigator:

Leonel E. Lagos, Ph.D., PMP®

Prepared for:

U.S. Department of Energy
Office of Environmental Management
Under Cooperative Agreement No. DE-EM0000598

FIU | Applied Research Center
FLORIDA INTERNATIONAL UNIVERSITY

Introduction

The Applied Research Center (ARC) at Florida International University (FIU) executed work on four major projects that represent FIU-ARC's continued support to the Department of Energy's Office of Environmental Management (DOE-EM). The projects are important to EM's mission of accelerated risk reduction and cleanup of the environmental legacy of the nation's nuclear weapons program.

The period of performance for FIU Performance Year 7 (from August 29, 2016 to August 28, 2017) has been revised due to the no-cost extension executed at the end of FIU Performance Year 6. This adjustment changed the period of performance of FIU Year 7 to the dates from September 29, 2016 to September 28, 2017. As a result, the upcoming FIU period of performance (FIU Year 8, DOE MOD 31) has been projected from September 29, 2017 to September 28, 2018. The information in this document provides a summary of the FIU-ARC's activities under the Cooperative Agreement for the period of July 1 to September 30, 2017. Executive highlights during this reporting period include:

***Project 1*: High level waste (HLW)/waste processing**

FIU is aiding DOE EM by supporting a number of research efforts in the area of tank and pipeline integrity.

1. FIU is aiding DOE EM by developing a test loop that can bridge technical gaps associated with the transfer of HLW within the transfer systems at Hanford and Savannah River. The loop will be designed to address multiple issues including critical velocities and the formation of sediment beds within the transfer pipelines. FIU completed a literature review of technical articles related to experimental research and developed initial test plan that involves leveraging FIU's infrastructure and providing valuable information that will aid in optimizing flushing operation for HLW transport systems. The final test plan will be incorporate recommendations from the key stakeholders at Hanford and Savannah River.
2. FIU is also aiding DOE EM by developing a test loop that can be used to evaluate the potential for sensors to detect erosion and corrosion in pipelines caused by the transfer of HLW. This information will provide an understanding of the structural integrity of the waste transfer pipelines without the need to exhume pipe sections and take random measurements. FIU recently developed a test plan that includes the use of a test loop that can be eroded or corroded with caustic or abrasive solutions. The test plan has been provided to engineers at WRPS, SRNL and PNNL for their feedback and recommendations.
3. Recently, FIU attended a two-day meeting hosted by SRNL which brought together researchers and engineers from WRPS, SRNL, ORP and FIU. During the two-day Tank and Pipeline Integrity meeting, research being conducted for both Hanford and Savannah River was presented. FIU presented a number of efforts that included: 1) development of miniature inspection tools for the evaluation of double-shell tanks (DSTs), 2) development of a full-scale sectional mock-up of the DSTs, 3) evaluation of non-metallic

materials aged with multiple stressors, and 4) evaluation of ultrasonic transducers to provide real-time monitoring of transfer lines.

Project 2: **Environmental remediation (ER)**

FIU is assisting DOE EM to meet the challenges of managing the environmental restoration of subsurface contamination in soil and groundwater.

1. Two graduate students who have been performing research for Project 2 graduated FIU with their masters' degrees this summer. Alberto Abarca graduated with a master's degree in environmental engineering and successfully defended his thesis entitled, "The stability of uranium-bearing precipitates created as a result of ammonia gas injections in the Hanford Site vadose zone," which was based on research conducted for Task 1. DOE Fellow Juan Morales graduated with a master's degree in environmental and occupational health; he plans to further his education by completing a Ph.D. in the same field.
2. Research for this project was recently presented at several venues. DOE Fellow Frances Zengotita presented research on the role of *Chromohalobacter* on the transport of lanthanides and cesium in the dolomite mineral system at the LANL summer intern poster competition on August 9. At the Fall American Chemical Society meeting on August 23, Dr. Hilary Emerson presented research on the role of ionic strength on sorption of neodymium on dolomite and Dr. Vasileios Anagnostopoulos presented his research on autunite dissolution in the presence of *Shewanella oneidensis* in different bicarbonate concentrations under anaerobic conditions. At the same conference Dr. Anagnostopoulos chaired a session titled, "Fate, transport and remediation of radionuclides in the environment." In addition, research DOE Fellow Awmna Rana presented a poster at the Emory STEM Research and Career Symposium titled "Effect of Acidic Plume on Soil's Properties and Capacity to Retain Uranium at the Savannah River Site." Ms. Rana was also awarded the Emory STEM Research and Career Symposium Travel Award.
3. FIU has completed a set of batch experiments for uranium removal by Huma-K sorbed on SRS sediments (Milestone 2016-P2-M6). From these kinetic sorption experiments, FIU determined that the sediments amended with Huma-K significantly increased the removal of uranium compared to plain sediments without Huma-K (68% vs 11%). This subtask is part of the assistance that FIU is providing to SRS and involves research to understand and predict uranium mobility using F-Area aquifer sediments.

Project 3: **Deactivation and decommissioning (D&D)**

FIU is assisting DOE EM to meet high priority D&D needs and technical challenges across the DOE complex through technology development, demonstration and evaluation.

1. FIU is investigating the use of intumescent coatings to mitigate the release of radioisotopes during fire and/or extreme heat conditions that can potentially occur at a DOE contaminated facility/building. Standardizing and implementing proven processes to refine and better synchronize DOE-EM technology needs, requirements, testing, evaluation, and acquisition by development of uniformly accepted testing protocols and performance metrics is an essential component of these efforts. On July 24, 2017, ASTM International's E10 Committee on Nuclear Technology and Applications published the two new international

standard specifications for fixative technologies that aim to immobilize radioactive contamination, minimize worker exposure, and protect uncontaminated areas against the spread of radioactive contamination during the decommissioning of nuclear facilities. FIU has been working with the ASTM International subcommittee on the development, review, revision, and ultimate approval of these standards as part of the D&D effort. The first specification, Specification for Strippable & Removable Coatings to Mitigate Spread of Radioactive Contamination (E 3104-17), establishes performance specifications for a coating that is intended to be removable during subsequent decontamination operations. The second specification, Specification for Permanent Coatings Used to Mitigate Spread of Radioactive Contamination (E 3105-17) is for coatings that are intended to be permanent, non-removable, long-term material for fixing contamination in place during decommissioning.

2. As part of the effort towards preserving and transferring D&D knowledge and information to assist future D&D projects and the future workforce, FIU is maintaining the D&D knowledge base by developing tools to enhance communication, share and distribute information, and promote collaboration within the D&D community of practice. FIU completed the initial development of a pilot native mobile application using the D&D Fixatives Module for the Android platform. This module can assist in the selection of commercially available fixatives, strippable coatings, and decontamination gels for application during D&D activities. A native application is an app that is developed for use on a specific platform and which is downloaded onto a mobile device in order to be accessed. As such, the native app does not need an internet connection to be used. FIU provided a demonstration of the pilot native mobile app on the fixative module to DOE on August 10, 2017 via Adobe Connect and then provided a broader presentation on the potential for applying native mobile apps to a wide variety of DOE EM challenges on August 24, 2017.
3. As part of the effort to identify robotic technology systems applicable to the challenges and needs of the SRS 235-F Facility, FIU is leveraging the research already completed to assist in identifying cross-cutting applications of robotic technologies being developed at FIU in the high-level waste research area that could potentially be used in support of D&D activities. A potential requirement for a remote dry film thickness gauge capability was identified during FIU's research with intumescent coatings. Determining the precise thickness of a coating applied in restricted spaces and confirming they are within specified parameters throughout the area has proven exceptionally challenging. FIU is investigating the potential for one of ARC's existing remote / robotic platforms to be modified and paired with a dry film thickness gauge to validate the thickness of the fixative application throughout the radioactive space. FIU is currently developing a conceptual design for a technology based on an existing wall climbing platform currently being developed at FIU to be successfully deployed to measure thickness of fixative coatings.

Project 4: **STEM workforce development**

FIU created the DOE Fellows Program in 2007 to assist DOE EM to address the problem of an aging federal workforce. The program provides training, mentorship, and professional development opportunities to FIU STEM students. The DOE Fellows provide critical support to the DOE EM research being conducted on high impact/high priority research being conducted at FIU.

1. Twelve (12) DOE Fellows completed 10-week internships across the DOE Complex and at two universities. The DOE Fellows engaged in research projects at DOE Headquarters in Maryland, DOE national laboratories (Savannah River Nat. Lab and Sandia Nat. Lab), Savannah River Ecology Lab, the Waste Isolation Pilot Plant, University of Texas-Austin Nuclear and Applied Robotics Group, and San Jose State University*. The DOE Fellows returned to ARC in August and will develop a summer internship technical report based on the research they performed over the summer. (*The internship at San Jose State University is separate from and not funded by the DOE-FIU Cooperative Agreement
2. DOE Fellows participated and ten (10) presented their research accomplishments during FIU's Research Review with DOE HQ and the national labs on July 18, 2017, as a part of technical projects 1, 2 and 3 as well as during the workforce development project 4.
3. Three DOE Fellows are scheduled to complete the Workforce Development Program and graduate FIU in December 2017, including Alexis Smoot, Max Edrei, and Jesse Viera. FIU is extremely proud of the accomplishments of these remarkable students and wish to highlight their many successes. A DOE Fellow Spotlight is included under Project 4 for Alexis and the next couple of monthly reports will include a Spotlight on Max and Jesse.
4. Alexis Smoot will successfully complete the DOE-FIU Science and Technology Workforce Development Program in December 2017 and graduate with a Bachelor's of Science in Environmental Engineering from Florida International University (FIU). She is actively pursuing career opportunities at DOE EM, other government agencies, and the national research laboratories as well as industry environmental companies and consultants. Alexis has special interests and abilities in environmental remediation, energy efficiency, and sustainable and renewable energy technologies.

Milestones and Deliverables

Project 1: No milestones or deliverables for this project were due during this reporting period.

Project 2: FIU completed a set of batch experiments for uranium removal by Huma-K sorbed on SRS sediments (milestone 2016-P2-M6).

Project 3: Milestone 2016-P3-M2.3 was completed with the participation in the ASTM E10 committee meeting to coordinate developing standardized testing protocols and performance metrics for D&D technologies (subtask 2.2.1). A deliverable for a second infographic was completed with a postcard style infographic on the DOE-FIU Cooperative Agreement and the DOE Fellows program. Milestone 2016- P3-M3.4 was completed on August 3, 2017 with the completion of the initial development of a pilot native mobile application using the D&D Fixatives Module for the Android platform.

Project 4: No milestones or deliverables for this project were due during this reporting period.

Program Wide: The program-wide milestones and deliverables that apply to all projects (Projects 1 through 4) for FIU Performance Year 7 are shown on the following table. The FIU Research Review presentations to DOE HQ and site points-of-contact was conducted on July 18-19, 2017. These presentations included the progress and accomplishments of the current

performance year (FIU Performance Year 7) as well as the planned scope of work for the next performance year (FIU Performance Year 8).

Task	Milestone/ Deliverable	Description	Due Date	Status	OSTI
Program-wide (All Projects)	Deliverable	Draft Project Technical Plan	9/30/16	Complete	
	Deliverable	Monthly Progress Reports	Monthly	Complete	
	Deliverable	Quarterly Progress Reports	Quarterly	Complete	
	Deliverable	Draft Year End Report	10/13/17	Reforecast to November 3, 2017	OSTI
	Deliverable	Presentation overview to DOE HQ/Site POCs of the project progress and accomplishments (Mid-Year Review)	4/7/17*	Complete	
	Deliverable	Presentation overview to DOE HQ/Site POCs of the project progress and accomplishments (Year End Review)	9/29/17*	Complete	

**Completion of this deliverable depends on availability of DOE-HQ official(s).*

Project 1
Chemical Process Alternatives for Radioactive Waste

Project Manager: Dr. Dwayne McDaniel

Project Description

Florida International University has been conducting research on several promising alternative processes and technologies that can be applied to address several technology gaps in the current high-level waste processing retrieval and conditioning strategy. The implementation of advanced technologies to address challenges faced with baseline methods is of great interest to the Hanford Site and can be applied to other sites with similar challenges, such as the Savannah River Site. Specifically, FIU has been involved in: modeling and analysis of multiphase flows pertaining to waste feed mixing processes, evaluation of alternative HLW instrumentation for in-tank applications and the development of technologies to assist in the inspection of tank bottoms at Hanford. The use of field or *in situ* technologies, as well as advanced computational methods, can improve several facets of the retrieval and transport processes of HLW. FIU has worked with site personnel to identify technology and process improvement needs that can benefit from FIU's core expertise in HLW. The following tasks are included in FIU Performance Year 7:

Task No	Task
Task 17: Advanced Topics for Mixing Processes	
Subtask 17.1	Computational Fluid Dynamics Modeling of HLW Processes in Waste Tanks
Task 18: Technology Development and Instrumentation Evaluation	
Subtask 18.2	Development of Inspection Tools for DST Primary Tanks
Subtask 18.3	Investigation Using an Infrared Temperature Sensor to Determine the Inside Wall Temperature of DSTs
Task 19: Pipeline Integrity and Analysis	
Subtask 19.1	Pipeline Corrosion and Erosion Evaluation
Subtask 19.2	Evaluation of Nonmetallic Components in the Waste Transfer System

Task 17: Advanced Topics for HLW Mixing and Processing

Task 17 Quarterly Progress

Subtask 17.1: Computational Fluid Dynamics Modeling of HLW Processes in Waste Tanks

An abstract based on this research was accepted by the Waste Management 2018 Symposium for a poster presentation:

> **Abstract**: 18374
> **Title**: Development of a Testbed for Pipeline Flushing and Critical Velocity Studies
> **Authors**: Ahmadreza Abbasi Baharanchi, Dwayne McDaniel, Joseph Coverston (DOE Fellow)

During this period, the primary activity was focused on developing a test matrix for the flushing study. Different strategies for flushing tests were developed and application of two ultrasonic sensors was investigated.

Test plan for flushing study

In this study, a stationary bed will be manually created in the system. The procedure will be based on the sequential creation of sliding and stationary beds in the loop. FIU will initially run the system without the flushing tank/pump components in order to fill the system. Then, by changing valve configurations, the slurry will be circulated in the system without running through the mixing tank. This step is necessary to keep the solid content constant in the loop. At this stage, the system will function similar to the WRPS Waste Certification Loop. Then, the system will be run in steady state mode and near the deposition velocities to obtain a sliding bed that will be moving in the entire horizontal sections of the system. The effort will first focus on achieving a uniform bed in the entire system. FIU will later achieve different sediment shapes by ramping velocity in different modes and rates.

FIU is currently considering instrumentation that is capable of detecting particles in dilute concentrations in high-velocity streams. This condition occurs close to the end of the flushing operation. According to Denslow et al. (2011), PulseEcho cannot be used for this application because of insufficient backscattered signals. This issue was not reported for the Lasentec sensor. Results reported by Bontha et al. (2000) showed the capability of this sensor to detect particles in the range of 0.8 to 1000 µm. Lasentec can produce particle size distributions (PSD) and update this information every two seconds (according to Poloski et al., 2009a) which is a relatively long time for this application. FIU is currently interested in the possibility of obtaining data from Lasentec in much shorter time intervals.

The proposed test plan includes the following general steps:

1. Create and mix the simulant in the mixing tank.
2. Run the slurry pump to fill the system.
3. Circulate the slurry by bypassing the mixing tank and create a stationary bed after creating a sliding bed and stopping it. At this stage, the system will function similarly to the WRPS Waste Certification Loop (Bontha et al., 2010).
4. Control the solids loading by changing the concentrations in the slurry mixing tank and bring the mixing tank back to the loop. Return to step 3.
5. Start the flushing test and stop after a certain time or after a certain flush volume.
6. Evaluate how much solid is left behind after step 5. One of the following will be used:
    a. Capture the residual solids in a special filter bag inside the capture tank.
    b. Circulate the residuals in a loop using the slurry pump and capture the residual solids progressively in a special filter inside a water tank. This step requires cleaning the slurry pump using water in a special cleaning line.

Proposed test matrix

Initial phases of this study will involve simple simulants which can physically represent actual waste in the WTP. Simple simulants that were used in PNNL's M1 tests (Poloski 2009a, b and Yokuda et al., 2009) will be considered. The goal will be to compare results obtained by FIU's loop with those obtained in M1 test results as a baseline test. Other important criteria in the

selection of simulants was the availability of flushing test results and the similarity of test loops to FIU's loop. For this reason, simulants used in the *PNNL-17639, WTP-RPT-175 Rev. 0* report (Poloski 2009a) were considered. Various simulants in the form of glass beads (two sizes, 10 µm and 100 µm), 50 µm alumina, and 316 stainless steel (two sizes, 10 µm and 100 µm) in water-kaolin suspension will be considered.

For the initial studies, FIU will choose one or two simulants from a matrix of 10 non-Newtonian simulants based on ease of testing and availability of material. FIU will consider instability issues associated with some similar simulants used in critical study tests as were reported in the *PNNL-18316 WTP-RPT-189 Rev. 0* document (Poloski et al., 2009b). In preparation of the test matrix for simulant selection, size, density, yield stress, and viscosity will be considered. Water will be the primary component of the carrier fluid. Kaolin clay and $MgSO_4$ (in 10 ppm) will be used to adjust the shear viscosity and yield stress, respectively. Kaolin clay with particle size of 1 µm and density of 2~3 g/cm^3 will be considered. Medium- and high- rheology simulants (τ_y =3 and 6 Pa) with small, medium, and high density, and medium and large particle sizes will be considered in the initial test matrix. Table 1-1 shows the matrix for simulant selection for FIU's flushing tests. Gray and cyan colors indicate material used in the first and second rounds of tests, respectively.

Table 1-1. Candidate Simulants for Use in Initial Phases of the Flushing Tests

Name	**Al_2O_3-MR**	**GB-MR**	**SS-MR**	**Al_2O_3-HR**	**GB-HR**	**SS-HR**
Volume fraction % (Mass fraction %)*						
Coarse Particle	9.5(25.6)	8.4(16.9)	3.9(22.9)	9.7(25.7)	10.7(20.6)	4.8(26.5)
Kaolin Clay	8.9(16.0)	7.7(15.5)	6.5(11.8)	10.7(18.7)	9.6(18.4)	6.4(11.2)
water	81.6(58.4)	83.9(67.6)	89.6(65.3)	79.6(55.6)	79.7(61.1)	88.8(62.2)
Al_2O_3: Aluminum Oxide, density: 4~6 g/cm^3, particle size:50µm G.B. : glass beads, density: 2~4 g/cm^3, particle size: 100µm SS: Stainless Steel, density:8~10 g/cm^3, particle size: 100µm MR and HR stand for medium rheology (τ_y = 3 Pa) and high rheology (τ_y = 6 Pa), respectively. * Mass fraction will be varied in each round of tests. Values are available in Poloski et al. (2009a) and are the baseline for future variations. Solid loading will be changed with ±5% and ± 10% increments.						

FIU will start with a 165-foot loop which is similar to PNNL's M1 test loop in length. In the initial phase, FIU will not consider glass beads due to instability issues reported by Poloski et al. (2009b). Also, FIU will focus on mid-density material which is aluminum oxide in both high and medium rheologies. Studies will continue with high-density stainless steel in later phases in addition to the full range of particle sizes in other test loops.

As a summary, the variables considered in the test matrix will include: simulant material (carrier material type, particle type and concentration), operation of pump mode (fixed, ramped, pulsing), flush duration, number of flushes (1, 2, and 3), bed formation (triangular, rectangular, and waveform) and loop length (165, 330, 495, 660, and 825 ft).

In initial phases of the flushing study, FIU will consider a fixed-volume test strategy. As indicated in Table 1-2, a total of 24 tests will be considered in the initial phases of the project. The table shows the test matrix using a simulant with 16% kaolin clay, 25.6% AL_2O_3 and 58.4% water for the 165 foot test loop that creates a uniform sediment bed. Resultant flush duration and line to volume ratio are also calculated and shown in the left two columns. The sediment shape

will not be the priority in the initial phases and FIU will try to obtain uniform beds in the system. FIU will also evaluate best flush practices by starting the flushing with a resulting total flush-to-line volume of 2. Low values were selected because testing results in *WTP-RPT-175 Rev. 0* showed a sudden drop of velocity after the velocity reached a maximum. FIU's challenge will be to examine low values by keeping the flow velocity constant during flushing. In this test phase, FIU will use the tank level indicator for flush volume calculations. FIU will also use the indicator signal for stopping the pump.

FIU will use the signals received from the Lasentec to stop the pump when no particles are detected. For performance evaluations, signals from a Coriolis meter will be considered as well. Therefore, columns related to total and per-flush line-to-volume ratio are tentative. This practice will be similar to those reported in *WTP-RPT-175 Rev. 0*. In subsequent phases, FIU may consider target flush volumes and stop the pump based on the signal received from the tank level indicator. In addition, FIU may include non-uniform sediment shapes in a future test matrix and continue the same tests with stainless steel beads and in longer test loops.

Table 1-2. Matrix for Flushing Test using 165-foot Test Loop

Test Number	Flush Mode	Number of Flushes	Flush-to-Line Volume Ratio (per flush)	Resultant Duration per Flush (sec)	Resultant Flush-to-Line Volume Ratio
1	Constant*	1	2	27.4	2
2	Ramped	1	2	27.4	2
3	Pulsed	1	2	27.4	2
4	Constant*	2	1	13.7	2
5	Ramped	2	1	13.7	2
6	Pulsed	2	1	13.7	2
7	Constant*	1	3	41	3
8	Ramped	1	3	41	3
9	Pulsed	1	3	41	3
10	Constant*	2	1.5	20.5	3
11	Ramped	2	1.5	20.5	3
12	Pulsed	2	1.5	20.5	3
13	Constant*	1	4	54.8	4
14	Ramped	1	4	54.8	4
15	Pulsed	1	4	54.8	4
16	Constant*	2	2	27.4	4
17	Ramped	2	2	27.4	4
18	Pulsed	2	2	27.4	4
19	Constant*	1	5	68.4	5
20	Ramped	1	5	68.4	5
21	Pulsed	1	5	68.4	5
22	Constant*	2	2.5	34.2	5
23	Ramped	2	2.5	34.2	5
24	Pulsed	2	2.5	34.2	5

* This value must be found experimentally. The default value is 12 ft/s if no plugging formation will be observed.
Ramping starts from a safe velocity (default 8 ft/s) that must also be found and the continues to 12 ft/s
Pulse will be between the safe velocity (default 8 ft/s) and the maximum velocity (12 ft/s)

Proposed test loop

The proposed test loop at FIU will be an integrated test loop for both critical velocity and flushing studies. This loop, as is shown in Figures 1-1 and 1-2, is designed to have the following features: (1) detection of the onset of particle deposition using the PulseEcho sensor, (2) inline monitoring of particles in the flush stream, (3) post-flush evaluation of solid residuals, (4) cleaning of slurry pump and its attached line, (5) modularity in length (165, 330, 495, 660, and 825 ft), (6) automatic control of valves and the flush pump, (7) automatic termination of flush operation using signals from Lasentec and an in-tank level transmitter, (8) several visualization sections for easy visualization of the flow.

An existing 270-ft carbon steel 3-inch schedule 40 pipeline at FIU is also shown in Figure 1-2. This pipeline is ready to be connected to the tanks, pumps, and other instrumentations to develop a closed loop for these studies.

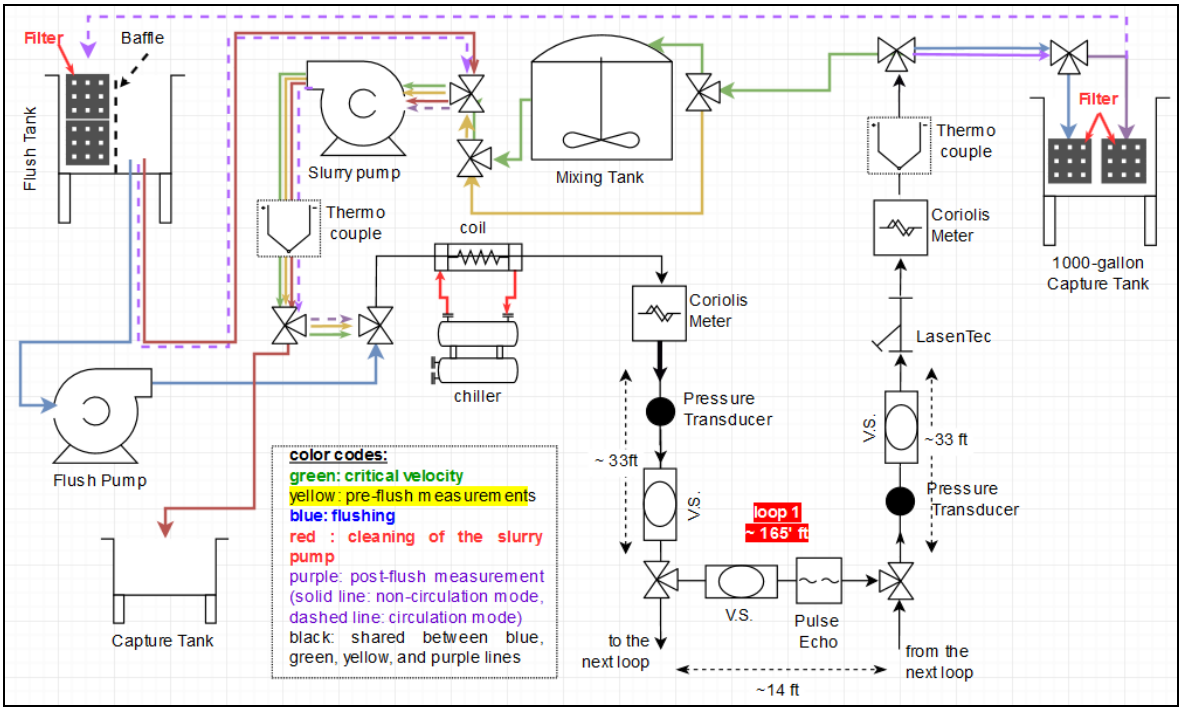

Figure 1-1. FIU's proposed test loop.

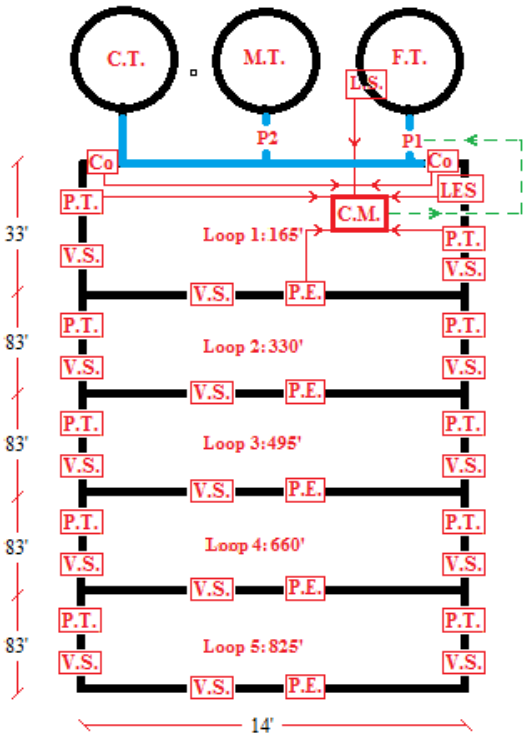

F.T. : flush tank
L.S.: tank level sensor
C.M.: controller module
P1 : flush pump
Co. : Coriolis meter
P2 : slurry pump
C.T. : capture tank
P.E.: PulseEcho sensor
M.T.: mixing tank
V.S.: Visualization section
LES : Lasentec

Figure 1-2. FIU's proposed variable-length loops (left) and an existing 270-ft pipeline at FIU (right).

Table 1-3. Information Required from Flushing and Critical Velocity Tests

No.	variable	Instrument type	#
F & C	Mass flow rate	Coriolis meter Micro-Motion F series model 2700	2
F & C	Density		
F & C	Pressure	differential pressure transducer	2,4,5, 6,8,10
C	Mixing tanks with agitator	400 Gallons	1
F	Water tank	1000 Gallons	1-2[(a)]
F & C	Capture tank	1000 Gallons	1-2
F	Electric water pump	TBD [(b)]	1
C	Slurry velocity and stratification	PulseEcho	2[(c)]
F	Sediment bed characterization	PulseEcho	1
F	Particle trace measurement	The Mettler Toledo Lasentec	1
F	Control module	TBD	1
F	Motor-operated valves	TBD	1
F	Tank level transmitter	TBD	1
C	Rhrometer	TBD	1
C	Slurry pump	TBD (15 HP for 165' loop)	1
C	Particle size analyzer	TBD	1
F & C	Data Acquisition (DAQ)	TBD	1
F & C	Flow characterization/observation	Visualization section	3,5[(d)]
F & C	Slurry temperature control	Chiller	1
F & C	Slurry temperature	Thermocouple	2

F: flushing C:critical velocity TBD: To be determined
[(a)] One tank for the 165, 330, 495-ft loops and two tanks for 660, 825-ft loops.
[(b)] Taco CSI series, Model SCI3009-3600-75, 110 psi @ 263 gpm
[(c)] Two PulseEcho sensors will be placed on circumference of a test spool.
[(d)] Three for 165 and 330-ft loops, 5 for 495, 660, and 825-ft loops.

FIU is currently investigating the potential use of the dynamic shear rheometer (DSR) manufactured by Bohlin Instruments for viscosity measurements of its simulants. This equipment is primarily used for measurement of liquids and may need some modifications to extend its functionality to slurries.

Figure 1-3. Dynamic shear rheometer (DSR) available at FIU (left) and water cooling bath (right).

Future work will include determination of the pressure requirements during flushing of different sediment heights. This will create a basis for pump selection in future steps. FIU will use different correlations suggested by Crowe (2006) and computational fluid dynamic simulations in order to emulate the available data in the literature and then utilize the conditions considered in FIU's test matrix.

During the month of September, FIU discussed a proposed flushing test plan with engineers from SRNL and PNNL in order to incorporate the most recent updates and requirements. Additionally, requirements associated with the initial phases of pumping were revisited.

Discussions with SRNL and PNNL

FIU engaged in multiple calls with the national labs to obtain feedback on the recently proposed test plan for the flushing study. The following points were noted during these calls:

1. FIU's proposed test plan aims to flush large volumes and infrequent waste transfers. Flushing of lines with small volumes and frequent waste transfer is more relevant at the present time.
2. The focus should be on understanding the relationship between re-suspension, deposition, and critical velocities and application of these quantities for flushing studies.
3. FIU's proposed test matrix focuses on non-Newtonian slurries with a yield stress of 3 to 6Pascal. It was recommended to consider a higher yield stress for particle suspension in the range of 10 to 30 Pascal.
4. Cohesive particles, not alumina, might be a better choice in the simulant. The alumina concentration of 25% is too high. Softer particles would constitute a better test, as they are more representative of the waste.
5. Incorporate coupons for erosion/corrosions testing.
6. Incorporate methodologies to set and validate the initial conditions at the start of the flushing tests.

Pumping requirements

In order to understand the pressure variations obtained in PNNL's previous flushing studies, efforts were made to theoretically predict the startup pressures. Proper startup pressures will avoid potential plugging issues in the lines. Two approaches were used to estimate the initial startup pressures. First, FIU investigated the correlations suggested by Crowe (2006) to estimate the pressure head needed at startup. According to the handbook of multiphase flows for fluid-solid transport in ducts, the pump startup pressure is:

$$P_{startup} = \frac{4\,\tau_y L}{D}$$

Where: τ_y is the yield stress of the sediment bed, and L and D are the length and diameter of the pipeline, respectively.

FIU considered cases with τ_y = 3 Ps, L = 28 m or 92 ft (the length of the horizontal section), and a hydraulic diameter of 0.065 m (as compared to D_{pipe} = 0.076 m) for a 3-inch pipe having

sediment with ß = 90° and sediment height of H_{bed} = R(1-cos(ß/2)) = 0.3R = 0.011 m = 0.44 inch. This calculation results in 0.75 psi of pressure at the start in a completely horizontal pipe, which is significantly lower than expected.

In an alternate approach to obtain the startup pressure, the pressure needed to overcome the friction between the lower suspension (bed) and pipe was considered as the maximum pressure needed for startup. The force of friction was calculated based on a normal force exerted by the weight of the upper suspension layer (supernatant fluid). The coefficient of friction between the sediment bed and the pipe wall varies between 0.42 and 0.5 according to the handbook of multiphase flows for fluid-solid transport. FIU used 0.5 to provide a maximum value. Figure 1-4 shows a pipe partially filled with sediment at an angle ß.

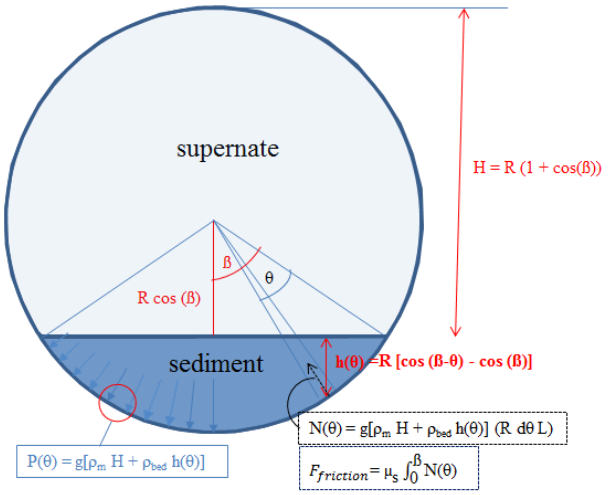

Figure 1-4. Calculation of normal and friction force in a sediment flow.

A simple derivation of forces along with integration of the local normal force caused by hydrostatic pressure leads to the following equation for the calculation of the friction force between the bed and pipe wall:

$$F_{Friction}=\mu s\ g\ R^2\ [\sin(ß)\ (\rho_{bed}+\rho_{mix})+\rho_{mix}\sin(ß)-\rho_{bed}ß\cos(ß)]$$

The pressure drop will be the combination of the following two terms: 1) pressure drop as a result of supernatant fluid flow, and 2) pressure drop associated with the effect of bed-pipe friction. Combining the two terms leads to the following:

$$\frac{Pressure_{drop}}{L}=\frac{4F_{Friction}}{L\pi d_{hyd}^{\ 2}}+f_{tur}\frac{\rho_{mix}}{2}\frac{vel^2}{d_{hyd}}$$

Here, the pressure drop coefficient for the turbulent flow was defined as 0.001and alumina-kaoline-water simulant was considered. This resulted in 0.230 and 0.232 psi pressure drop per foot of pipeline at zero and 12 ft/s velocities, respectively, which indicated pronounced effect of the first term in the above formula. For a 92-ft pipeline (92 ft horizontal out of a 165 ft loop) this resistance will require 21.3 psi which is significantly more than 5 psig value reported at PNNL-17639 WTP-RPT-175 Rev. 0 (Poloski et al., 2009a). However, this calculation is based on

moving the entire sediment bed along the length of the pipe. A more realistic approach is to consider that the process of bulk pushing of the bed will occur in the vicinity of the pipe inlet, then the length can be estimated to be 5/21.3*92=21.6 ft (instead of 92 ft) from the pump. Note that startup pressures that are elevated can cause sediment ramping and accumulation near the pump. This behavior is in agreement with pressure rise trend in PNNL's report. This means that upon start of the flow, the entire sediment bed will move 21.6 feet. Then lateral solid accumulation occurs that reduces the cross section area of the flow and causes the pressure difference and flow velocity to rise until a minimum cross section point is reached. After that point, shear stress will erode the sediment ramp layer by layer and a wider cross sectional area will be obtained, which results in decrease of pressure difference.

Variations in the startup requirements are likely due to estimates in the parameters utilized, such as the sediment angle, friction coefficient, pressure drop coefficient, and estimated pipe lengths. Future steps will be to refine the calculations to match PNNL data and to understand the sediment build up process during flushing.

References

Bontha J.R., Adkins H.E., Denslow K.M., Jenks J.J., Burns C.A., Schonewill P.P., Morgen G.P., Greenwood M.S., Blanchard J., Peters T.J., MacFarlan P.J., Baer E.B., Wilcox W.A., 2010, Test Loop Demonstration and Evaluation of Slurry Transfer Line Critical Velocity Measurement Instruments, PNNL-19441 Rev. 0.

Bontha J.R., Adkins H.E., Denslow K.M., Jenks J.J., Burns C.A., Schonewill P.P., Morgen G.P., Greenwood M.S., Blanchard J., Peters T.J., MacFarlan P.J., Baer E.B., Wilcox W.A., 2010, Test Loop Demonstration and Evaluation of Slurry Transfer Line Critical Velocity Measurement Instruments, PNNL-19441 Rev. 0

Crowe C.T., Multiphase flow Handbook: Fluid-Solid Transport in Ducts, CRC Press-Taylor & Francis Group, Chapter 4, Boca Raton, 2006.

Denslow K.M., Jenks J.J., Bontha J.R., Adkins H.E., Burns C.A., Schonewill P.P., Bauman N.N., Hopkins D.F., 2011, Hanford Tank Farms Waste Certification Flow Loop Phase IV: PulseEcho Sensor Evaluation, PNNL-20350 FINAL

Subtask 17.1.2: Computational Fluid Dynamics Modeling of a Non-Newtonian Fluid Undergoing Sparging for Estimating PJM Mixing Times

For this reporting period, the results obtained for the CFD modeling of the sparging were evaluated and analyzed. After the review, it was noted that the solution was mesh dependent with respect to refinement in the axial direction. This was confirmed by a grid dependence study on the amount of axial (z direction) cell divisions.

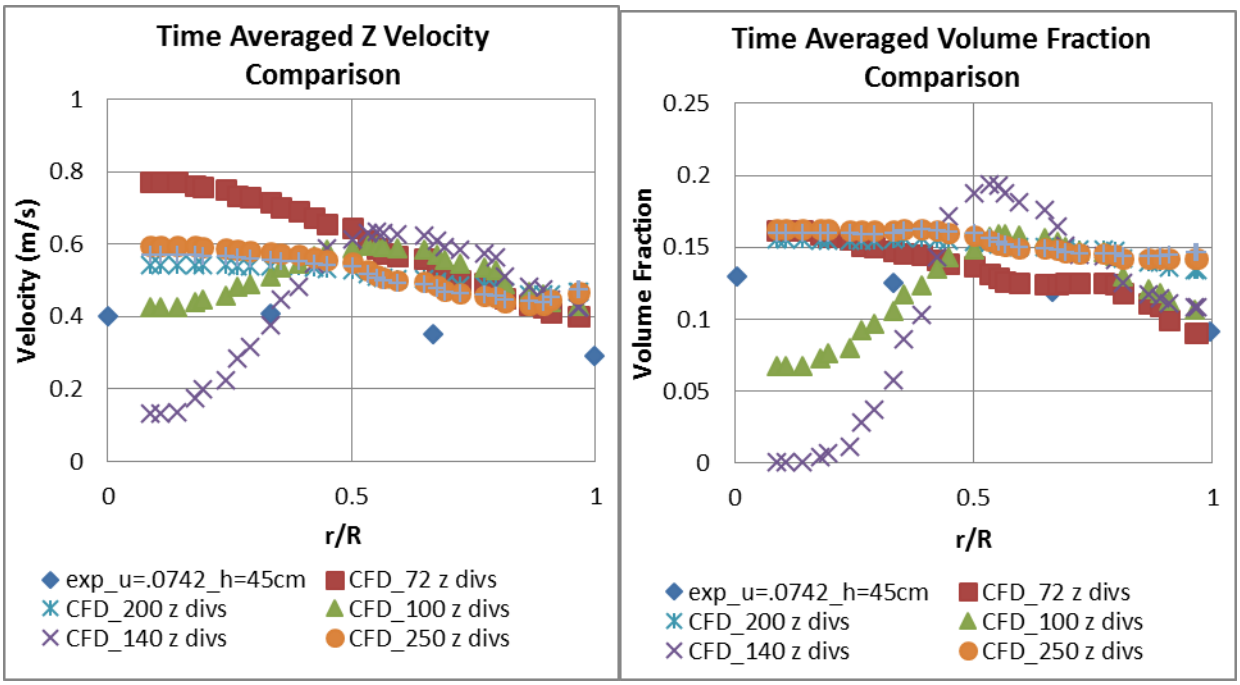

Figure 1-5. Sensitivity analysis on the axial mesh (Z direction).

It was observed that after 200 divisions in the z direction, the results began to converge. Thus, this was the discretization chosen to repeat the parametric study. Furthermore, the distribution of the mesh in the radial and circumferential direction was re-evaluated. The total mesh size has significantly increased to over one hundred thousand cells. The two mesh profiles being considered are shown below:

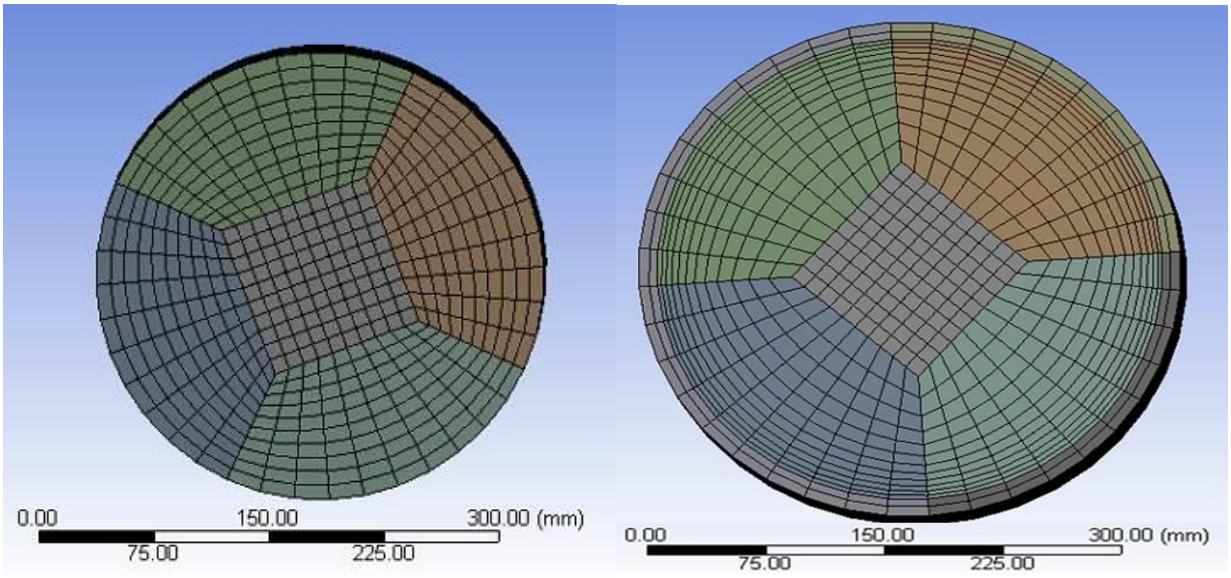

Figure 1-6. Proposed circumferential and radial mesh profiles.

The mesh on the left of Figure 1-6 increases the mesh count for higher and even resolution but wastes mesh on the center of the column. The mesh on the right of Figure 1-6 concentrates meshing near the wall where there will be higher velocity gradients, giving better resolution near

the wall at the cost of resolution near the center. These two meshes will be run and the simulation with the best results will be the one chosen for the final parametric study.

During this reporting period, further simulations on the work of Esmaeli, et al. (2015), which investigated sparging non-Newtonian fluid, were continued. Previous simulations were able to predict volume fraction profiles with reasonable accuracy, but lacked accuracy in predicting the velocity profiles of the bubble column. Simulations were run with different drag models and turbulent dispersion effects were added in order to attempt to address the observed discrepancies. A few of the results are shown below.

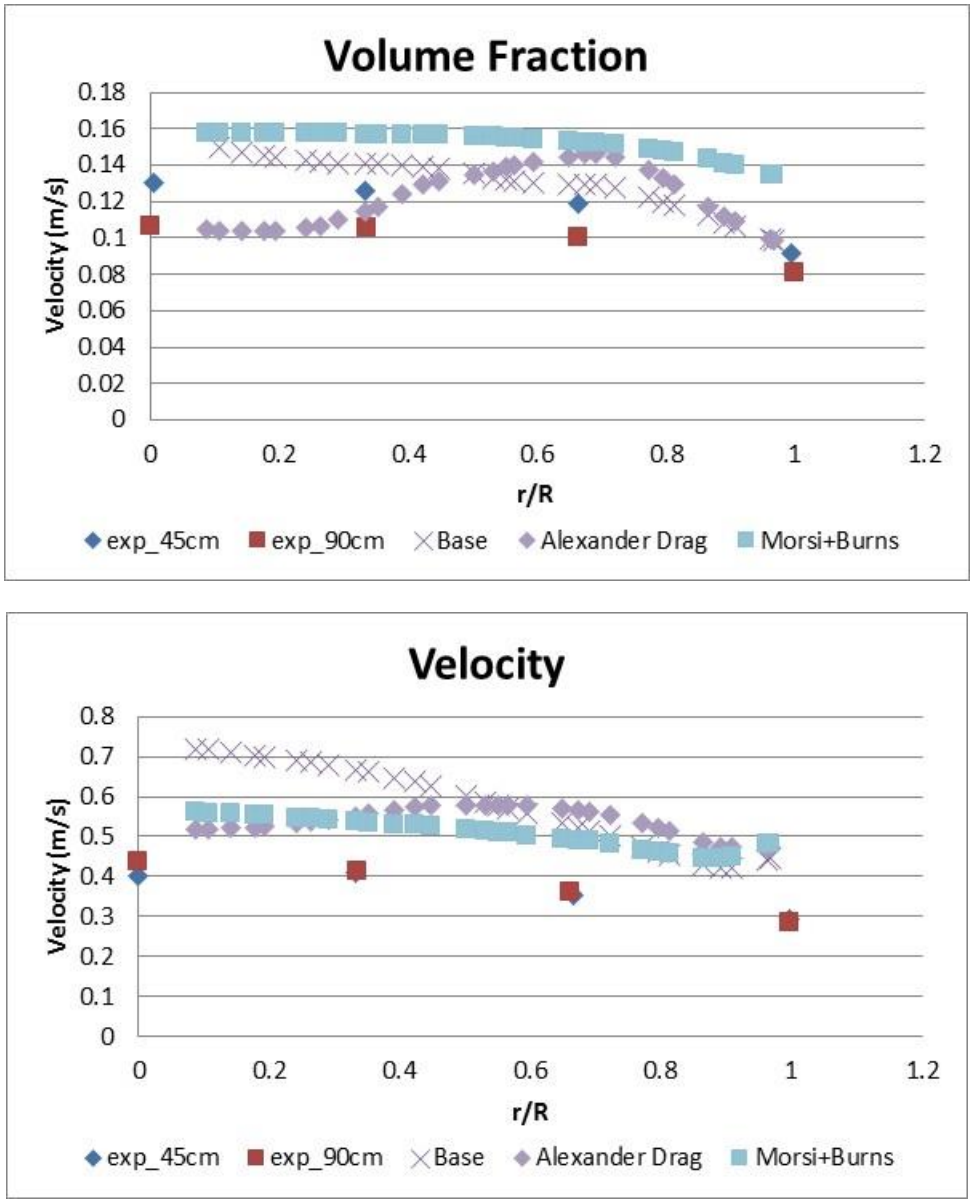

Figure 1-7. Comparison of experiments against a base CFD case and altered drag law and turbulent dispersion models.

A base case simulation was used as reference to the different viscosity and turbulent dispersion models. It was observed that with Morsis's drag law and Burns et al. turbulent dispersion model

the velocity profiles were much better matched. This comes at the expense of loss in volume fraction profile accuracy, but this aspect is still accurate within a reasonable range.

Lastly, two different experimental works on a bubble column operating with a Bingham type fluid were found. One investigation was headed by Koichi et al. (2003) on oxygen transfer in yield stress fluids and the other was directed by Kawase et al. (2005) having investigated the hydrodynamics in bubble columns for fermentation broths. Although both works investigate the fluid of interest, none account for a radial distribution of velocity or volume fraction profiles. Both of these works are concurrently being simulated using the same models as previous simulations, with exception of the viscosity model which now includes the characteristic of yield stress. Both simulations are currently diverging and are being evaluated in order to retrieve results. The path forward involves developing a working model of a bubble column with yield stress fluid, so that a validated computational fluid dynamics model may be completed.

Due to a lack of quality experimental data of bubble columns with yield stress fluids, time would be best spent investigating sparging of power law fluids. The simulations replicating Esmaeli, et al. (2015) were refined as shown in Figure 1-8.

From the figure, it can be seen that the volume fraction profile is well matched to experimental data. The small discrepancies observed are due to the lack of bubble coalescence modeling in the current simulation. The time averaged axial velocity profiles are qualitatively similar but lack in quantitative accuracy. Because the nature of this study is more concerned with qualitative analysis, the current results are deemed appropriate to use for validation.

Simulations of sparged non-Newtonian fluids using the validated model were conducted in a manner that reveals characteristic behavior in bubble columns with non-Newtonian fluids. This is achieved by altering the height-to-diameter ratio of the bubble column and the power law index of the continuous fluid in a systematic fashion. The status of these efforts are shown in Figure 1-9.

It can be observed from Figure 1-9 that the H/D effects are more pronounced at lower inlet velocities. It also appears to be the case that lowering the H/D ratio increases the volume fraction when looking at radial distributions. From Figure 1-10, it can be observed that lowering the power coefficient in the viscosity model tends to flatten the volume fraction profile for H/D = 3.8. Lowering the H/D ratio appears to flatten the volume fraction profile, lessening the effects of changing the power index on the volume fraction profile.

Gas volume fraction and axial air velocity profiles will continue to be studied for qualitative trends as a function of the altered variables. The progression of the total gas hold up in the simulation will also be studied. The study will be finalized and trends will be inferred from the simulation results.

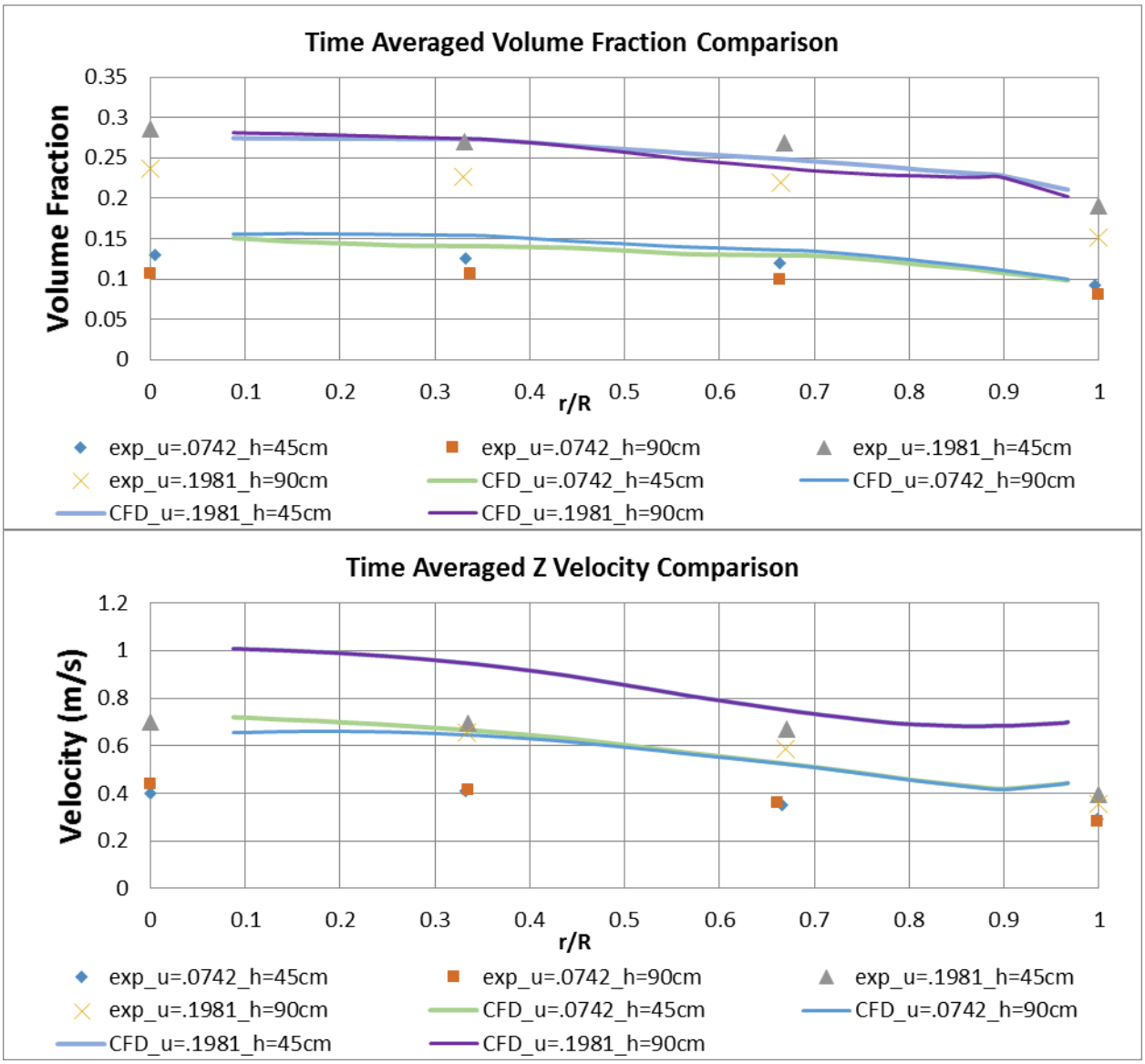

Figure 1-8. Comparison between Amin's experimental data and current simulation at two different inlet superficial gas velocities.

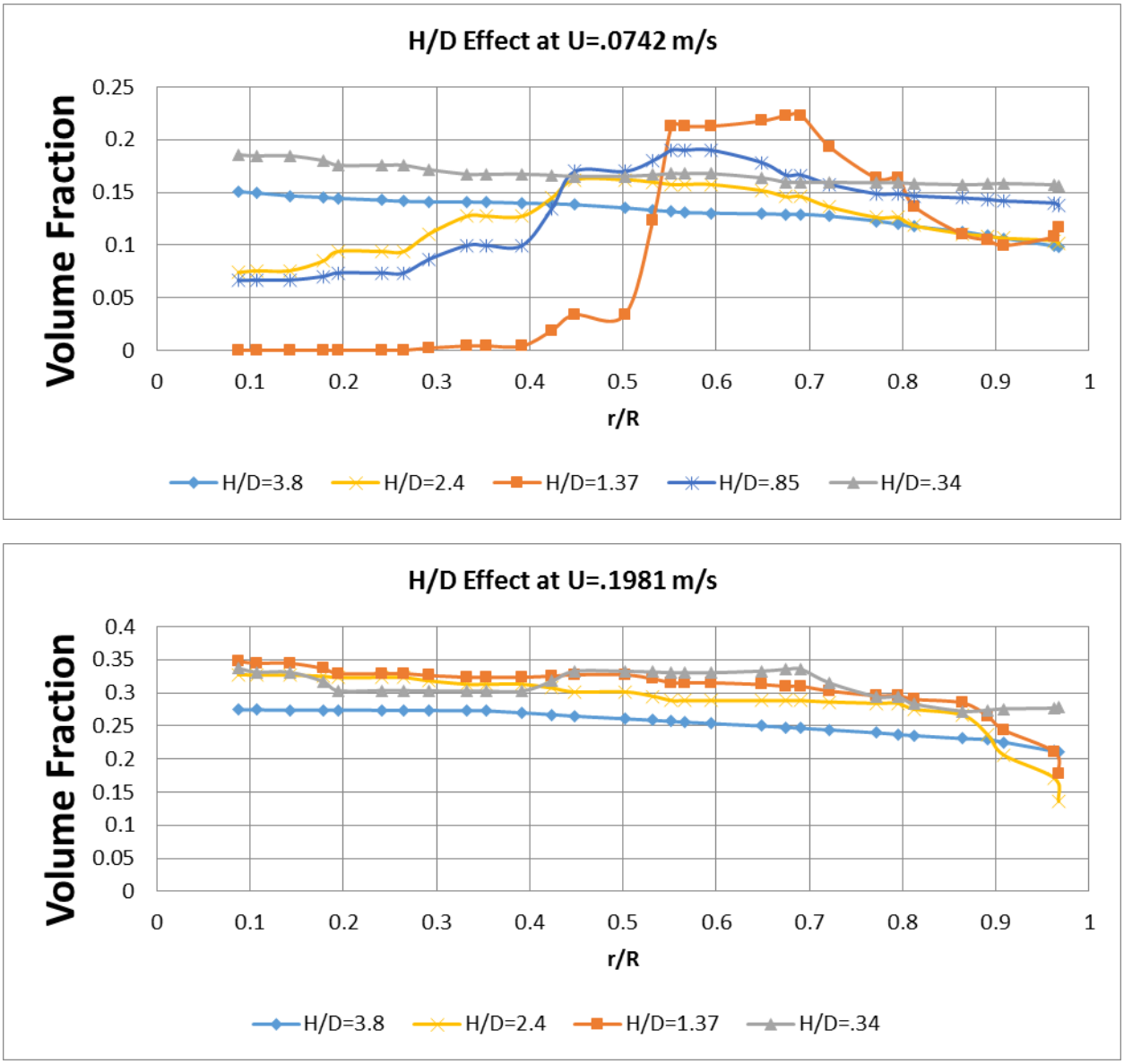

Figure 1-9. H/D Effect on volume fraction with inlet velocity U=.0742 (top) and U=.1981 (bottom).

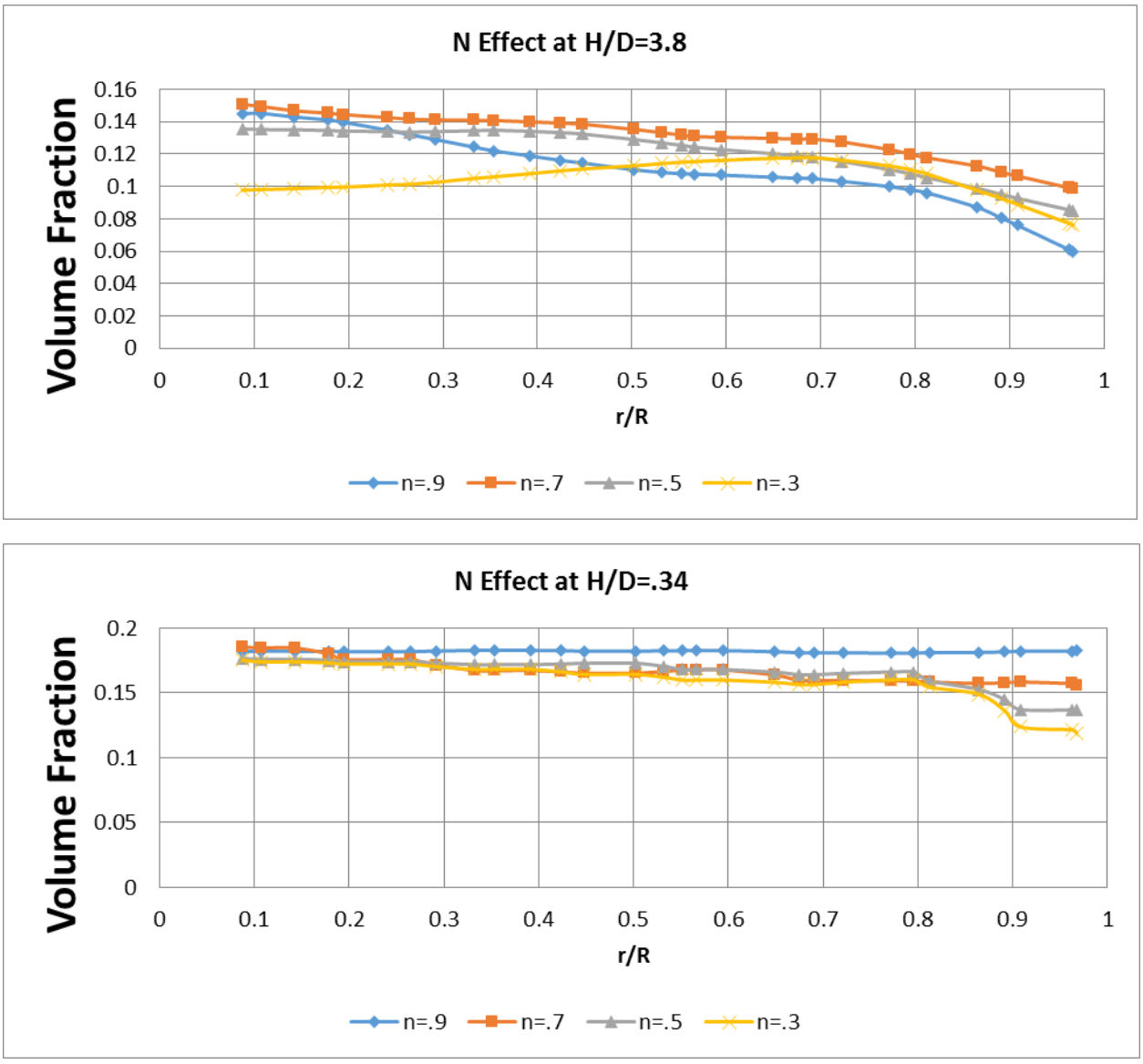

Figure 1-10. Effect of power law on volume fraction profile at H/D=3.8 (top) and H/D=.34 (bottom).

Task 18: Technology Development and Instrumentation Evaluation

Task 18 Overview

The objective of this task is to assist site engineers in developing tools and evaluating existing technologies that can solve challenges associated with the high level waste tanks and transfer systems. Specifically, the Hanford Site has identified a need for developing inspection tools that provide feedback on the integrity of the primary tank bottom in DSTs. Under this task, FIU is developing inspection tools that can provide visual feedback of DST bottoms from within the insulation refractory pads and other pipelines leading to the tank floor.

As part of the Hanford DST integrity program, engineers at Hanford are also interested in understanding the temperatures inside the primary tanks and to safeguard against exceeding specified limits. These limits are set to ensure that the tanks are not exposed to conditions that

could lead to corrosion of the tank walls. Previously, analysis was conducted to determine the viability of using an infrared (IR) temperature sensor within the annulus space to estimate the temperature of the inside wall of the tank. The analysis suggested that variations due to heat loss would be minimal and reasonable estimates using the sensor within the annulus is viable. Under this task, FIU is also evaluating the ability of IR sensors to detect inner tank wall temperatures via bench scale testing.

Task 18 Quarterly Progress

In September, FIU attended a two day meeting hosted by SRNL that focused on tank and pipeline integrity issues. Updates on Tasks 18 and 19 were presented to engineers from SRNL, WRPS and ORP.

Subtask 18.2: Development of Inspection Tools for DST Primary Tanks

An abstract based on this research was accepted by the Waste Management 2018 Symposium for an oral presentation:

> **Abstract**: 18349
> **Title**: Engineering Scale Testing of Robotic Inspection Tools for Double Shell Tanks at Hanford
> **Authors**: Michael DiBono (DOE Fellow), Dwayne McDaniel, Anthony Abrahao, William Tan, Leonel Lagos

Miniature Rover Inspection Tool

For the miniature rover, efforts included populating the electronic components on the printed circuit boards (PCBs) and testing the overall functionality of the populated PCBs. The following figure shows the two sensor hoops that are populated with both the temperature and iButton (temperature and humidity) sensors. The sensor hoop has a generic hardware interface with the base-PCB, such that different sensor hoods can be interchangeable when needed.

Figure 1-11. Sensor hoops populated with both the temperature and iButton sensors.

The following figure shows the populated camera PCBs. Two designs with different light emitting diode (LED) light configurations are being tested at the moment to determine the optimum lighting required for the camera in the refractory slots. The first design uses all patch

LEDs, which provide good localized lighting, while the second design mixes both the patch and bulb LED lights, with the hope of providing both localized and distance lighting. Tests will be conducted in the in-house built mock up facility to determine the best lighting choice.

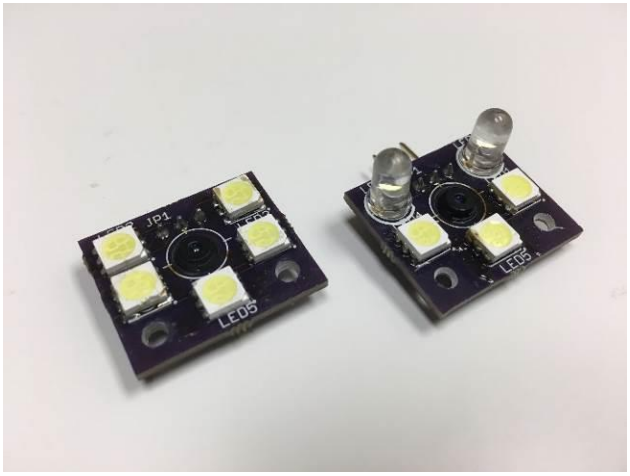

Figure 1-12. All patch LED lights on the left, mixed LED lights on the right for the lighting source of the mini inspection tool.

In addition, FIU also worked on overall rover system integration and functional testing. This included motor and camera integration, wiring and ensuring all the electronic components are operating correctly. The following figure shows two fully integrated mini-inspection tool fitted with radiation, temperature and humidity sensor hoods. The sensor hoods share a common electrical and communication interface, thus allowing the sensor hoods to be interchangeable onto the inspection tool's base for different sensing missions. The next step is to conduct testing in the mock-up facility.

Figure 1-13. Temperature sensor hood (left), inspection tool fitted with iButton (humidity and temperature) sensor (middle), and inspection tool fitted with RD2014 Radiation sensor (right). The sensor hoods share a common electrical and communication interfaces.

The team also worked on the design of an automated tether management system that will be used in the mini-rover deployment. This design, shown in Figure 1-14, will be scaled accordingly to other inspection tools currently being developed at FIU.

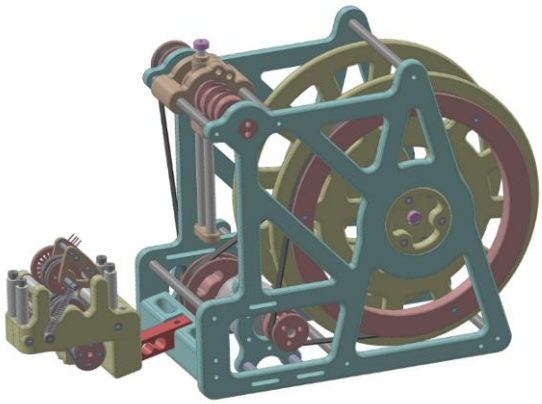

Figure 1-14. Redesigned automated tether management systems.

Since the mini-inspection tool has limited pull force when navigating in the air refractory, FIU incorporated an active cable releasing capability onto the cable management system. This capability makes use of a strain gauge to sense the tension on the cable and actively releases the cable to minimize the cable tension. Figure 1-15 shows the integrated cable management system equipped with the active cable release capability.

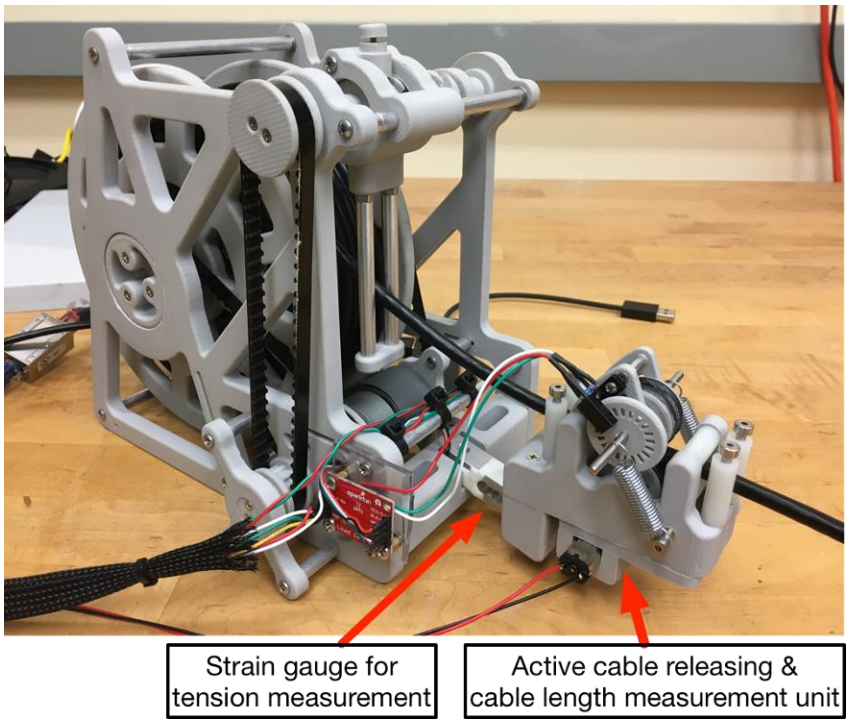

Figure 1-15. Cable management system equipped with active cable release capability.

The cable release and retrieval sub-systems are currently being controlled by the Adafruit Feather M0 and DC motor FeatherWing boards. Figure 1-16 shows the block diagram of the cable management system with its sub-components. Whenever the cable tension (output signal of the strain gauge) is higher than a pre-defined threshold, the M0 controller board will generate a control signal for the DC motor controller to release the cable. Concurrently, the Opto Encoder will record and estimate the length of the cable that is being released. Conversely, whenever the operator commands the inspection tool to maneuver in the backward direction, and the cable tension is below the threshold, the controller will command the DC motor controller to retrieve the cable. The feedback control would allow the cable management to operate autonomously. The current setup is having some issues. When the strain gauge is operational and providing readings, the M0 board fails to generate a control signal for the DC motor control. This may be a problem at the software level where the Feather M0 board is sharing the same communication channel for both the strain gauge and the DC motor controller. This issue is currently being addressed.

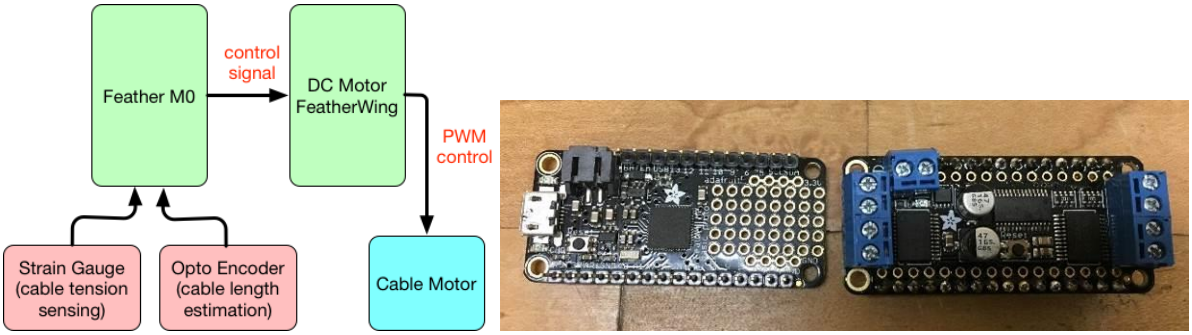

Figure 1-16. Block diagram of the cable management system showing sub-components and the control system passing (left), Adafruit Feather M0 and FeatherWing (right).

A concurrent effort is also being pursued to develop a simulation environment for both the mockup facility and the mini-inspection tool. The simulation uses a physic-based Gazebo engine (http://gazebosim.org/) and the robotic operating system (ROS). The simulation is useful for testing various designs of the mini inspection tool, as well as different simulation environments that mimic the layout of different tank configurations. The simulation also allows the systems' designs (both the mockup and inspection tools) to be fine-tuned before fabrication. Furthermore, once the simulation is fully developed, it can be used for the operator training for inspection tasks before field deployment. Figure 1-17 shows the screen captures of the mockup simulation environment that is currently being developed (left), as well as the deployment of a mini inspection tool maneuvering on top of a duct with the camera view shown in the insert (right).

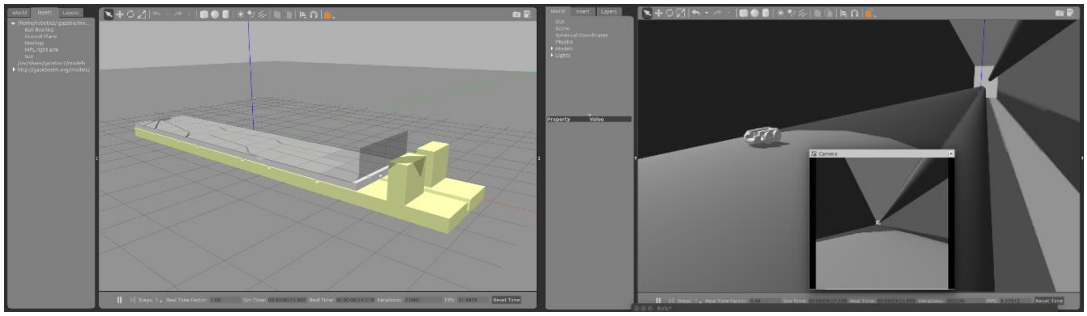

Figure 1-17. Simulation environment for tank mockup currently being developed at FIU (left) and simulation of mini inspection tool maneuvering on top of a duct work, with the insert showing the camera view (right).

Full-Scale Sectional Mockup

During this performance period, the main activity was focused on continuing the construction of the full-scale sectional mockup of the double shell tank (DST). The following figure shows the mockup foundation during construction at FIU. The construction of the shell foundation was completed. The concrete coating was successfully applied to the wooden frame and the steel plates of the secondary tank liner were laid in place.

Figure 1-18. The full-scale HLW tank mockup.

The following figure shows the design of the refractory pad with cooling channels. Similar to the concrete foundation, the pads have a wooden structure, which will be coated with concrete.

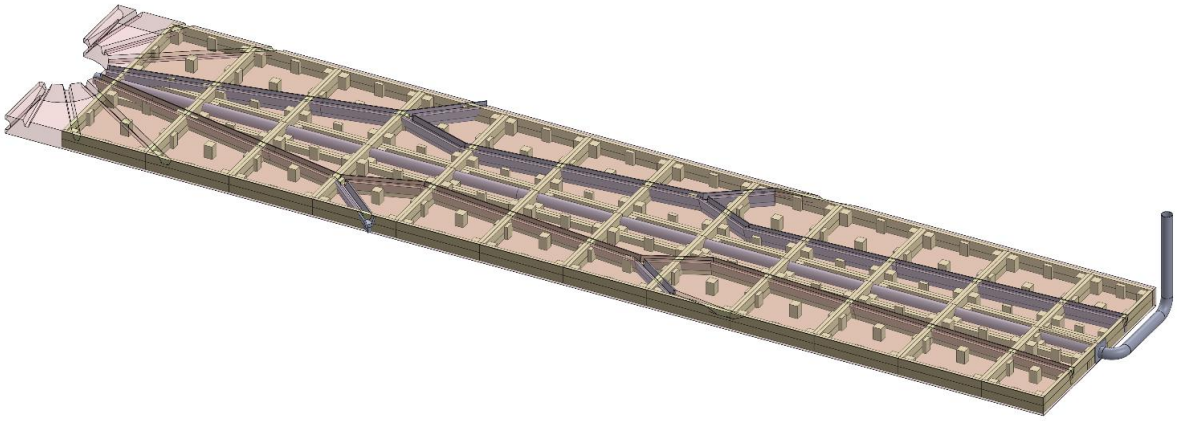

Figure 1-19. Design of the refractory pad structure with cooling channels.

The design is modular, which is suitable for testing, customization, assembly and maintenance. The following figure shows some modules laid on top of the secondary tank liner.

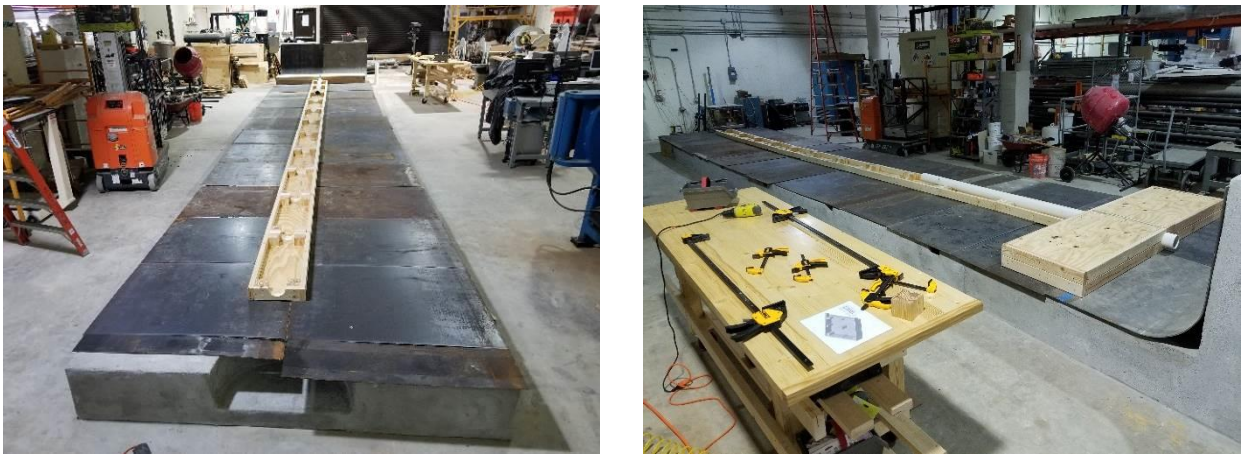

Figure 1-20. Modular refractory pad.

Figure 1-21 shows the refractory being constructed from sectional boxes made of plywood. Construction of these boxes were completed. The boxes will have slots cut to form the network of refractory channels. The design and procedure for the cuts was recently developed. After the slots are created, the wood boxes will be covered in an asphalt felt and metal lath will be placed on top. A thin layer of concrete will then be added onto the lath and the secondary liner will be installed. This will complete the initial construction of the test bed.

Figure 1-21. Plywood boxes that form the refectory.

Subtask 18.3: Investigation Using an Infrared Temperature Sensor to Determine the Inside Wall Temperature of DSTs

This task has been completed. FIU will discuss with Hanford engineers whether additional testing is needed. Currently, FIU is researching options for permanently integrating the IR sensor with the mini rover and testing it on the full-scale mockup testbed being constructed at FIU ARC.

Task 19: Pipeline Integrity and Analysis

Task 19 Overview

The objective of this task is to support the DOE and site contractors at Hanford in their effort to evaluate the integrity of waste transfer system components. The objective of this task is to evaluate potential sensors for obtaining thickness measurements of HLW pipeline components. Specific applications include straight sections, elbows and other fittings used in jumper pits, evaporators, and valve boxes. FIU will assess the accuracy and use of down selected UT systems for pipe wall thickness measurements. FIU will also demonstrate the use of the sensors on the full-scale sectional mock-up test bed of the DSTs. An additional objective of this task is to provide the Hanford Site with data obtained from experimental testing of the hose-in-hose transfer lines, Teflon® gaskets, EPDM O-rings, and other nonmetallic components used in their tank farm waste transfer system under simultaneous stressor exposures.

Task 19 Quarterly Progress

In September, FIU attended a two day meeting hosted by SRNL that focused on tank and pipeline integrity issues. Updates on Tasks 18 and 19 were presented to engineers from SRNL, WRPS and ORP.

Subtask 19.1: Pipeline Corrosion and Erosion Evaluation

An abstract based on this research was accepted by the Waste Management 2018 Symposium for a poster presentation:

Abstract: 18368
Title: Real-time Erosion-Corrosion Detection in Waste Transfer Pipelines using Ultrasonic Sensors
Authors: Aparna Aravelli, Dwayne McDaniel, Clarice Davila (DOE Fellow)

During this quarter, a test loop has been designed, a test plan has been established for bench scale testing, and the process of procuring the required loop components has been initiated. In addition, a simulant has been selected and additional literature review has been conducted to support the current research. The test loop is designed to evaluate the Permasense sensors under real-time erosion-corrosion.

During the month of July, efforts were focused on the design of the test loop. Based on the initial design, the head losses in the loop were calculated. Accordingly, an appropriate pump was selected. Previously, the option of circulating caustic solutions was investigated for erosion. The practical implementation of the method included the use of a fume hood and ensuing stringent chemical use regulation standards. Hence, a more environmentally friendly method of sand and water slurry was pursued.

The test loop was designed for a soil and water mixture. The average volume fraction of solids was assumed to be 10% (based on literature). The basic diagram is as shown in the following figure and consists of 2- and 3-inch pipe sections connected via a reducer. The pump will be attached at the lower horizontal 2-inch pipe section next to the tank bottom.

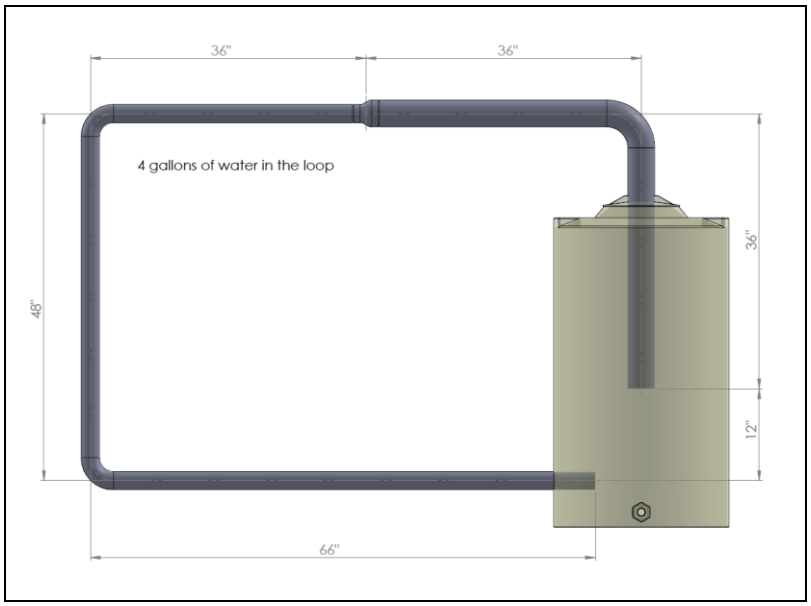

Figure 1-22. Pipe loop design.

The head loss calculations for the pipe sections were conducted using a standard approach, Bernoulli's equation. The input data included mean fluid flow rate (Q) of 160 gpm to provide a velocity of 3 m/s (9.8 ft/s), density of the sand particles was 2650 kg/m^3 (165.4 lb/ft^3) and sand size was 900 µm. The slurry viscosity was calculated as 1.25 cP. According to the obtained

Reynold's number, the flow was turbulent and, hence, is assumed to cause erosion at a faster rate. The fundamental equations used in calculations included:

$$Hp = \frac{Q}{2g}\left(\frac{1}{A_2^2} - \frac{1}{A_1^2}\right) + (Z_2 - Z_1) + H_{pipe} + H_{fittings} \quad (1)$$

Where *Hp* is the pump head, *Q* the flow rate, A_i represents the pipe's cross-sectional area, Z_i, the inlet and outlet height, H_{pipe} is the head for the pipe sections and the $H_{fittings}$ the head for the fittings. The equations used for the pipe and head fittings were:

$$H_{pipe} = f\left(\frac{l}{d}\right)\left(\frac{v_i^2}{2g}\right) \qquad H_{fittings} = k\left(\frac{v_i^2}{2g}\right) \quad (2)$$

Where *f* is calculated based on the value of the Reynold's number, v_i represents the flow velocity at each cross section, and *k* is an equivalent constant calculated based on the fittings. Using the above equations, the head for the pump was determined to be 10 ft.

During the month of August, efforts were focused on developing a test plan for the UT sensors task, finalizing the actual sizing of the test loop and procuring the necessary pump. The test plan document includes a description of the Permasense sensors, initial sensor validation tests and results, new loop design for real-time corrosion monitoring, the test matrix for the loop testing phase using sand water mixture as simulants and a future plan to use caustic and saline solutions as potential simulants.

The actual sizing of the test loop considered features such as a by-pass added to the loop design. A final design of the loop is as shown in Figure 1-23. This design incorporates 2- and 3-inch schedule 40 carbon steel straight pipe sections along with long radius elbows and a reducer. The loop is approximately 6½ ft x 7 ft in dimension and consists of a pump and a reservoir to circulate the simulants. The reservoir is a 70-gallon vertical polyethylene tank with a stirrer/mixer. The design includes a bypass with steel ball valves to control the flow of the simulant as the pump does not have a variable frequency drive (VFD). The loop consists of several sections attached with flanges and connectors for ease of installation and removal/replacement, as needed. A total of four Permasense sensors will be placed on the 2- and 3-inch diameter straight and bend sections (elbows) of the loop as shown in the figure below.

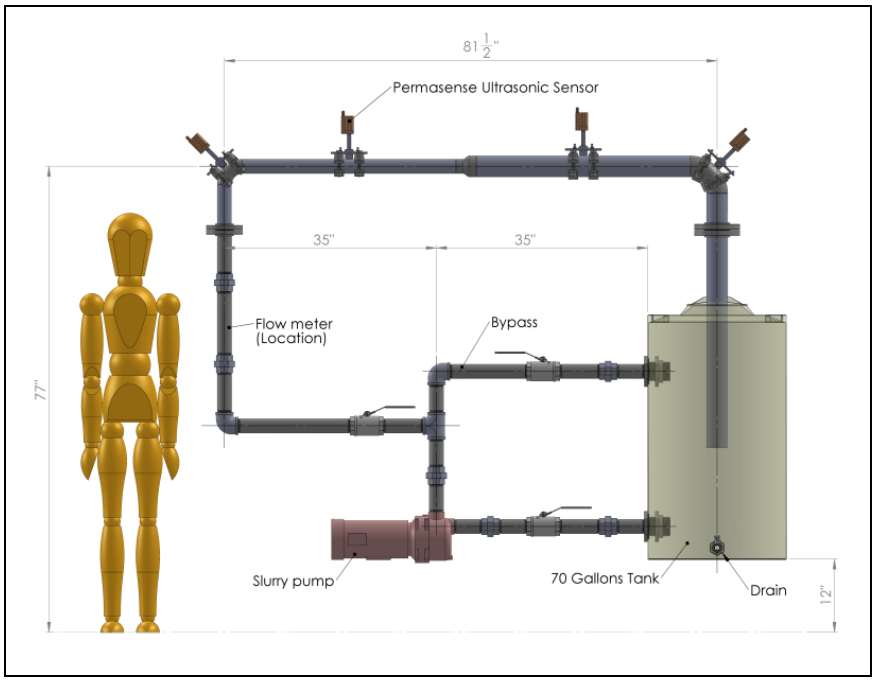

Figure 1-23. Pipe loop design for aging.

An important feature in the test loop is a slurry pump that can handle abrasive simulants and generate flow velocities up to 2.5 m/s and flow rates up to 110 gpm. The maximum values are based on typical flow requirements needed for erosion found in the literature [1]. A number of pumps were evaluated for this purpose and the candidate selected is a 3-HP self-priming centrifugal pump with 230V, 12.5Amps, 1 phase, 2-inch inlet/outlet and a maximum head of 60 ft. The slurry pump, manufactured/distributed by Dayton [2], includes a stainless steel impeller which makes it suitable for corrosive media. It can also handle solids up to 1 inch in diameter and can pump liquids with temperatures up to 160°F.

Since there are suspended solids in the simulant, a mixture or agitator is also needed. Some of the options include tank mixers, drum mixers or laboratory mixers. Two of the potential options for the mixers are as shown in Figure 1-24. The mixer shown in Figure 1-24 (left) is a Dayton drum mixer (1/2 HP) and is made of 316 stainless steel propeller blades and shaft. The shaft diameter is 5/8 inches and the shaft length is 29 inches. It contains a 115/23V 1-phase electric motor. The mixer is designed and manufactured for efficient mixing of closed-head steel drums. The mixer mounts on the drum lip; this mounting will provide the correct shaft angle through the bung opening. The propeller vanes collapse to allow entry through the bung hole and open when operating to provide thorough mixing. The mixer unit can be easily moved from one container to another and the propeller opens to a 3-3/4" diameter when the mixer is in operation. Figure 1-24 (right) shows a laboratory drum mixer (1/20 HP) with 316 stainless steel propeller blades and shaft. The shaft diameter is 5/16 inches and the shaft length is 30 inches. It contains a 115V 1-phase electric motor. The mixer is designed for economical mixing of small tanks and open head drums. The mixer can be easily mounted and the shaft angle can be easily adjusted for optimum mixing. The mixer can be conveniently moved from one container to another, and can be mounted directly to tanks or on rails with opening adjustable clamp and a mounting bracket which adjusts for unlimited mixing angles. It is well-suited for mixing/blending low viscosity

fluids and suspending or dissolving low concentrations of solids in water or water-like liquids, including light oils and syrups. One of these two or similar options will be considered for testing.

Figure 1-24. Drum mixers: closed drum (1/2 HP) and open drum (1/20HP) [3].

As discussed in the previous monthly report, there are several options of simulants for circulation in the loop to determine real-time wear rate. In the first stage of testing, a sand and water solution was selected due to its ease of procurement, testing and disposal. Based on the results obtained during the first phase of testing, other options might be considered in the future. The schedule for the testing is shown in Table 1-4. The sand media used will be up to 10% of solids by volume and the size of the sand particles will be typically 200, 600 and 900 microns. The volume concentration and size of particles for testing have been selected based on similar literature values [1, 4].

Table 1-4. Sand and Water Testing

Simulant	Circulation Period (estimated)
Water (loop validation)	1 week
Sand and water slurry (5%)	3 months
Sand and water slurry (8%)	2 months
Sand and water slurry (10%)	2 months

The test loop will be constructed as indicated by the final design and the testing will be conducted based on the schedule above to measure real-time thinning of the carbon steel pipe sections. The measurements will be obtained every 6 hrs and the data will be analyzed to determine if modifications to the system need to be made.

The bill of materials for the loop components has been generated and currently FIU is in the process of obtaining quotations for the procurement and welding of the pipe sections as well as procurement of the reservoir, mixer and the flowmeters. In addition, FIU is looking into procedures for removing the sensors from the old test piece and replacing them on the new simulant loop with the assistance of the Permasense manufacturer.

References

1. Wood R. J. K and Jones T. F., "Investigations of sand–water induced erosive wear of AISI 304 stainless steel pipes by pilot-scale and laboratory-scale testing", Wear, Vol. 255, Issue 1-6, Aug-Sep 2003, Pg. 206-218.
2. http://www.sciencedirect.com/science/article/pii/S0043164803000954.
3. https://www.grainger.com/ec/pdf/4YU37_1.pdf
4. https://www.grainger.com/ec/pdf/Dayton-Drum-Mixer-32V126-OIPM.pdf
5. Naz, M. Y., Ismail, N. I., Sulaiman, S. A., Shukrullah, S., "Characterization of erosion of gas pipelines by dry sand", Instrumentation Science and Technology, 2017, VOL. 45, NO. 1, 62–72. http://dx.doi.org/10.1080/10739149.2016.1194295.

During the month of September, efforts were focused on disseminating the test plan to key stakeholders at WRPS, SRNL, and PNNL and incorporating their feedback. Additional documentation was also reviewed on the use of the sand-water slurry for erosion effects on the carbon steel pipe sections. The test plan containing the test loop development and the testing procedures for the erosion/corrosion detection using Permasense sensors was circulated to meet the site needs. In addition to carbon steel, WRPS had suggested the use of alternative materials such as 304L stainless-steel for testing. Additional comments included exploring the effect of ambient temperature and humidity conditions on the sensors.

SRNL is interested in the potential investigation of radiation exposure of the sensors and in validating their novel method of erosion/corrosion testing using coupons. These are replaceable erosion/corrosion coupons to measure the mass change (loss or gain) and to obtain and study the surface roughness profiles obtained from wear and pitting corrosion while conducting real-time UT sensor measurements. Testing and evaluation of SRNL erosion/corrosion coupon system will require the coupon(s) to be inserted into elbow/straight sections of the pipe which will be detachable. The testing phase will be interrupted for short intervals of time while the coupons are removed from the loop. Gravimetric weight loss measurements will be conducted on the removed coupons. The coupons will then be re-inserted into the loop. In addition, an external UT sensor and a micro-meter will be used to measure the pipe thinning manually.

The literature review for erosion in pipes and ductile materials with sand and water included a number of reference articles. A few of the relevant papers are summarized below.

Comparison of predicted and experimental erosion estimates in slurry ducts [1]

This article compares predicted and experimental erosion estimates using a full-scale loop rig with AISI 304 stainless steel pipework. Computational models are used for the prediction of erosion, which also focuses on the impact velocity and impact angle in a bend. Slurry consisting of water and sand is used as the cause of the erosion within the loop system. Three methods are used to gather data on thickness loss: 1) ultrasonic measurements, 2) gravimetric measurements, and 3) micrometer measurements (requires cutting into the pipe and bends sections). These measurements are then compared to the predicted erosion damage levels by the models developed.

Slurry erosion of surface imperfections in pipeline systems [2]

This article focuses on the erosion of imperfections on the surfaces and welds within the pipes that handle slurry. The data collected from the experiments are compared to computational fluid dynamics models. The erosion results for two sizes of circular cavities as well as a regular and an irregular weld bead-configuration commonly encountered on pipeline surfaces are analyzed and it is concluded that the maximum erosion occurs on the forward-facing edge of the pipe cavities, while the maximum erosion rate occurs on the wind-ward side of the weld. One of the cases of the computational model results for erosion is shown in Figure 1-25. The images in the figure are a simulation of an imperfection caused by a cavity and the effect on the edge that is impacted by the flow of the slurry (eroded at different rates though the flow is consistent). The time of slurry flow is 16 and 32 hrs, respectively, for the two cases shown.

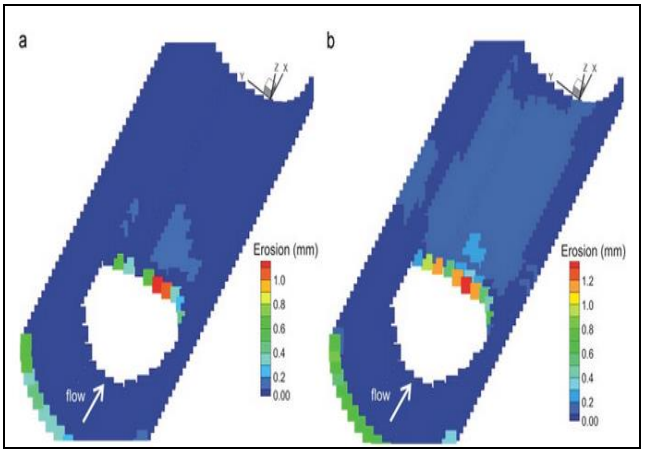

Figure 1-25. Erosion results using the computational models.

Abrasion erosion modeling in particulate flow [3]

This article demonstrates the use of a model that displays abrasion erosion within a pipe, caused by a slurry mixture of sand and water. In this work, the mechanistic erosion equation, the abrasion erosion equation, and empirical constants developed from previous works are implemented in a commercially available CFD code (ANSYS FLUENT) to calculate erosion for submerged impingement jet geometry, and the result is compared with the experiment. It also takes into consideration erosion without the presence of an abrasive to determine the significance of the thickness loss when an abrasive is present. In Figure 1-26, the results obtained from the experiments are compared to those obtained from models with sand particle sizes of 150 and 300 microns.

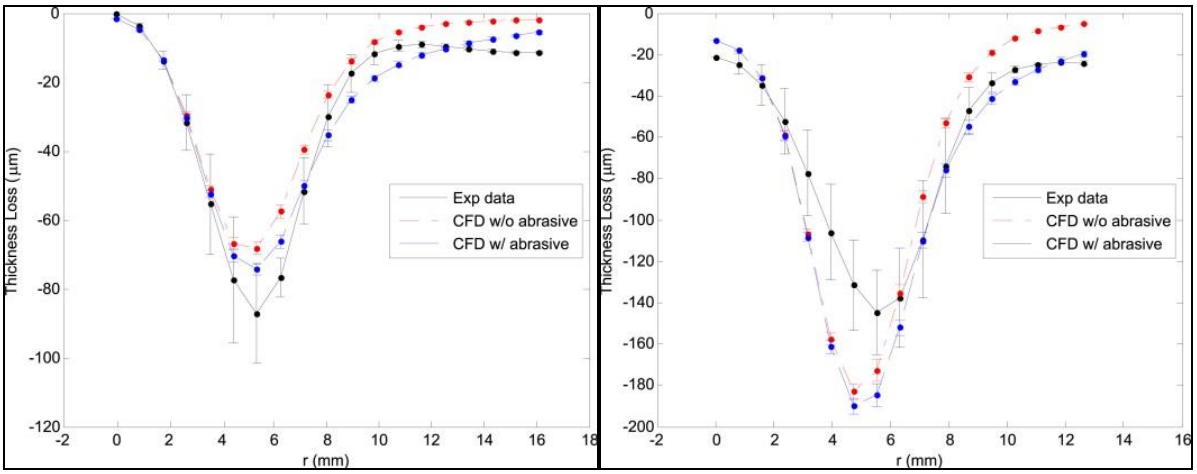

Figure 1-26. Thickness loss results from experiments and using CFD at 150 microns (left) and 300 microns (rt).

Numerical investigation of erosion threshold velocity in a pipe with sudden contraction [4]

This article discusses how velocity through turbulent flow with particles present plays a role in causing the erosion rate to increase within slurry pipes with sudden contraction. This is mainly tested through mathematical models for the calculations of the fluid velocity field and the motion of the solid particles that have been established and overall used to predict the erosion rate. A slurry mixture of sand and water are taken into consideration as well. Figure 1-27 compares the erosion rate in the models with regards to its direction of flow, which in this case involves downward and upward flow.

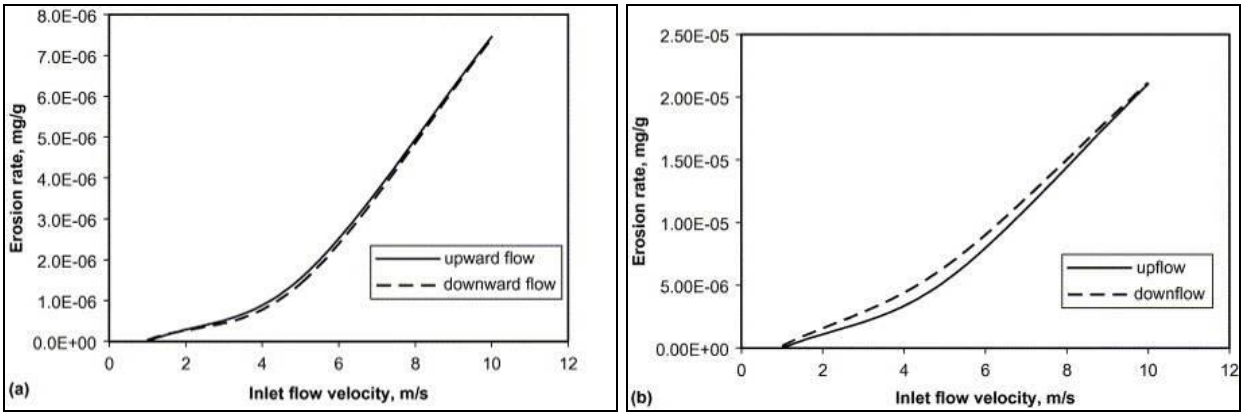

Figure 1-27. Erosion rate with flow velocity.

Slurry erosion of ductile materials under normal impact condition [5]

This article focuses on the erosion of a variety of ductile materials within a slurry pot tester. A slurry mixture of water and sand is taken into consideration within the experiment followed by the comparison and analysis of the erosion results of the materials used. The hardness of the materials is analyzed to understand how that affects the increase or decrease of the erosion rate. Figure 1-28 displays the accuracy of the correlation for normal impact wear of ductile materials within a margin of 12%.

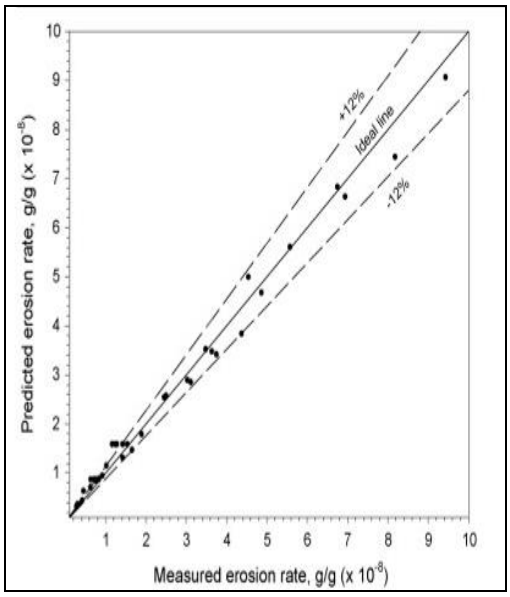

Figure 1-28. **Correlation accuracy of predicted and measured erosion.**

References

1. R.J.K. Wood, T.F. Jones, J. Ganeshalingam, N.J. Miles, Comparison of predicted and experimental erosion estimates in slurry ducts, In Wear, Volume 256, Issues 9–10, 2004, Pages 937-947, ISSN 0043-1648, https://doi.org/10.1016/j.wear.2003.09.002.

2. Chong Yau Wong, Christopher Solnordal, Lachlan Graham, Gregory Short, Jie Wu, Slurry erosion of surface imperfections in pipeline systems, In Wear, Volumes 336–337, 2015, Pages 72-85, ISSN 0043-1648, https://doi.org/10.1016/j.wear.2015.04.020.

3. H. Arabnejad, A. Mansouri, S.A. Shirazi, B.S. McLaury, Abrasion erosion modeling in particulate flow, In Wear, Volumes 376–377, Part B, 2017, Pages 1194-1199, ISSN 0043-1648, https://doi.org/10.1016/j.wear.2017.01.042.

4. H.M. Badr, M.A. Habib, R. Ben-Mansour, S.A.M. Said, Numerical investigation of erosion threshold velocity in a pipe with sudden contraction, In Computers & Fluids, Volume 34, Issue 6, 2005, Pages 721-742, ISSN 0045-7930, https://doi.org/10.1016/j.compfluid.2004.05.010.

5. Girish R. Desale, Bhupendra K. Gandhi, S.C. Jain, Slurry erosion of ductile materials under normal impact condition, In Wear, Volume 264, Issues 3–4, 2008, Pages 322-330, ISSN 0043-1648, https://doi.org/10.1016/j.wear.2007.03.022.

Subtask 19.2: Evaluation of Nonmetallic Components in the Waste Transfer System

An abstract based on this research was accepted by the Waste Management 2018 Symposium for an oral presentation:

Abstract: 18371
Title: Extensive Aging and Evaluation of Nonmetallic Components in the Waste Transfer System at Hanford
Authors: Dwayne McDaniel, Amer Awwad, Jose Rivera

Sample coupons were taken from the hoses used during the 6-month burst pressure tests as well as the non-aged hoses. These samples were given to FIU's AMERI lab for analysis using a scanning electron microscope with energy dispersive X-ray spectroscopy (SEM-EDS). The intention is to be able to determine how far the NaOH penetrated into the ethylene propylene diene monomer (EPDM) inner hose samples. Figure 1-29 shows the results from the unaged (baseline) sample. As expected, there is no NaOH found within the EPDM. Figure 1-30 shows the results of the hose sample aged for 6-months at 170°F. As can be seen in the figure, there are low levels of both sodium and calcium present within the sample. From these preliminary results, it appears that the sodium hydroxide has some level of penetration into the inner hose at the higher temperatures. Once FIU obtains the results from the lower temperature samples, FIU will correlate how the temperature effects the penetration of the NaOH into the EPDM hoses. In addition, the samples will be analyzed in order to determine the source of the calcium inside the samples.

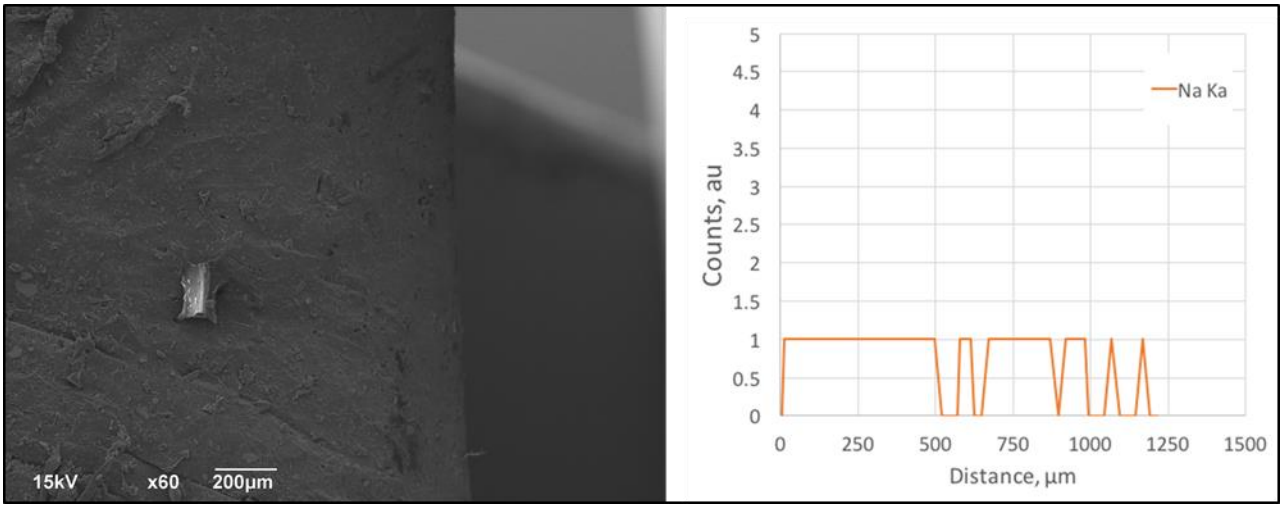

Figure 1-29. Unaged (Baseline) hose sample.

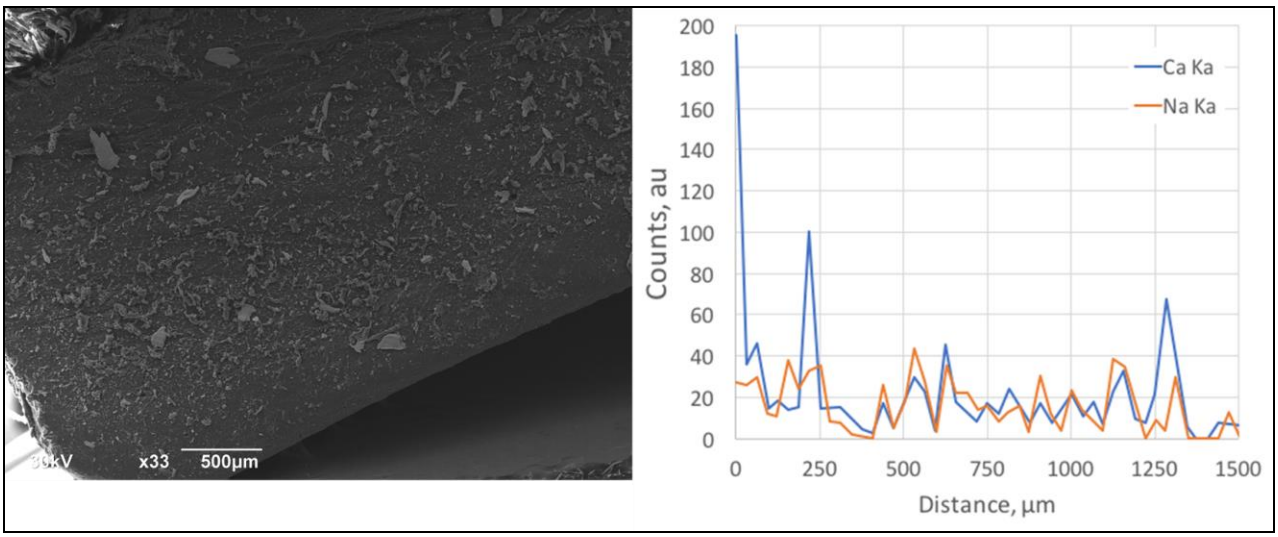

Figure 1-30. 6-Month aged hose sample (170F).

The one-year aging of the remaining specimens was also completed. Preparations began for the burst pressure tests of the HIHTL specimens that were aged for one year. FIU has also been in contact with key personnel to develop the next phase of material testing. Although burst pressure tests for the 6-month specimens did not demonstrate a significant change in strength from the baseline coupons, the material coupons did see significant changes in material properties. During the recent tank and pipeline integrity meeting at SRNL, engineers from SRNL, WRPS and FIU discussed each of their respective research efforts to understand how testing should move forward. SRNL has done a significant amount of material research to determine the effects of radiation, as well as caustic and elevated temperature exposure to polymer liners. Efforts will be made to draw correlations between material properties determined from specimens cut from the aged HIHTLs with the material dog bone coupons. After discussions with key personnel, FIU is planning on conducting the following tests during the next quarter; 1) Burst pressure test 2 high temperature aged hose specimens aged for 1 year. If the burst pressures are compatible with the baseline, then FIU will attempt to irradiate the others prior to burst pressure testing in order to determine what effect radiation exposure has on the burst pressure of the hoses. 2) Test all EPDM dog bone coupons that were aged for 1 year at the three temperatures of 100°F, 130°F and 170°F. 3) Extract dog bone coupons from the inner layer of the EPDM hoses that have been aged at the three temperatures of 100°F, 130°F and 170°F for the 6 months and have been burst. FIU will then conduct tensile tests on sets from each temperature as well as attempt to irradiate additional sets from each temperature and repeat the tensile test on the irradiated samples to determine the effect of radiation on the EPDM material.

Milestones and Deliverables

The milestones and deliverables for Project 1 for FIU Performance Year 7 are shown in the following table. Milestones and deliverables reforecast to be completed as carryover scope with the last increment of FIU Performance Year 7 funding from DOE are also shown below. No milestones or deliverables for this project were due in this quarterly reporting period.

FIU Performance Year 7 Milestones and Deliverables for Project 1

Task	Milestone/ Deliverable	Description	Due Date	Status	OSTI
Task 17: Advanced Topics for Mixing Processes	2016-P1-M17.1.1	Complete literature review and selection of baseline experimental cases	2/3/17	Complete	
	Deliverable	Draft Summary Report for Subtask 17.1.1	2/17/17	Complete	OSTI
	2016-P1-M17.1.2	Complete CFD simulations of air sparging experiments	4/21/17	Reforecast to 10/13/17	
	Deliverable	Draft Summary Report for Subtask 17.1.2	5/5/16	Reforecast to be included in YER	OSTI
Task 18: Technology Development and Instrumentation Evaluation	2016-P1-M18.2.1	Complete assembly of full-scale sectional mock-up test bed	12/16/16	Reforecast to 10/31/17	
	Deliverable	Draft Summary Report for Subtask 18.3.1	4/14/17	Complete	OSTI
	2016-P1-M18.2.2	Complete evaluation of sensor integration into inspection tools	5/26/17	Complete	

	Deliverable	Draft Summary Report for Subtask 18.2.3	6/30/17	Reforecast to 11/30/17	OSTI
	2016-P1-M18.2.4	Complete conceptual design of miniature rover platform	8/25/17	Reforecast to 11/30/17	
	2016-P1-M18.2.5	Complete conceptual design of 6 inch peristaltic crawler	8/25/17	Reforecast to 11/30/17	
	2016-P1-M18.3.1	Complete bench-scale testing for temperature measurements using IR sensors	3/31/17	Complete	
Task 19: Pipeline Integrity and Analysis	2016-P1-M19.1.1	Assess the accuracy of the down selected UT system via bench-scale testing	5/12/17	Complete	
	2016-P1-M19.1.2	Develop test loop for evaluating UT sensors	8/25/17	Reforecast to 11/30/17	
	2016-P1-M19.2.1	Complete experimental testing of 6 month aged materials	3/17/17	Complete	
	Deliverable	Draft Summary Report for Subtask 19.2.2	3/31/17	Complete	OSTI
	Deliverable	Draft Summary document on UT assessment for Subtask 19.1.1	5/26/17	Complete	OSTI

Work Plan for Next Quarter

Project-wide:

- Draft the Year End Report (YER) for FIU Performance Year 7.
- Draft the Project Technical Plan (PTP) for FIU Performance Year 8.

Task 17: Advanced Topics for Mixing Processes

- During the next quarter, FIU will focus on feedback received from engineers from PNNL and SRNL during multiple conference calls. Work will continue to find a consensus on the most representative simulant to be used and the test plan will be updated, accordingly. The feedback received has directed the focus to be on small and more frequent transfers and use of softer particles than Al_2O_3. FIU will consider various scenarios in which formation of crystalline UDS in sodium-bearing supernatants and slurry transfer lines occur during or after completion of a transfer. In addition, the sequence of processes from retrieval, solid/liquid separation, enhanced solids washing, and evaporation will be studied with emphasis on the requirements of flushing for those processes.

Task 18: Technology Development and Instrumentation Evaluation

- FIU will continue to develop the sectional full-scale mock-up of the DSTs that will allow for the demonstration of robotics/sensor systems from FIU as well as other collaborators. In the up-coming quarter, the refractory channels will be completed and the pipes and tank liners will be installed. Testing of the miniature rover and the peristaltic crawler within mock-up will be conducted and any modifications required for successful operation will be integrated.

- For the mini inspection tool, focus will be on testing the tool in the full-scale sectional mock-up. Efforts will also be allocated to improvement of the cable management system, image quality of the live inspection video streaming, and fine tuning the semi-autonomous operation of the mini inspection tool. System testing with the integrated sensors will also be conducted and the results will be validated at the full-scale mock-up.

Task 19: Pipeline Integrity and Analysis

- For the UT sensors task, the test loop will be assembled according to the final design. Upon assembling the test loop, the Permasense sensors will be mounted on the specified sections of the loop. Finally, the engineering-scale tests will be initiated based on the test plan.
- For the non-metallic materials task, FIU is planning on conducting burst pressure tests on two hose specimens aged at high temperature for 1 year. If the burst pressures are compatible with the baseline, then FIU will attempt to irradiate the other specimens prior to burst pressure testing in order to determine what effect radiation exposure has on the burst pressure of the hoses. FIU also plans to test all of the EPDM dog bone coupons that were aged for 1 year at all three temperatures (100°F, 130°F and 170°F).

Project 2
Environmental Remediation Science and Technology

Project Description

This project will be conducted in close collaboration between FIU and national laboratory scientists and engineers at SRNL, SREL, PNNL and LANL in order to plan and execute research that supports the resolution of critical science and engineering needs, leading to a better understanding of the long-term behavior of contaminants in the subsurface. Research involves novel analytical methods and microscopy techniques for characterization of various mineral and microbial samples. Tasks include studies which predict the behavior and fate of radionuclides that can potentially contaminate the groundwater system in the Hanford Site 200 Area; laboratory batch and column experiments, which provide relevant data for modeling of the migration and distribution of natural organic matter injected into subsurface systems in the SRS F/H Area; laboratory experiments investigating the behavior of the actinide elements in high ionic strength systems relevant to the Waste Isolation Pilot Plant; surface water modeling of Tims Branch at SRS supported by the application of GIS technology for storage and geoprocessing of spatial and temporal data. The following tasks are included in FIU Performance Year 7:

Task No	Task
Task 1: Remediation Research and Technical Support for the Hanford Site	
Subtask 1.1	Remediation Research with Ammonia Gas for Uranium
Subtask 1.2	Investigation on Microbial-Meta-Autunite Interactions - Effect of Bicarbonate and Calcium Ions
Subtask 1.3	Investigation of Electrical Geophysical Response to Microbial Activity in the Saturated and Unsaturated Environments
Subtask 1.4	Contaminant Fate and Transport Under Reducing Conditions
Task 2: Remediation Research and Technical Support for Savannah River Site	
Subtask 2.1	Investigation on the Properties of Acid-Contaminated Sediment and its Effect on Contaminant Mobility
Subtask 2.2	The Synergistic Effect of Humic Acid and Colloidal Silica on the Removal of Uranium (VI)
Subtask 2.3	Humic Acid Batch Sorption and Column Experiments with SRS Soil
Task 3: Surface Water Modeling of Tims Branch	
Subtask.3.1	Modeling of Surface Water and Sediment Transport in the Tims Branch Ecosystem
Subtask 3.2	Application of GIS Technologies for Hydrological Modeling Support
Subtask 3.3	Biota, Biofilm, Water and Sediment Sampling in Tims Branch Watershed
Task 5: Research and Technical Support for WIPP	

Project Wide:

An abstract based on this research was accepted by the Waste Management 2018 Symposium for a poster presentation:

> **Abstract**: 18547
> **Title**: FIU Research on Soil and Groundwater Contamination at DOE's Hanford and Savannah River Sites
> **Authors**: Leo Lagos, Yelena Katsenovich, Elizabeth Hoffman (SRNL), Vicky Freedman (PNNL)

Task 1: Remediation Research and Technical Support for the Hanford Site

Task 1 Overview

Radioactive contamination at the Hanford Site has created plumes that threaten groundwater quality due to downward migration through the unsaturated vadose zone. FIU is supporting basic research into the fate and remediation of radionuclides such as uranium in the vadose zone as a cost effective alternative to groundwater pump and treat technologies. One technology under consideration to control U(VI) mobility in the Hanford vadose zone is a manipulation of sediment pH via ammonia gas injection to create alkaline conditions in the uranium-contaminated sediment. This project also investigates the biodissolution of autunite solids created in sediments after injections of polyphosphate amendments and studies the potential detection of biofilms via the spectral induced polarization method (SIP). Another focus of this project is to investigate the properties of Tc and its compounds under Hanford Site conditions to better understand and predict Tc fate and transport in the subsurface and for designing remedial strategies for this contaminant.

Task 1 Quarterly Progress

Subtask 1.1. Remediation Research with Ammonia Gas for Uranium

An abstract based on this research was accepted by the Waste Management 2018 Symposium for an oral presentation:

> **Abstract**: 18279
> **Title**: Base Treatment for Uranium Immobilization at DOE Hanford's Site
> **Authors**: Hilary Emerson, Silvina Di Pietro, Yelena Katsenovich, Jim Szecsody (PNNL)

During the period of July through September, summer 2016 internship data and FIU batch experimental data were begun to be organized for peer-reviewed publications. There are two ongoing sets of experiments at FIU. These experiments include (1) a series of filtration experiments to quantify the cation exchange capacity of the inorganic minerals and sediments used in experiments both at FIU and during Silvina Di Pietro's 2016 internship at PNNL; and (2) batch experiments to understand U fate and mineral dissolution data for both NaCl and synthetic groundwater under the three base treatments (NaOH, NH_4OH and NH_3 gas).

Cation Exchange Capacity – Summer 2016 Internship Minerals

Table 2-1 provides the cation exchange capacity measured by DOE Fellow Silvina Di Pietro for the minerals that she used for dissolution experiments during her summer 2016 internship as

determined by standard methods developed by the American Standards for Testing and Materials (ASTM) (ASTM D7503-10, 2010).

Table 2-1. Cation Exchange Capacity (CEC) for Minerals Utilized for Summer 2016 Internship Experiments Conducted at Pacific Northwest National Laboratory by DOE Fellow Di Pietro

Mineral	CEC (cmol/kg)
Calcite	2.22
Epidosite	13.1
Illite	17.6
Microcline	10.8
Montmorillonite	9.73
Muscovite	16.2
Quartz	12.9

FIU – Uranium fate following base treatment

Air stripping was conducted on select samples (muscovite, illite, and Hanford sediments in the presence of 7.2 mM NaCl or synthetic groundwater) aged for five months in the presence of 5% NH_3/95% N_2 prior to stripping of NH_3 gas with high purity air at an approximate flow rate of 6 mL/min. Figure 2-1 shows a decrease in pH with respect to the cumulative volume of air injected into the samples. This indicates that removal of ammonia gas occurred although it was slow (occurring over approximately 24 hours).

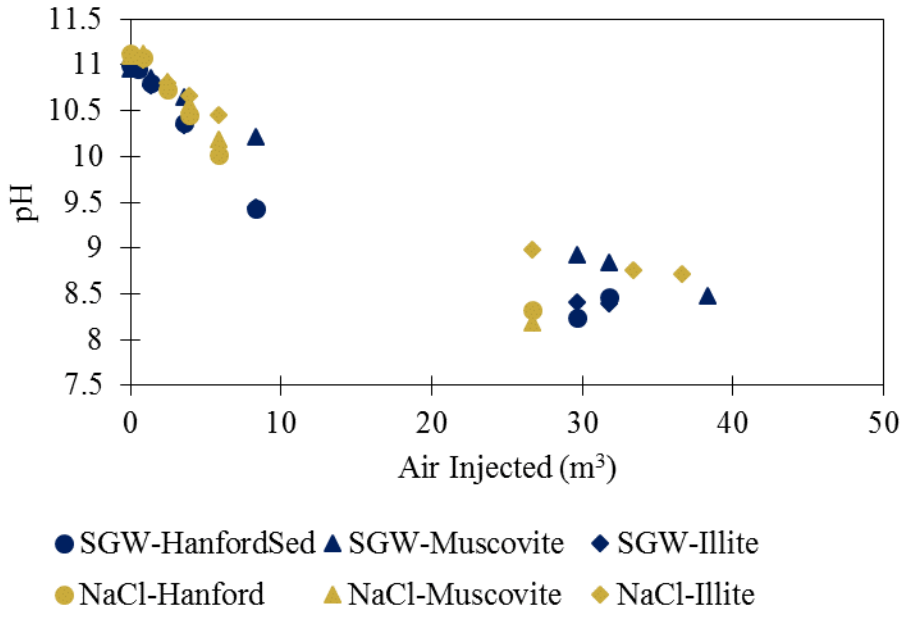

Figure 2-1. Results for pH change with respect to the volume of air injected into 25 mL batch samples (1 g/L mineral concentration) with synthetic groundwater (blue) or 7.2 mM NaCl (yellow).

Overall, the treatment of Hanford sediment, muscovite, and illite samples with NH_3 gas increases the removal of U with respect to the initial natural conditions at pH 7.5 by increasing the pH above 11. Following treatment and aeration, there is a significant removal of U from the minerals

into the aqueous phase. However, this is still representative of significantly greater partitioning coefficients (K_d, mL/g) than initial conditions for synthetic groundwater. For the simpler NaCl background electrolyte, there is a significant increase in K_d's for Hanford sediments but not for the minerals muscovite and illite. For the muscovite mineral, there is an apparent increase in U above the initial mass after five months of treatment and aeration. FIU is currently investigating whether or not this is an experimental artifact or there is natural U within the mineral that was not removed in the previous shorter term experiments.

Table 1-2. Comparison of Partitioning Coefficients (K_d, mL/g) for U to Hanford Sediments, Muscovite, or Illite in the Presence of 7.2 mM NaCl

Note: mass balance discrepancy for five month treatment and aerated muscovite sample

Mineral	K_d (mL/g)			
	Initial, pH 7.5	NH_3 (gas), 3 day	NH_3 (gas), 5 months	After aeration
Hanford Sediment	5±5	5170±970	1109±35	583±32
Muscovite	106±8	370±120	23±1	-486±-27
Illite	910±240	16200±300	5560±60	710±30

Table 2-3. Comparison of Partitioning Coefficients (Kd, mL/g) for U to Hanford Sediments, Muscovite, or Illite in the Presence of Synthetic Groundwater

Mineral	K_d (mL/g)			
	Initial, pH 7.5	NH_3 (gas), 3 day	NH_3 (gas), 5 months	After aeration
Hanford Sediment	2±1	28800±120	59600±700	640±30
Muscovite	1270±200	28500±270	26000±300	3740±180
Illite	140±30	33000±5000	60500±700	1000±50

Reference

1. ASTM D7503-10 Standard Test Method for Measuring the Exchange Complex and Cation Exchange Capacity of Inorganic Fine-Grained Soils, ASTM International, West Conshohocken, PA, 2010, https://doi.org/10.1520/D7503-10

Low Si/Al Experiment

In the month of July, FIU continued a column experiment with the objective of evaluating the relative leaching of uranium from artificially prepared U-bearing precipitates. Two columns were set up for two types of precipitates with the only difference in composition for the concentration of bicarbonate: 3 mM for a "low" concentration of bicarbonate in the precipitate composition for Column 1 and 50 mM for a "high" concentration of bicarbonate in the precipitate for Column 2. The mass of precipitate in each column was 0.5 g with an estimated 70 ug of U present in the precipitate. The following figures show the results of the U dissolved from the continuous flow-through experiment after approximately 35 sample collections.

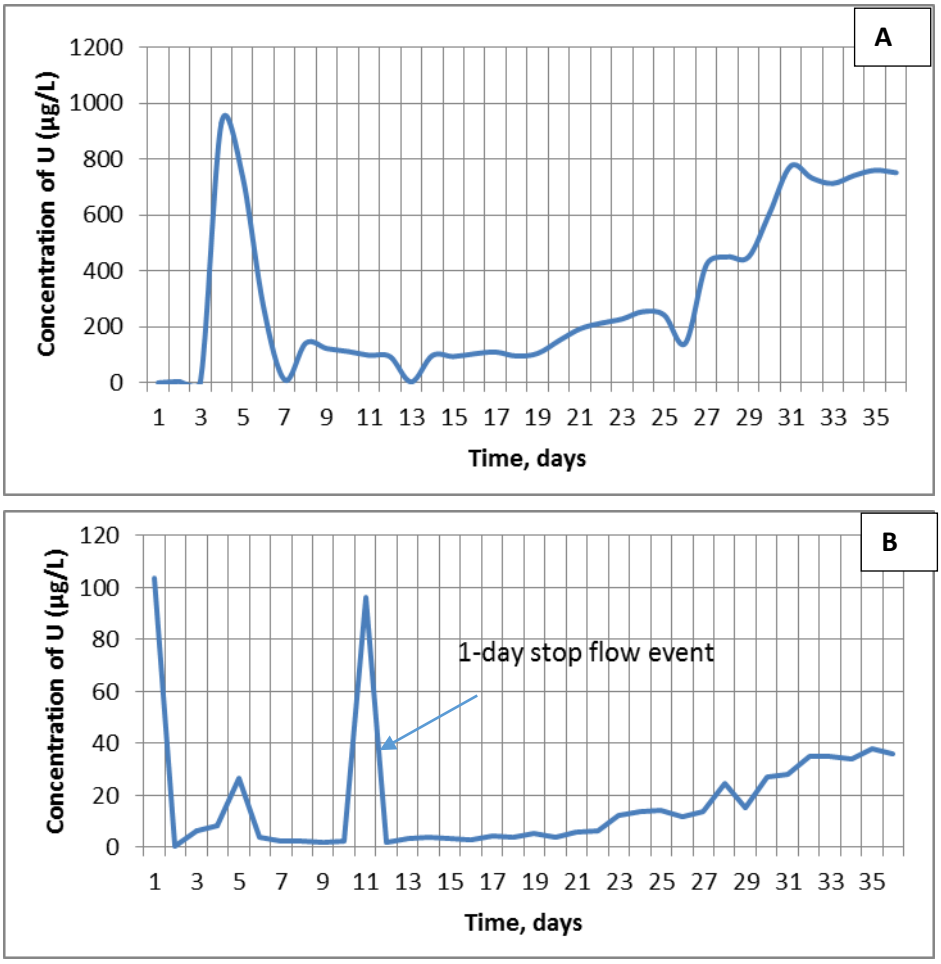

Figure 2-2. Concentration of measured U (ug/L) vs. time (days) from A) column no. 1 (low bicarbonate) and B) column no. 2 (high bicarbonate).

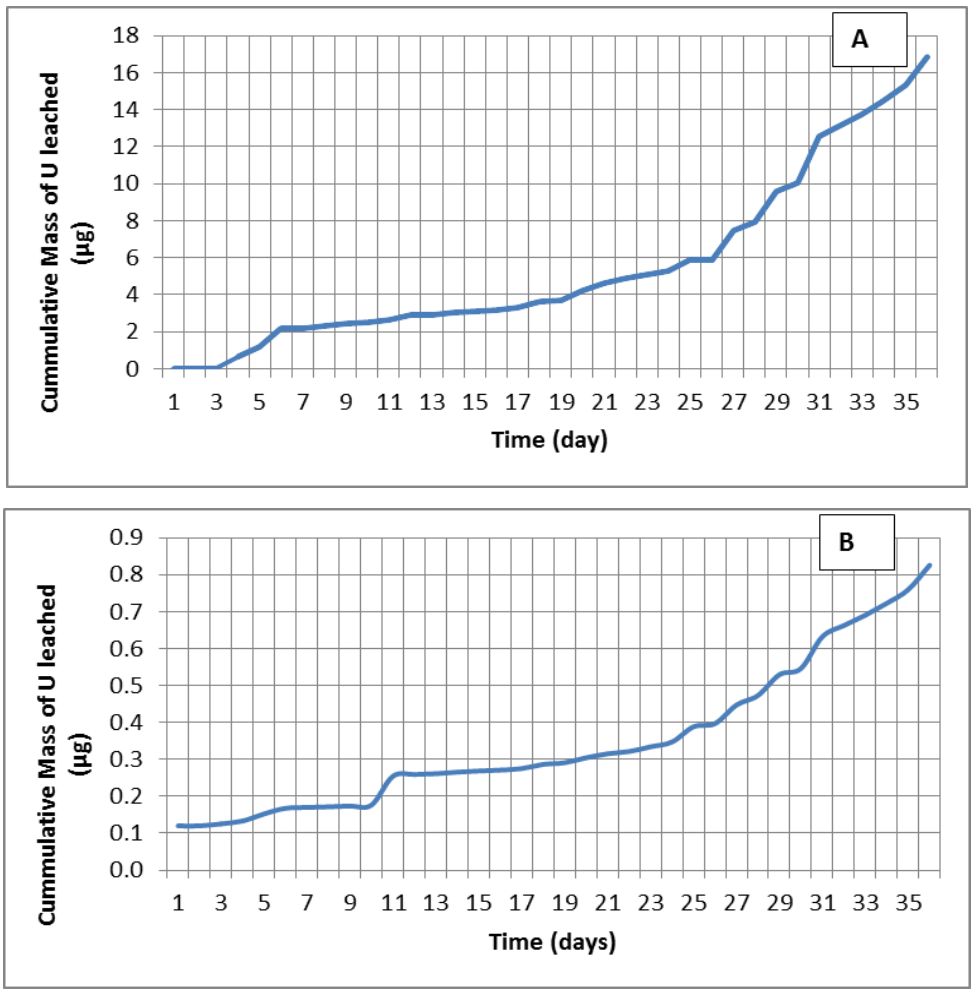

Figure 2-3. Cumulative mass of leached uranium (µg) vs. time (days) from A) column no. 1 (low bicarbonate) and B) column no. 2 (high bicarbonate).

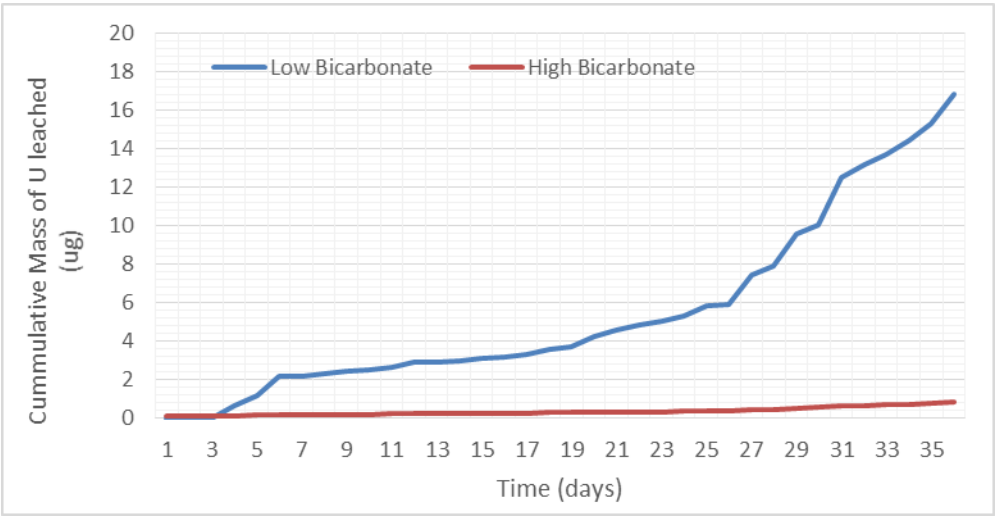

Figure 2-4. Cumulative mass of U in ug from both columns for comparison.

From Figures 2-2, 2-3 and 2-4, it is evident that there is a significantly higher mass of U leached from precipitate samples prepared with low bicarbonate concentration in the composition, up to 18 ug after 35 sample collection events, which is equivalent to 25% of U leached from the solid precipitates, as opposed to only approximately 1 ug leached (2% after 35 sample collection events) from precipitates prepared with high bicarbonate concentrations in the composition. This experiment will be continued to investigate the stability of each precipitate. However, initial results show that, in the presence of low bicarbonate concentrations, the potential leaching from the NH_3-treated samples is higher compared to precipitates formulated using higher bicarbonate concentrations. This experiment with sample collection and uranium analysis of leached uranium is still on-going.

In the month of August, FIU continued a column experiment with the objective of evaluating the relative leaching of uranium from artificially prepared U-bearing precipitates. Additional samples have been collected from two mini-columns that contain precipitates; column 1 represents a "low" concentration of bicarbonate in the precipitate (3 mM of bicarbonate) and column 2 represents a "high" concentration of bicarbonate in the precipitate for (50 mM of bicarbonate). The collected samples were processed for uranium concentration analysis via the KPA instrument and results are pending.

In addition, FIU conducted speciation modeling via the Geochemist Workbench (GWB) version 10.0.04 to predict aqueous speciation and solid phases likely to be saturated for samples amended with calcium or iron prepared at "low" and "high" bicarbonate concentrations. Modeling results were compared to uranium removal data obtained for silica concentrations of 15 mM, Ca of 10 mM, and both "low" and "high" concentrations of bicarbonate in the solution (Figure 2-5).

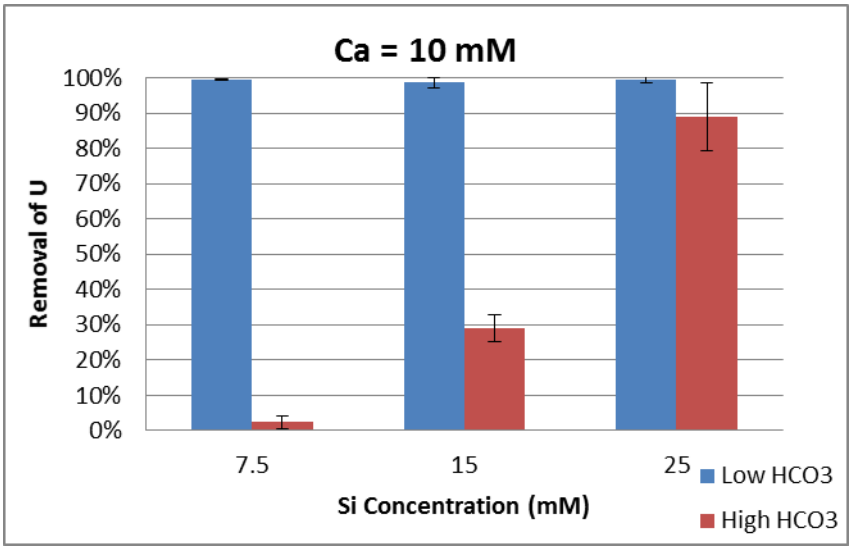

Figure 2-5. Percent removal of U (VI) tested at variable bicarbonate and silica concentrations in solutions amended with 5 mM Al, 2 mg/L U (VI) and 10 mM of Ca.

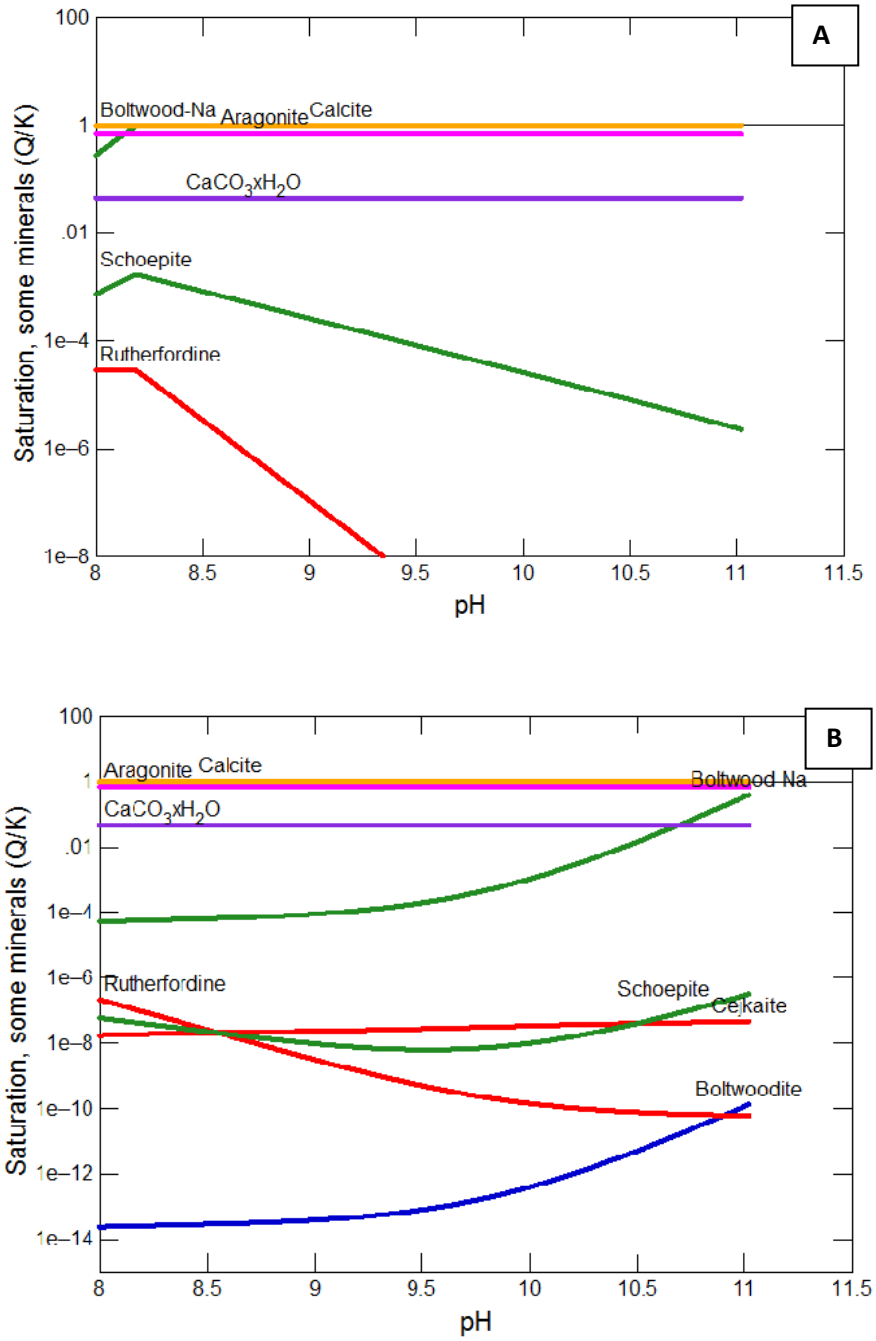

Figure 2-6. Diagrams of saturation indices of uranium-bearing mineral phases plotted as a function of pH. Sample composition includes 15 mM Si, 10 mM Ca and HCO_3^- concentrations of 3 mM (A) and 50mM (B).

Speciation modeling suggested that for the studied range between 7.5 mM and 25 mM, silica concentration has not affected the speciation and the saturation indices of formed minerals. However, there was a noticeable effect of bicarbonate concentration on the formation of solid phases. At "low" bicarbonate concentrations, modeling identified the highest saturation indices for uranyl silicate Na-boltwoodite [$(Na)(UO_2)(HSiO_4)\cdot 0.5H_2O$] and calcium carbonate phases such as aragonite and calcite (Figure 2-6). Apparently, strong complexation of uranium and silica

resulting in the formation of Na-boltwoodite contributed to the higher removal of uranium, on the level of 98-99%, from the solution mixture. At "high" bicarbonate concentration, the system was saturated with calcium carbonate minerals such as aragonite and calcite. Na-boltwoodite was found close to saturation only at pH 11. This suggests that uranium removal is mostly controlled by the co-precipitation with calcite and aragonite at pH conditions from 8 to 10.5; however, as pH increased to 11, Na-boltwoodite at saturation becomes an additional solid phase contributing to the removal of uranium from the solution mixture. The addition of iron into the solution composition resulted in the formation of iron phases such as iron hydroxide and goethite. However, the increase in the concentration of ferric iron from 0.2 mM to 5 mM hasn't affected saturated indices of iron phases. As the speciation diagrams showed (Figure 2-7), the most significant factor affecting the formation of solid phases in the presence of iron was an increase in bicarbonate concentration. At "low" bicarbonate concentrations of 3 mM, solid phases were dominated by the uranyl silicate Na-boltwoodite phases; however, when bicarbonate concentration was increased, the formation of iron phases was predominant, except at elevated 10.5-11 pH conditions when the formation of Na-boltwoodite phases prevailed (Figure 2-7).

In the month of September, FIU continued a mini-column experiment with the objective of evaluating the relative leaching of uranium from artificially prepared U-bearing precipitates. The collected samples were processed for uranium concentration analysis via the KPA instrument and the results are presented below in Figures 2-8 to 2-10. These results of the U release from the continuous flow leach experiment was obtained after approximately 51 collections. This corresponds to approximately two months for the two columns filled with uranium containing precipitates prepared with "low" bicarbonate and "high" bicarbonate concentrations.

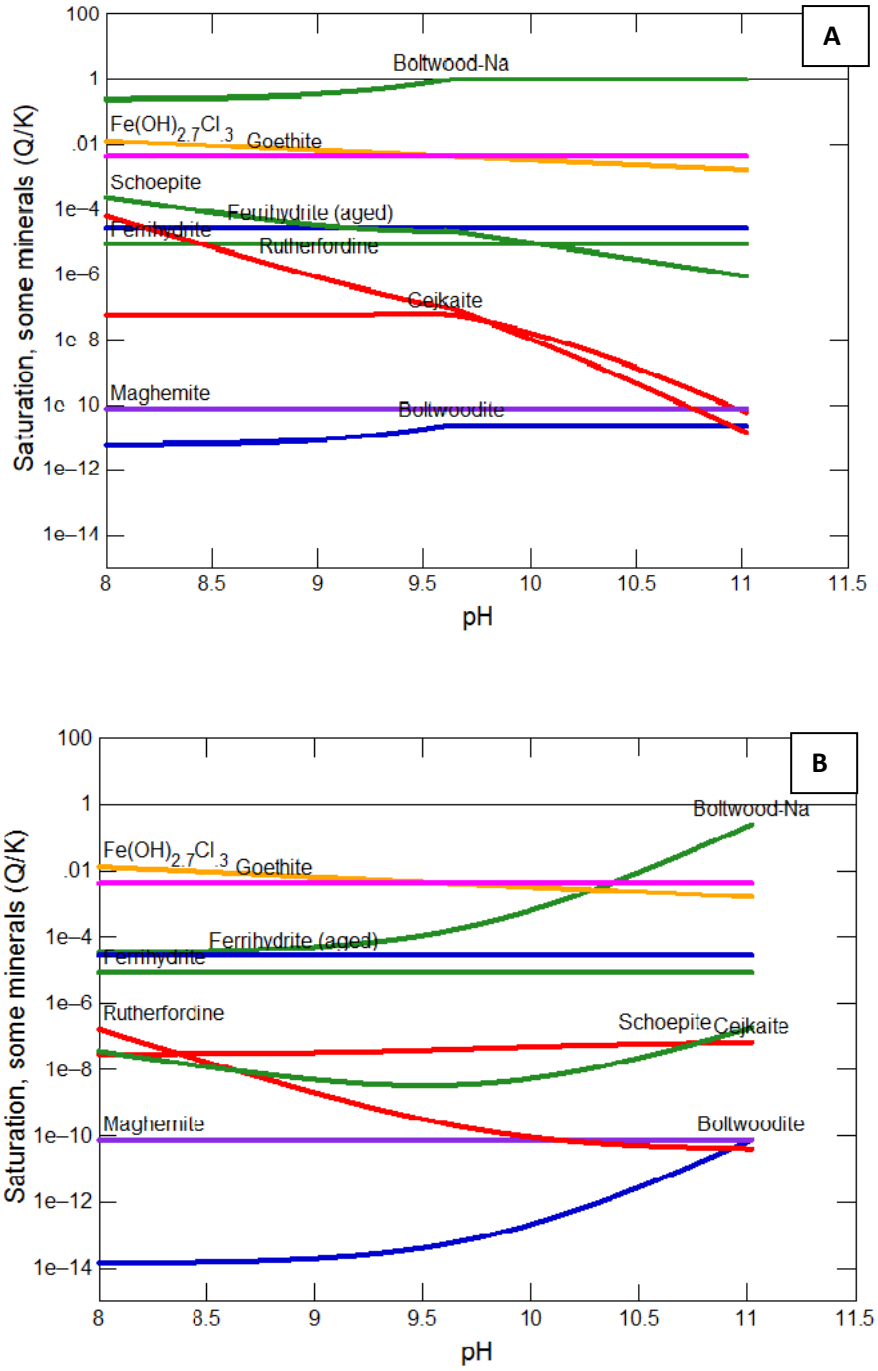

Figure 2-7. Diagrams of saturation indices of some of uranium-bearing mineral phases plotted as a function of pH. Sample composition includes 15 mM of Si and varied HCO_3^- concentrations: (A) 3 mM of HCO_3^-, 0.2 mM Fe or 5 mM Fe and (B) 50 mM of HCO_3^-, 0.2 mM Fe or 5 mM Fe.

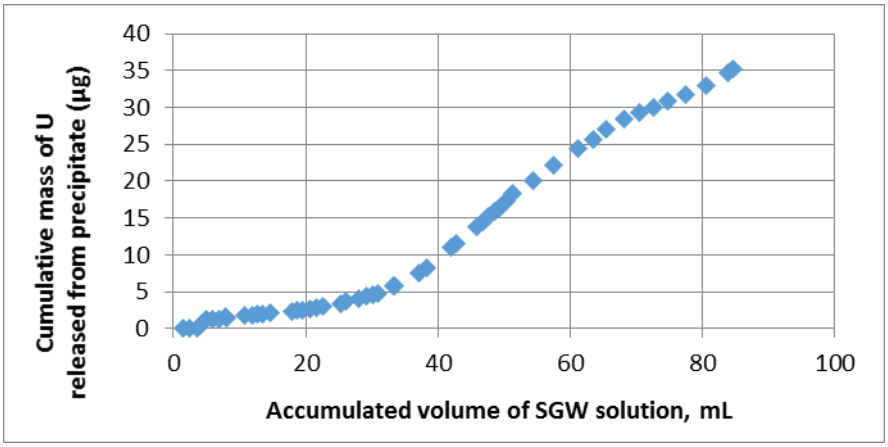

Figure 2-8. Cumulative mass of U in µg released from uranium-bearing precipitate in Column # 1 (Low bicarbonate).

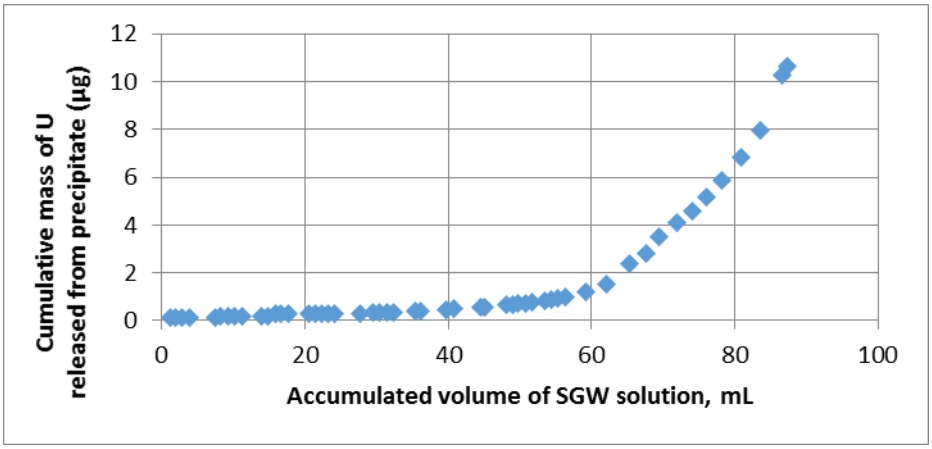

Figure 2-9. Cumulative mass of U in µg released from uranium-bearing precipitate in Column # 2 (High bicarbonate).

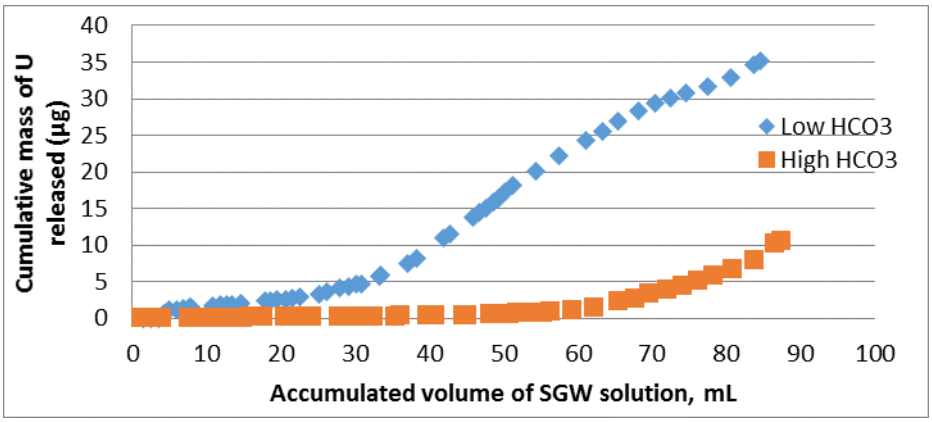

Figure 2-10. Cumulative mass of U in ug released from both columns for comparison.

It is important to note that an estimated 370 ug of U were contained in each column, which corresponds to the 100% of U present. The results show that there is a significantly higher mass of U leached from precipitate prepared with "low" bicarbonate in the samples (i.e., up to 35.2 ug after ~85 mL of SGW solution amended with 3 mM of HCO_3 was injection through the column).

This volume of SGW is equivalent of approximately of 220 pore volumes flowing through column 1 that resulted of 9.5% of U released from the solid precipitates. This is opposed to only approximately 2.6 µg leached (2.87% of U) in the presence of "high" bicarbonate concentrations. Therefore, there is evidence to state that in the presence of "low" bicarbonate concentrations, there is a higher risk of U release potential from the NH_3-treated sediments compared to "high" bicarbonate conditions using SGW solution amended with bicarbonate. In addition, FIU evaluated the analytical results to determine what component concentrations would maximize the fraction of U in the precipitate phase based on the concentrations of U left in the supernatants, or in other words, the U removal efficiency. This relied on the assumption that all uranium introduced to the sample solutions was either retained in solution or precipitated/adsorbed onto the solid phase.

The results of the KPA analysis of the supernatant solutions were visualized using response surface diagrams (Figure 2-11). For this assessment, all test concentrations for calcium bearing samples were evaluated to display the relationship between the two variable concentrations, Ca and HCO_3, and the concentration of uranium in the supernatant phase. The initial concentration of uranium in all experiments was 2212±232 µg/L based on measurements of the control samples prepared in triplicate.

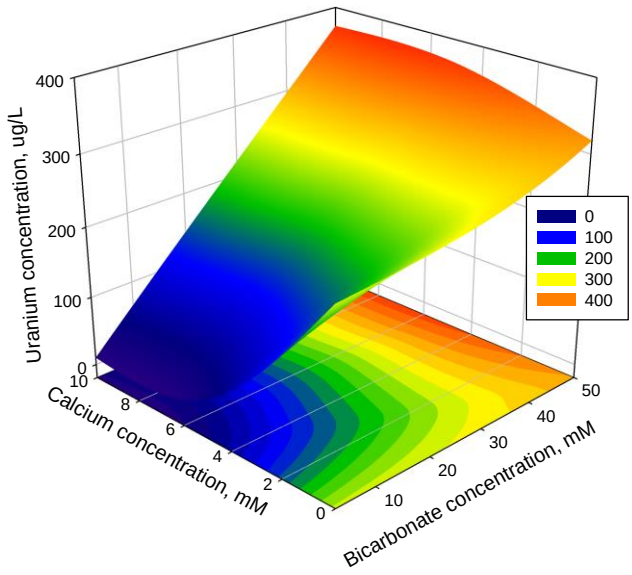

Figure 2-11. Response surface diagrams displaying filtrate solution uranium retention in samples.

The results of the sample set show a clear and demonstrative positive correlation between the increasing concentration of bicarbonate in synthetic pore water solutions and the concentration of uranium in the post-treated supernatant solution. This finding suggests that with increasing sample bicarbonate concentration, the amount of uranium in the precipitate decreases. It is therefore safe to conclude that the high bicarbonate samples would be least likely to precipitate the uranium analyte.

This observed trend of uranium in the supernatant solutions increasing with added bicarbonate is likely indicative of the formation of highly soluble uranyl carbonates. In contrast, the trends in

Figure 2-11 shows that low bicarbonate samples have the least uranium remaining in the supernatant solutions and, therefore, have the most in the precipitate phase. This may be explained by the formation of uranyl silicates, which are relatively stables in the solid phases.

Additionally, there is a correlation between the increasing calcium concentrations in the sample solution and the concentration of uranium in the supernatant. The increasing calcium is associated with a decrease of uranium concentration in solution and an increase in the uranium precipitated. It is hypothesized that the increase in calcium could favor the removal of uranium due to the co-precipitation with less soluble solids, such as calcium carbonates or calcium silicates, which could serve as nucleation sites, provoking Si polymerization reactions and precipitation of silica (Iler, 1979). Precipitated silica and calcium carbonate solid phases could lead to co-precipitation of uranium. In fact, considering the concentration of U injected as 2000 µg/L, the U precipitation/removal efficiencies from the aqueous phases ranged between 75-98%; the higher percentage was accounted for in samples containing 10 mM of Ca and low in bicarbonate.

Note that this subtask on Si/Al experiments is ending and will not be continued as FIU Performance Year 8 scope.

Reference

Smith and Szecsody, 2011. Influence of contact time on the extraction of 233uranyl spike and contaminant uranium from Hanford Site sediment. Radiochim. Acta 99, 693–704.

SEM-EDS imaging of Hanford sediments treated with U and NH_3 gas

SEM was conducted at the Florida Center for Analytical Electron Microscopy (FCAEM) at FIU MMC campus. A total of nine samples were taken to the facility to examine and analyze for morphology, particle size, and elemental composition using a scanning electron microscope with energy dispersive spectroscopy (SEM-EDS). Table 2-4 details the conditions of the samples prior to preparation for microscopy. All samples were washed with pH-adjusted distilled deionized (DDI) water prior to drying and prep on SEM studs. Figures 2-12 to 2-14 show representative images and EDS collected at 24 Pa vacuum pressure with an X-ray beam energy of 15 keV for the Hanford sediments. The EDS detector was used to conduct spot analysis on bright veins, precipitates, and pools with the exception of the location depicted in Figure 2-12D. Backscatter detection mode was utilized to allow for the heavier elements to appear brighter in order to search for particles and minerals associated with U.

Table 2-4. Uranium-Spiked Minerals (except control samples) and Treated Conditions

Mineral	Condition	Uranium (500 ppb) + NH_3 gas
Illite	Dry control (neither U nor base treatment)	
	7.2 mM NaCl solution	✓
	Synthetic GW	✓
Muscovite	Dry control (neither U nor base treatment)	
	Synthetic GW	✓
	7.2 mM NaCl solution	✓
Hanford Sediments	Dry control (neither U nor base treatment)	
	Synthetic GW	✓

Figure 2-12 represents four SEM-EDS analysis points from control Hanford sediments with neither U addition nor ammonia gas treatment. Elemental analysis data for Figure 2-12 reported U concentrations below detection limits with the exception of Figure 2-12C. However, the concentration is 0.037 wt% above the method detection limit (MDL), reported as 0.360 (Table 2-5 and 2-6). Therefore, these results are likely not significantly greater than the detection limits. Figure 2-13 represents three different SEM-EDS images of Hanford sediments in the presence 500 ppb U and a background electrolyte of 7.2 mM. As in Figure 2-12, MDL values for Figure 2-13 samples were higher than the measured U concentration. Thus, general conclusions about the minerals with which U is associated following NH_3 gas treatment cannot be formulated.

Figure 2-14 represents four different SEM-EDS images of Hanford sediments in the presence of synthetic groundwater solution and U. The U measurements are provided in Table 2-7. Unlike Figures 2-12 and 2-13, U measurements for synthetic groundwater (SGW) samples are above the detection limits. From batch experiments, the initial U loadings were estimated at 457 ppm for Hanford sediments with the synthetic groundwater solution based on aqueous phase measurements (Table 2-7). When comparing post-treatment U loadings, U concentration is significantly higher for the pools analyzed by point EDS (six times greater for Figure 2-12J and 36 times for Figure 2-12H and Table 2-6). This suggests that U was concentrated in the precipitates formed on the surface of the minerals in the SGW samples.

In addition, the lack of U detection for the NaCl electrolyte could demonstrate that bulk U loading was evenly distributed throughout the surface and, therefore, below detection limits based on estimated loadings. In other words, U likely adsorbed across the mineral's surface. It is expected that co-precipitation processes are more likely to control U in the sediments treated with NH_3 gas in synthetic groundwater (Figure 2-14). Geochemical speciation modeling presented in previous monthly reports suggests that the system would be saturated with respect to calcite at elevated pH in the synthetic groundwater. Zheng and collaborators also previously reported secondary Ca-Mg mineral phases forming at elevated pH in Hanford sediments (Zheng et al., 2008). This can be further correlated to the EDS results for point analyses presented in Figure 2-14. Based on the four measurements collected, there is a slightly positively correlated

relationship with Ca but not with Al and Si content (Figure 2-15). More data will be gathered to confirm or refute this relationship.

For the three conditions observed, Ca values were in the range of 1.14 to 7.36 wt% (with three exceptions: Figures 2-12C, showing a significantly higher value of 45.4 wt% and Figures 2-14J and 3K, showing values close to the MDL). Although these values are highly variable, they highlight that there is a significant amount of Ca naturally present in the Hanford sediments. Further, this is consistent with previous characterizations of Hanford sediments, predicting up to 5% calcite in the bulk phase (Serne et al., 2008; Zheng et al., 2008).

Table 2-8 provides the detected concentrations of Ca, Al and Si and their detection limits for all images presented in this report. Although the instrumentation provided elemental analysis on various elements, significant focus is given on these elements as they represent possible secondary neophases on the minerals and sediments under study (Table 2-4) and are a significant fraction of the natural sediments (Qafoku et al., 2011; Serne et al., 2008).

The morphology of the control sediments includes smaller precipitates (similar to Figure 2-12B) and veins (similar to Figure 2-12C) that are brighter and consistent with heavier elements due to the use of the backscatter detection mode for analysis. EDS analysis shows that the bright spots (small, round particles) are consistent with Fe-Ti minerals (Figures 2-12A-C and 2-13E, G) and veins are largely composed of calcium, suggesting potential calcite precipitates. It must be noted that when spot analysis was selected on the background 'dark' surface (Figure 2-12D), the Ti concentration was only 0.988 wt% (Table 2-5).

Like the control samples, the morphology of NaCl-treated samples also contains smaller precipitates. Because both NaCl and control samples show elevated concentrations of Ti and Fe within the small, round precipitates, it is suggested that these minerals are naturally present and not significantly solubilized by the ammonia gas treatment. It is important to note that the high Ti concentration is likely contributing to the brightness of these particles and not U as there is no U detected above MDL limits. However, further analysis needs to be conducted to understand the potential Fe-Ti changes with ammonia gas treatment and to gather more SEM-EDS images from both surface background and bright spots.

The morphology of SGW-treated samples shows larger precipitates or pools of particles than Figures 2-12 and 2-13. The absence of small, round, bright particles in SGW samples may be hidden due to the greater brightness or contrast of the heavier U-bearing precipitate particles that appear to be forming on the surface. However, further analysis is needed to compare particle size, morphology, and elemental analysis for each treatment with similar magnifications and a statistically representative sampling of locations by EDS.

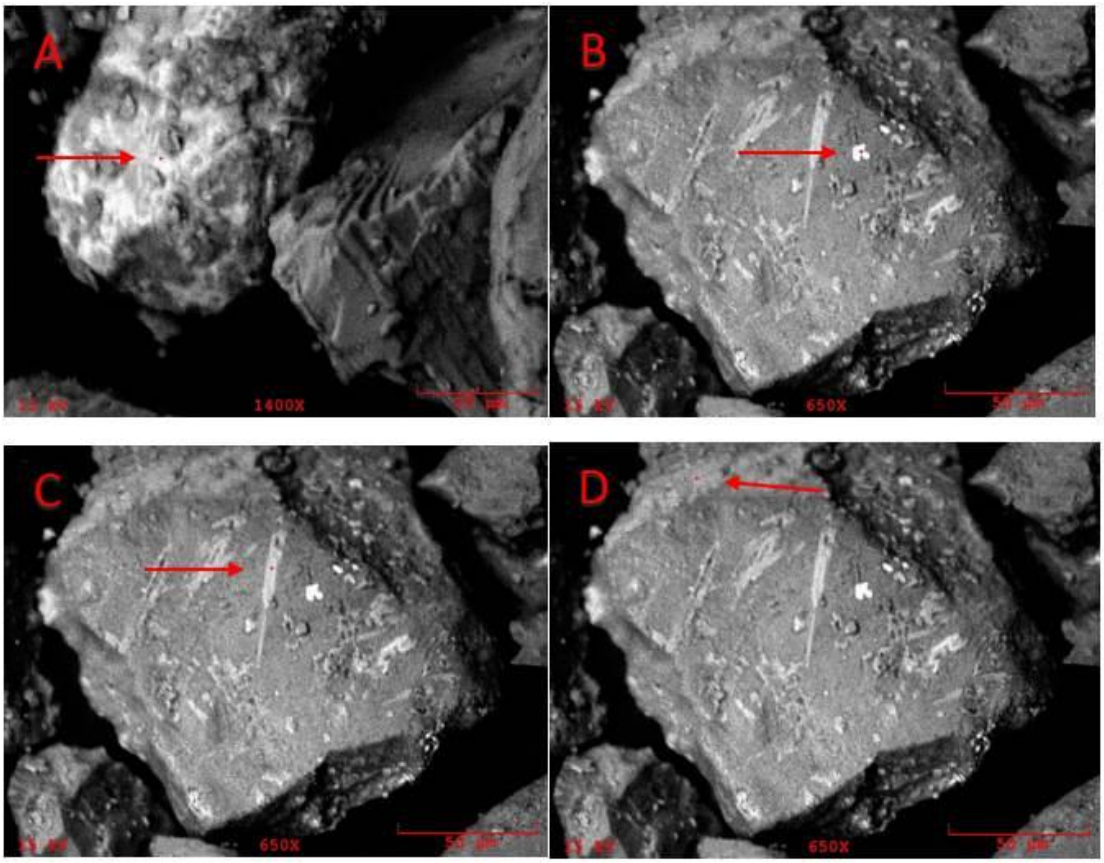

Figure 2-12. Representative SEM images with magnification of 1400x for A and 650x for B-D for Hanford sediment controls without base treatment. The red dot represents the location where elemental analysis was taken on the mineral's surface via energy dispersive x-ray spectroscopy (EDS).

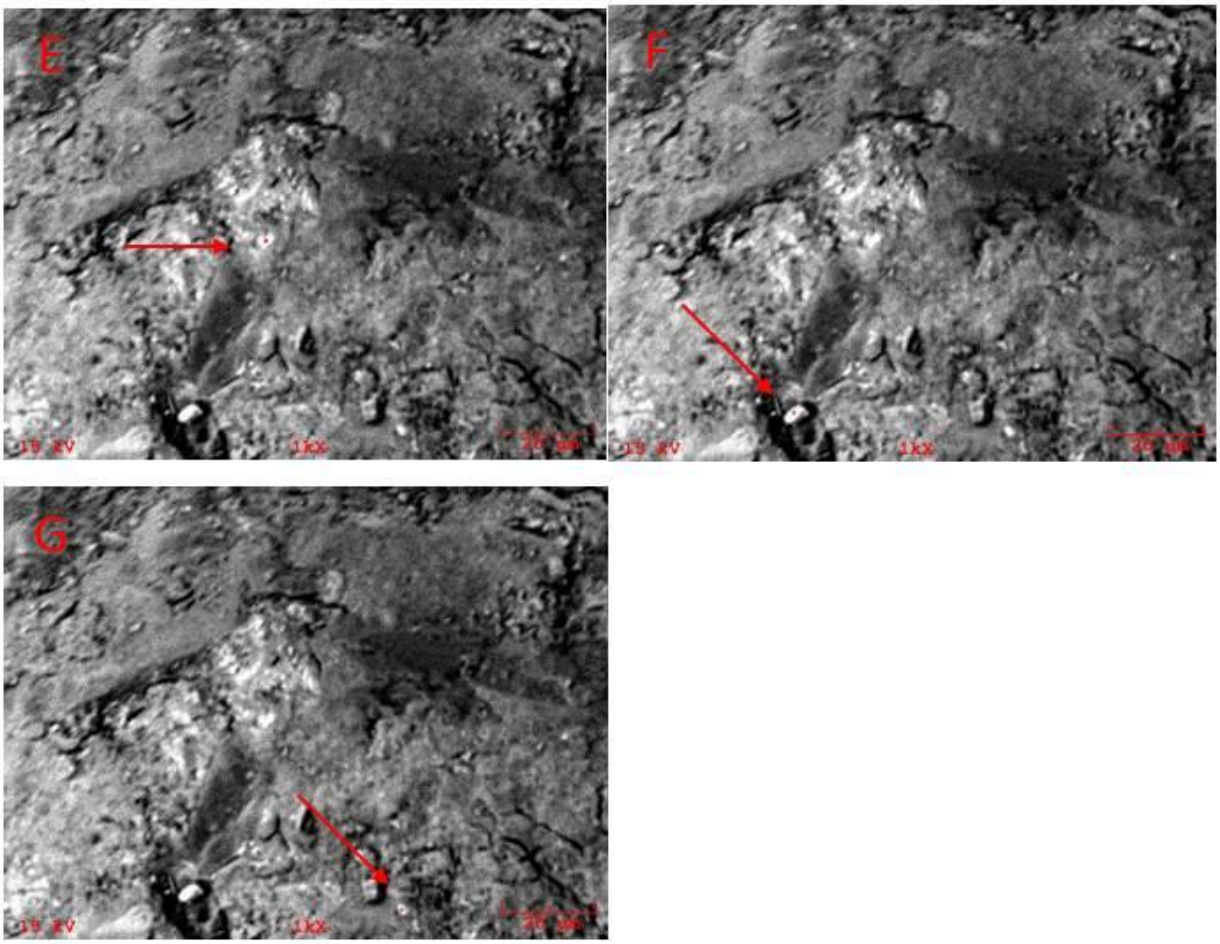

Figure 2-13. Representative SEM images with a magnification of 1000x for Hanford sediment in 7.2 mM NaCl treated with NH_3 gas for approximately five months in the presence of 500 ppb U. The red dot represents the location where elemental analysis was taken on the mineral's surface via EDS.

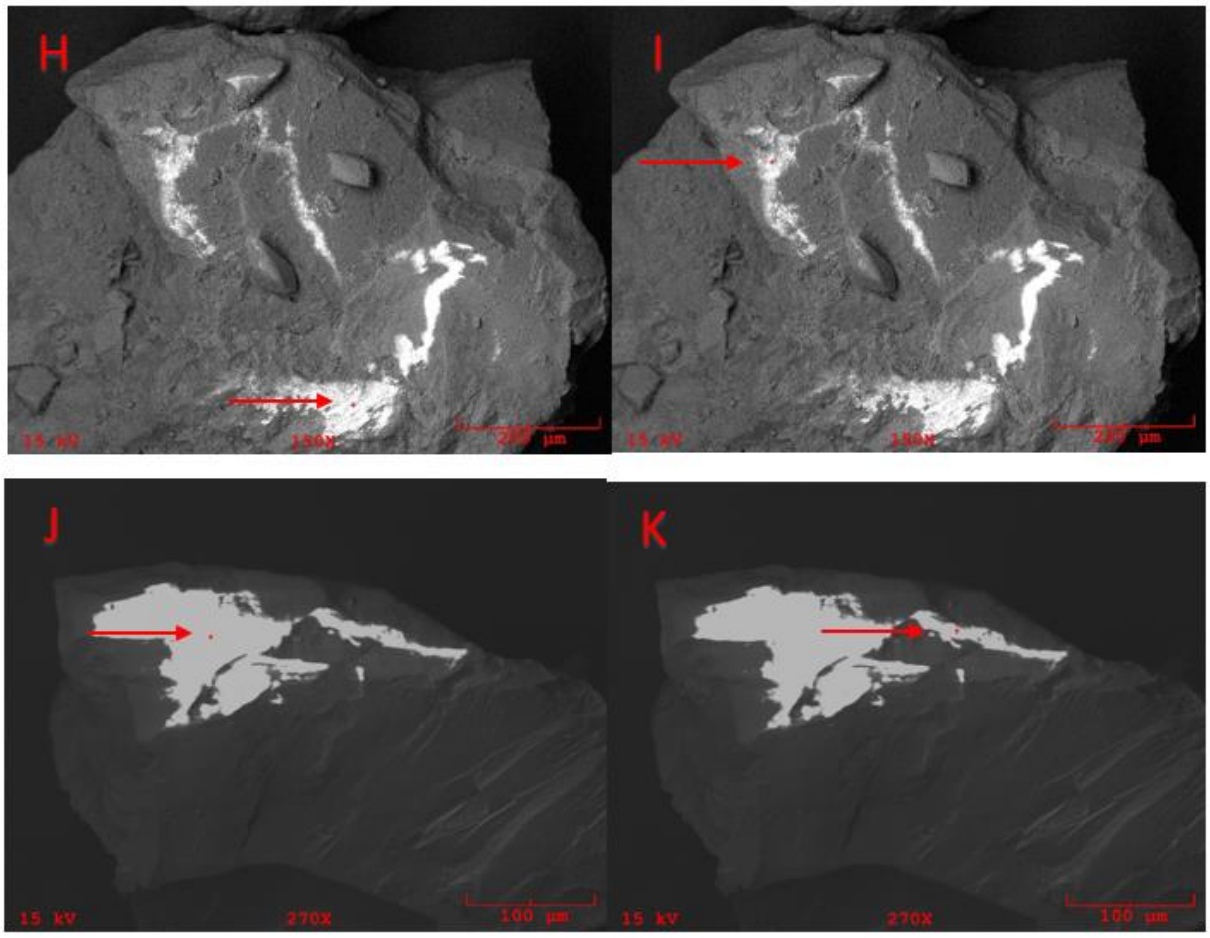

Figure 2-14. Representative SEM images with magnification of 150x for H and I and 270x for J and K for Hanford sediment in synthetic groundwater (SGW) solution treated with NH_3 gas for five months in the presence of 500 ppb U. The red dot represents the location where elemental analysis was taken from the mineral's surface.

Table 2-5. Fe and Ti Reported Concentrations and their MDL (wt %) for the SEM-EDS Images Presented in Figures 2-12 and 2-13 (Note: No EDS Ti measurement was taken for Figure 2-12C)

		Fe (wt%)	MDL (wt%)	Ti (wt%)	MDL (wt%)
Figure 2-12	A	39.1	0.318	34.8	0.185
	B	54.9	0.542	12.9	0.297
Control	C	4.91	0.309	-	-
	D	26.8	0.306	0.988	0.176
Figure 2-13	E	41.9	0.146	11.2	0.146
	F	8.66	0.254	55.3	0.156
NaCl	G	40.3	0.253	12.7	0.152

Table 2-6. U Reported Concentrations (wt% and ppm) for the EDS Analysis for Hanford Sediments Treated with NH_3 Gas in the Presence of Synthetic Groundwater and 500 ppb U from Figure 2-14

		U (ppm)	U (wt%)	MDL (wt%)
Figure 2-14	H	16,700	1.67	0.675
	I	5,590	0.559	0.322
SGW	J	2,750	0.275	0.190
	K	3,790	0.379	0.204

Table 2-7. Initial Uranium Loadings for Treated Minerals Exposed to 500 ppb U and 5% NH_3/95% N_2 Gas for Five Months in the Presence of NaCl or SGW Background Electrolyte

Sample ID	Solid (µg/g)
NaCl-Hanford	260±8
NaCl-Muscovite	11.4±0.4
NaCl-Illite	399±5
SGW-Hanford	457±5
SGW-Muscovite	481±5
SGW-Illite	461±5

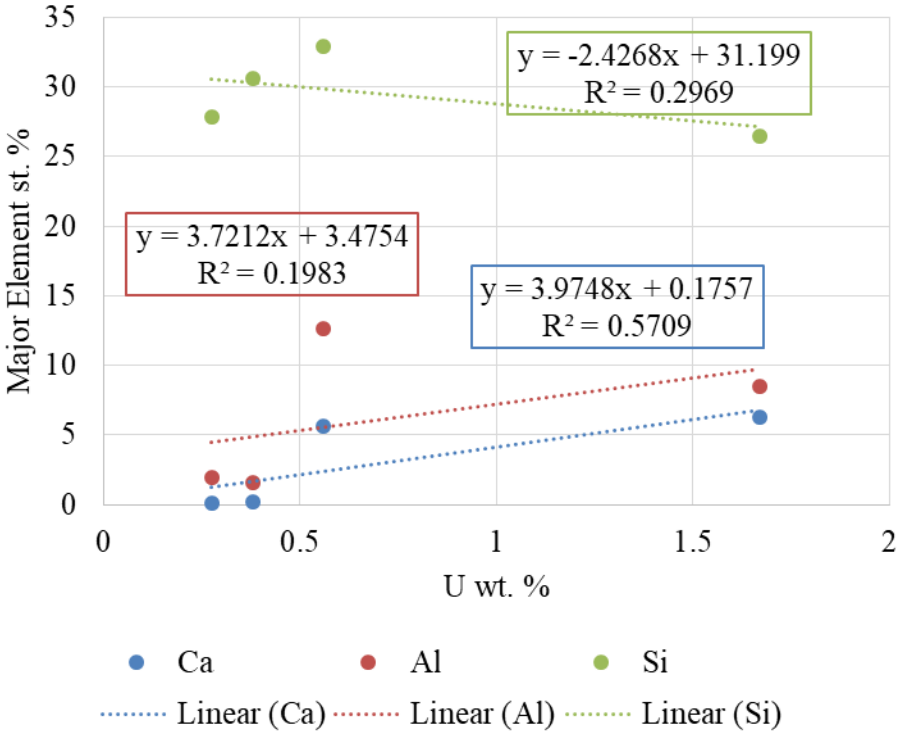

Figure 2-15. Comparison of the correlation between major elements and U content in Hanford sediments treated with ammonia gas in the presence of synthetic groundwater.

Table 2-8. Ca, Al and Si Reported Concentrations and their MDL (wt%) for the SEM-EDS Images Presented in Figures 2-12 to 2-14

		Ca (wt%)	MDL (wt%)	Al (wt%)	MDL (wt%)	Si (wt%)	MDL (wt%)
Figure 2-12	A	1.14	0.135	5.37	0.150	15.48	0.138
	B	1.98	0.259	6.89	0.281	17.82	0.265
Control	C	45.42	0.156	4.31	0.135	14.1	0.129
	D	7.36	0.149	5.50	0.152	46.6	0.14
Figure 2-13	E	4.48	0.118	9.25	0.119	25.9	0.113
	F	2.12	0.114	8.82	0.122	19.4	0.117
NaCl	G	1.99	0.124	9.73	0.122	27.3	0.119
Figure 2-14	H	6.26	0.207	8.49	0.117	26.5	0.124
	I	5.67	0.094	12.66	0.069	32.9	0.072
SGW	J	0.061	0.049	1.90	0.061	27.8	0.540
	K	0.171	0.053	1.58	0.067	30.6	0.059

During the month of September, solid phase characterization continued for select minerals aged in the presence of ammonia gas with uranium for three months and then re-equilibrated with air for thirty days to mimic the transient conditions during and after gas treatment. In addition, larger masses of clean minerals and sediments were treated in a similar manner for future characterization (including but not limited to BET, SEM-EDS, FTIR, and XRD). Progress also continued towards publications based on previous results for minerals treated with NaOH, NH_4OH or NH_3 gas. Finally, the scope of work for this subtask for FIU Performance Year 8 was finalized in conjunction with Dr. Jim Szecsody with a focus on the adsorption and co-precipitation processes of U on minerals following treatment.

Future efforts will include solid phase characterization of minerals and sediments before and after ammonia gas treatment to identify potential mineral transformations and uranium fate. A publication based on the work conducted in FIU Performance Year 7 is also being developed.

References:

Qafoku, N., Szecsody, J.E., Arey, B.W., Gartman, B.N., Zhong, L., and Truex, M.J. (2011). Subsurface solid and liquid phase interactions under NH_3 gas induced alkaline conditions: Moisture content (solid: solution) controls on aqueous elemental concentrations. Unpublished manuscript, Richland, WA.

Serne, R.J., Last, G.V., Gee, G.W., Schaef, H.T., Lanigan, D.C., Lindenmeier, C.W., Lindberg, M.J., Clayton, R.E., Legore, V.L., Orr, R.D., 2008. Characterization of vadose zone sediment: Borehole 299-E33-45 near BX-102 in the B-BX-BY waste management area. Pacific Northwest National Laboratory, Richland, WA.

Zheng, Z, Zhang, G., and Wan, J. (2008). Reactive transport modeling of column experiments on the evolution of saline–alkaline waste solutions. *Journal of Contaminant Hydrology, 97*(1-2), 42; 42-54; 54.

Subtask 1.2. Investigation on Microbial-Meta-Autunite Interactions – Effect of Bicarbonate and Calcium Ions

FIU completed preparations for the natural autunite dissolution experiments in the presence of consortia culture enriched at PNNL and initiated sampling of the sacrificial vials containing 18 mg of autunite mineral. In total, sixty sacrificial 20-mL glass scintillation vials were prepared for the experiments to have 20 vials for about 17 sampling events for each bicarbonate concentration. The vials were amended with 10 mL of sterile media solution containing 0, 3, and 10 mM $KHCO_3$. Three vials from each set were left abiotic, which will be sampled in parallel with biotic samples by extracting 0.2-0.3 mL for each sampling event. The reduction in volume for abiotic vials will be no more than 10%. After equilibration with the leaching solutions, the vials were inoculated with bacteria consortia obtained from PNNL. A consortia culture enriched at PNNL was kept frozen at -80^{o}C in 50% glycerol and then grown on sterile hard and liquid media prepared with 250 mg/L of tryptone, 500 mg/L of yeast extract, 0.024M of sodium lactate (3.4 mL of 60% (w/w) sodium lactate syrup), 0.6 g/L $MgSO_4 \cdot 7H_2O$, and 0.07 g/L $CaCl_2 \cdot 2H_2O$ (TYL). Hard media required an addition of 15.0 g/L of agar. The concentration of sodium lactate in the growth media was the same as was included in the sterile media amended by bicarbonate to conduct the biodissolution experiments. All prepared samples are being kept in an anaerobic glove box filled with nitrogen gas. Cell counting of the inoculating culture before inoculation was conducted by means of a hemocytometer using a light microscope. Samples were inoculated with the consortia culture at the level of log 6 cells/mL after three weeks of equilibration. The inoculated samples are sacrificed to collect aliquots for various analysis twice a week according to the sampling schedule. The oxidative-reduction potential (Hannah Instruments redox electrode) and the pH (Orion™ 9110DJWP double junction pH electrode) were recorded inside the glove box for each sample at the beginning of a sampling event. Redox readings were made using the Ag/AgCl reference electrode. The procedures also include filtering the 0.5 mL aliquot collected from the vials' supernatant through a PTFE 0.2 μm filter. Acidified filtered aliquots will be stored at 4°C for chemical analysis. Chemical analysis will include the determination of Ca and P by means of ICP-OES and measurements of U by means of KPA. Subsequently, aliquots are being isolated for the determination of cell viability on agar plates. The plates are incubated at 30°C to count the viable colonies. Sampling also includes collection of cell suspensions for future protein content analysis by means of a bicinchoninic acid assay. The cell suspension is stored at -20°C for future protein content analysis by means of a bicinchoninic acid assay.

In the month of August, FIU continued sampling from the remaining sacrificial vials containing autunite mineral inoculated with the consortia culture on the level of log 6 cells/mL. Inoculated samples were sacrificed to collect aliquots for various analyses twice a week according to the sampling schedule. Results from the sampled vials and plate cultures to this point are provided below. So far, the oxidation-reduction potential (ORP) of the samples fluctuated within the same ranges across all concentrations, but there is some tendency for the ORP values to decrease (2-15). The pH of the samples have stayed relatively constant. The cell viability in the samples has also stayed relatively constant across all concentrations but a peak can be seen at 10 days after inoculation. After this, it seems as if the cell viability of the samples stabilizes.

In the month of September, FIU continued sampling from the remaining sacrificial vials containing autunite mineral inoculated with the consortia culture on the level of log 6 cells/mL. Inoculated samples are sacrificed to collect aliquots for various analysis twice a week, in

accordance with the established sampling schedule. Aliquots for all of the samples collected so far have been processed for wet and dry ashing. The 0.5-mL filtered samples that were taken in the anaerobic glove box using a 1-mL syringe and a 2.0-uL filter were taken from the laboratory refrigerator for wet and dry ashing. Wet digestion was performed by the addition (0.5 mL of each) of concentrated nitric acid (HNO_3) and concentrated hydrogen peroxide (H_2O_2) to each vial. The vials were placed on a heating plate until all the solution present was evaporated and a white solid precipitate was present. During the process, some samples turned yellow or brown so additional peroxide was added and the process was continued until a white precipitate was obtained. The dry samples were then placed in a furnace preheated to 450°C for 15 min and then allowed to cool at room temperature. Precipitates obtained in the drying step will be dissolved in 1 mL of 2 mol/L nitric acid and analyzed by the kinetic phosphorescence analysis (KPA) instrument to determine uranium concentrations released into the aqueous phase as a function of time. Chemical analysis will also include the determination of Ca and P by means of ICP-OES. Some autunite samples were prepared for SEM-EDS analysis. Samples were filtered and then treated with 4 ml of 2% glutaraldehyde in 0.1 M HEPES at 4°C for 2h. Samples were then centrifuged, the supernatant was decanted and the material was washed with 4 mL of 0.05 M HEPES for 10 min. After discarding the supernatant, the material was dehydrated in 4 consecutive steps: treatment with 35%, 70%, 90% and 100% of ethanol for 10 min at room temperature. Viable cells were counted by plating on the petri dishes.

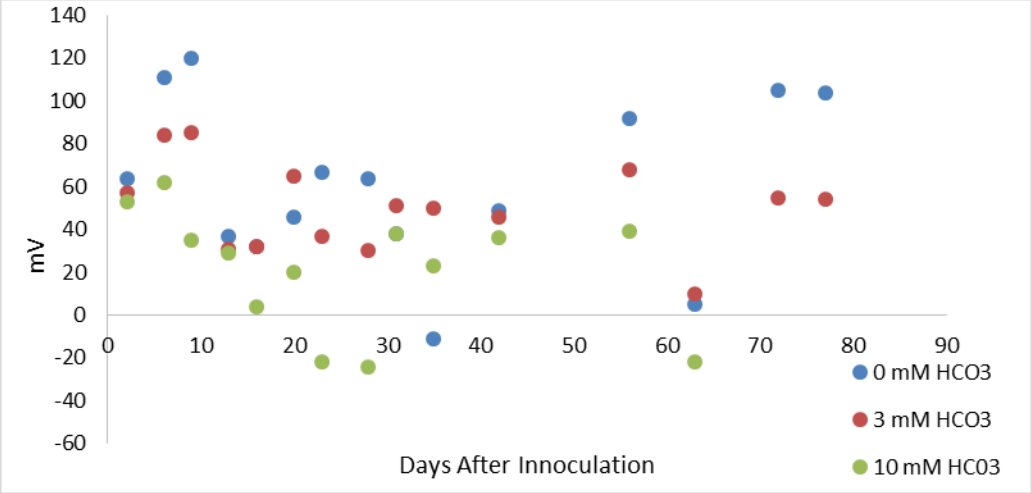

Figure 2-16. Oxidative-reduction potential (ORP) of samples.

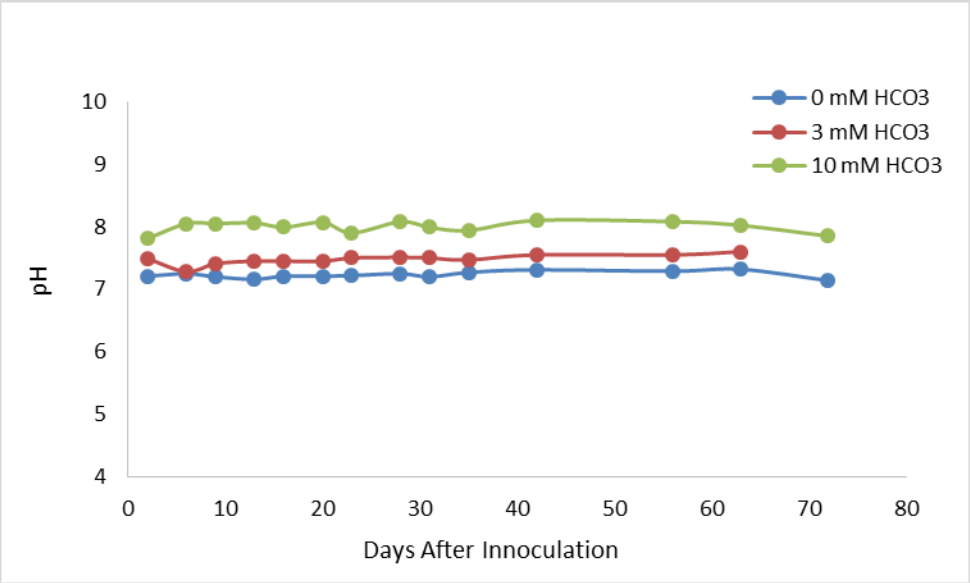

Figure 2-17. Changes in sample pH.

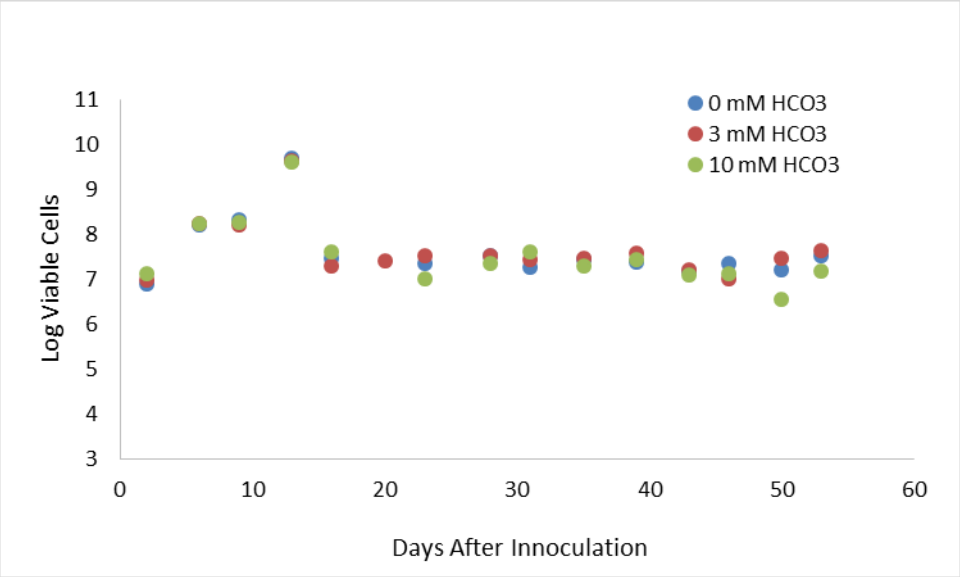

Figure 2-18. Total viable cells measured from plates.

In addition, a carryover scope was developed for this task that will focus on the chemical analysis of the collected samples, protein content in cells and microscopy analysis of post dissolution autunite solids. Note that this task is ending and will not be continued as FIU Performance Year 8 scope.

Subtask 1.3. Investigation of Electrical Geophysical Response to Microbial Activity in the Saturated and Unsaturated Environments

An abstract based on this research was accepted by the Waste Management 2018 Symposium for an oral presentation:

Abstract: 18440
Title: Evaluating the Effects of Microbes on Autunite Dissolution and the SIP Response in Hanford Sediment
Authors: Alejandro Garcia (DOE Fellow), Brady Lee, Yelena Katsenovich.

During July 2017, graduate student Alejandro Garcia successfully defended his thesis proposal titled, "Spectral Induced Polarization Response of Biofilm Formation in Hanford Vadose Zone Sediment." Alejandro also submitted abstracts for the 2017 American Geophysical Union annual conference in New Orleans and for the student poster competition session at the Waste Management 2018 Symposia in Phoenix. Both abstracts present results conducted in collaboration with PNNL researchers.

A scanning electron microscope (SEM-EDS) was used to analyze soil samples collected from columns 1 and 2 in order to search for the presence of biofilm. Six sediment samples were taken at different heights from the columns by removal of the sampling ports and prepared for the SEM/EDS analysis. Biofilm formation or presence of microorganisms was not visible via SEM (Figures 2-19 and 2-20). This may be due to the fact that columns 1 and 2 were only actively running for approximately 1 month, which may be not enough time for the development of biofilm by anaerobic bacteria that grow very slowly. Future SEM-EDS analysis to determine the presence of biofilm will use soil samples extracted from columns 5 and 6 that were in operation for a longer period of time (about 4 months).

Uranium was detected at the background level by the EDS analysis. This is likely due to a lack of data points since U is present in pore water samples and was added at the start of the experiments.

The fall 2016 pore water samples are currently being prepared for uranium analysis via KPA. The procedure for the preparation of these samples is the same as was used for the spring 2017 samples by following wet and dry ashing procedures.

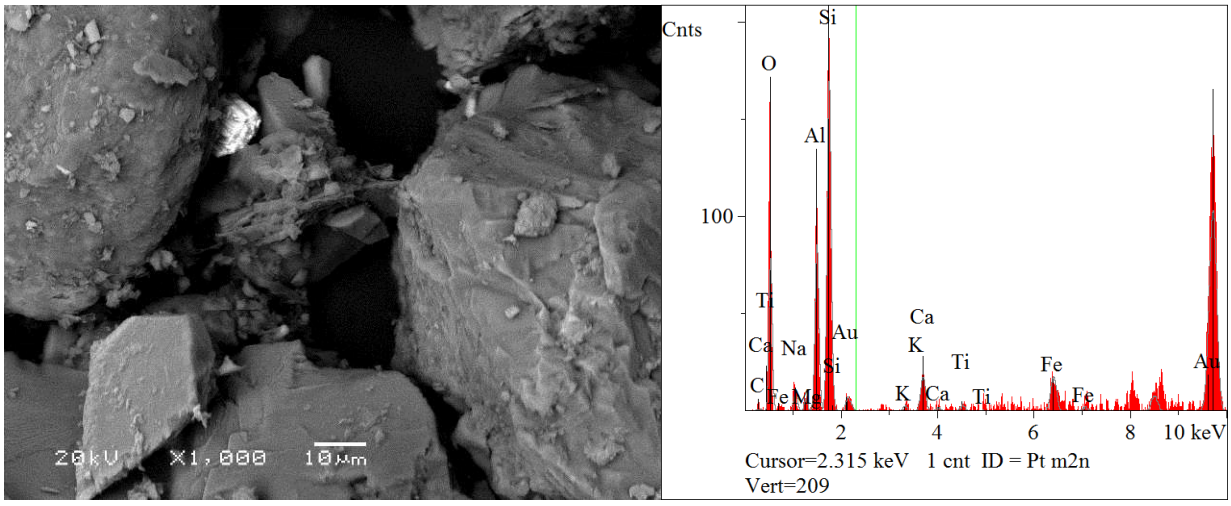

Figure 2-19. SEM-EDS image of sediment from column 2 port 3, bright spot seems to be gold, other major elements include oxygen, aluminum, and silicon.

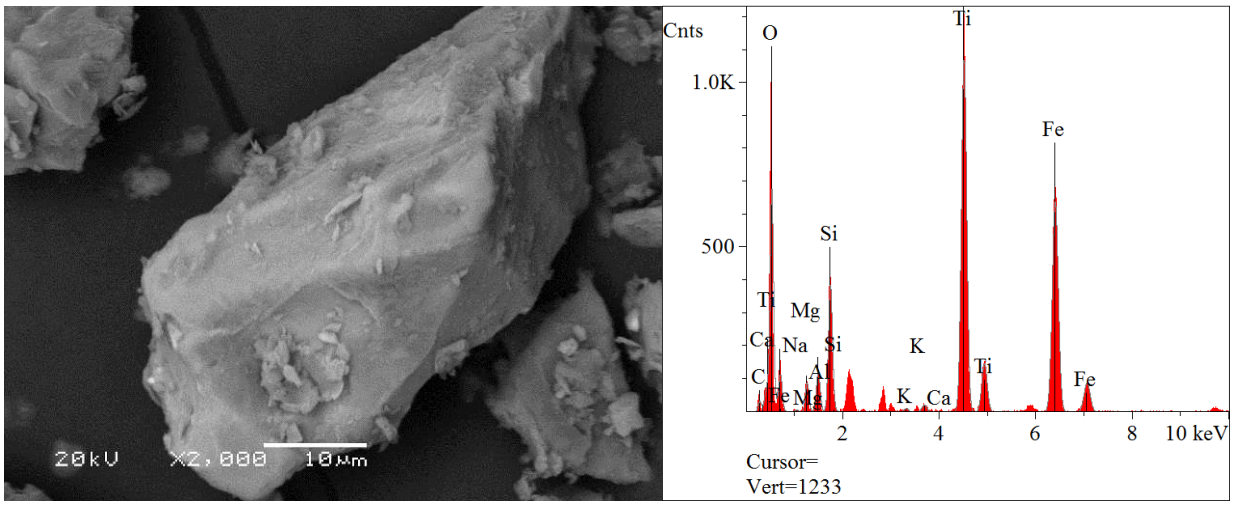

Figure 2-20. SEM-EDS image of column 1 port 2, major elements include oxygen, silicon, titanium, and iron.

During August, new graphs for the fall 2016 phase experiments were developed in the same style as existing graphs for the spring 2017 phase studies. These graphs have missing data towards the start of the experiment due to difficulties in data collection caused by the formation of gas bubbles in the columns. This missing data currently appears as blank space in the graph; however, FIU plans to give it a unique graphical identifier in the future to clearly identify the missing data (Figures 2-21 and 2-22). New graphs plotting resistivity versus frequency will also be developed to supplement the existing plots of bulk resistivity. This will allow for a better analysis of existing measurements.

The fall 2016 pore water samples were prepared for uranium analysis via KPA. The procedure for the preparation of these samples is the same as was used for the spring 2017 samples by following wet and dry ashing procedures.

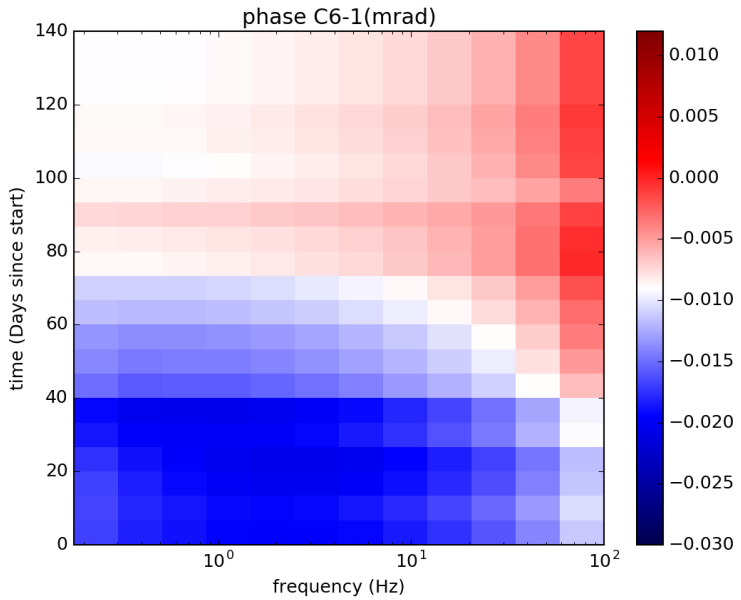

Figure 2-21. Phase graph of column 6 port 1. This graph has no missing data.

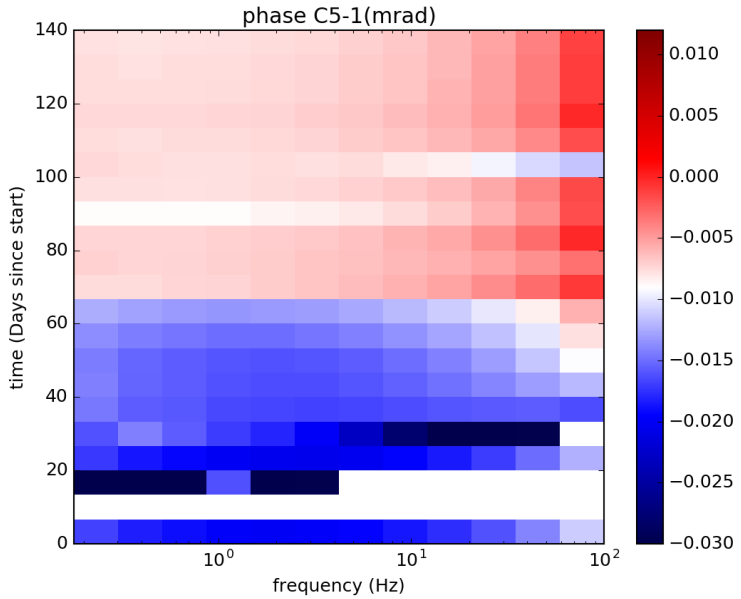

Figure 2-22. Phase graph of column 5 port 1. This graph has data missing towards the start (solid white) as well as some erroneous data (dark blue patches).

During September, a majority of the pore water samples collected during the fall of 2016 were analyzed for uranium with the KPA instrument. Uranium concentrations in these samples seem to show similar trends to that observed in the samples collected during the spring of 2017, showing that the uranium concentration decreased as conditions moved from oxidizing to reducing. There may be some correlation between the U concentration reduction and an increase in ferrous iron concentration. Completion of the KPA analysis is planned for the beginning of October. KPA analysis will be the final step for the existing samples apart from possibly repeating any samples with erroneous results.

Findings from the saturated column experiments (fall 2016 and spring 2017) will be presented by a DOE Fellow as a poster at the 2017 American Geophysical Union conference in New Orleans, LA as well as during an oral panel session at the 2018 Waste Management Symposia in Phoenix, AZ.

FIU is working on the Year End Report for Performance Year 7 with expected completion and submission at the beginning of November 2017. The scope of work for Performance Year 8 in the Project Technical Plan for this project has been discussed with PNNL scientists, including the possibility of conducting basic experiments to have better control throughout the experimental phase.

Subtask 1.4. Contaminant Fate and Transport under Reducing Conditions

During the month of July, FIU continued investigating the chemistry of Tc under reducing conditions in the presence of Hanford soil, as well as troubleshooting and setting up all the necessary parameters of the system. In the previous studies presented in the June monthly report, it was found that the presence of $NaBH_4$, as a reducing agent/electron donor in the aqueous phase at concentrations 0.001 and 0.002 M, was able to partially remove Tc(VII) from the aqueous phase, whereas ~65% of the total Tc-99 concentration in the aqueous phase remained in the +7

oxidation state. Two additional samples were prepared by bringing 1g of Hanford soil (average particle diameter d<300µm) into contact with 50 mL of the aqueous phase containing 50 µM initial concentration of $^{99}TcO4^-$, 10 mM HCO_3^-, 10^{-3} Na-HEPES (pH ~7.5) and 0.01M and 0.05 $NaBH_4$. All solutions were previously purged with high purity N_2 under vigorous stirring for 2h at room temperature. Eh (mV) and pH were also measured frequently by using a Hannah Instruments redox electrode and an Orion 9110D pH electrode, respectively. Tc(VII) and Tc(IV) aqueous phase speciation was done with a solvent extraction (CH_3Cl-TPPC). Tc-99 was measured by means of liquid scintillation counting. The pH was monitored for a period of 4 days and it was found to be stable at 7.5±0.1; hence, no additional adjustment to pH was made. ORP values were found to be stable and Eh was recorded at -70±5 mV and -98±6 mV for the samples containing 0.01 and 0.05 M $NaBH_4$, respectively. The calibration curve of the known mass of Tc-99 versus net cpm (after background subtraction) is presented in Figure 2-23. Experimental results are presented in Table 2-9.

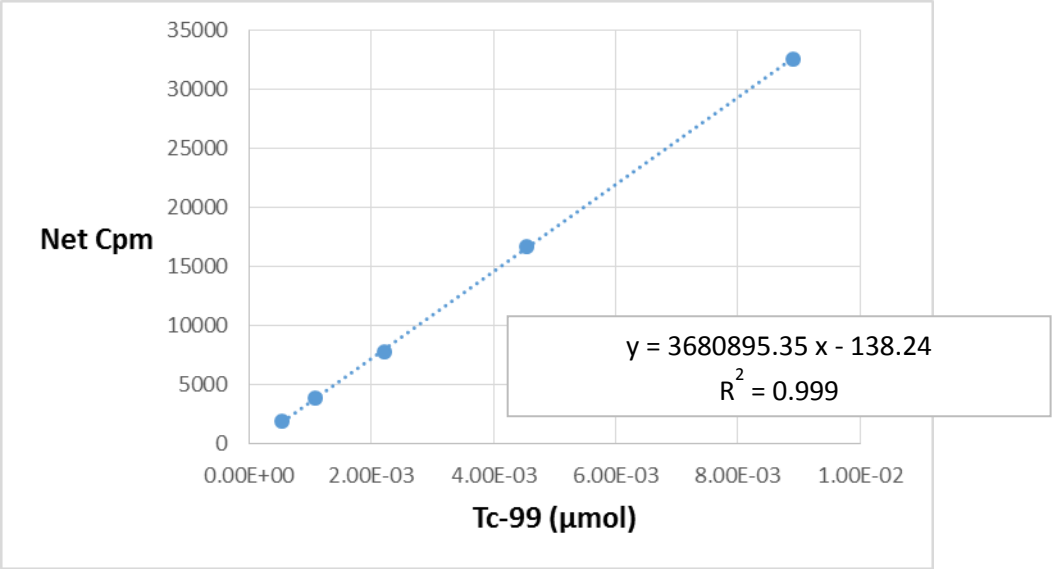

Figure 2-23. Calibration curve of Tc-99.

Table 2-9. Counts per Minute (cpm) for Hanford Soil Suspensions Containing Different $NaBH_4$ Concentrations, as a Function of Time

Sample	Separation Phase	Day 2 (cpm)	Day 3 (cpm)	Day 4 (cpm)
0.01 M $NaBH_4$	H_2O	224	325	275
	CH_3Cl	41	90	68
0.05 M $NaBH_4$	H_2O	32	88	70
	CH_3Cl	27	46	39
Background		24	30	27
Standard Tc-99 solution, 50µM		17650		

As can be seen in Table 2-9, as early as Day 2, Tc-99 is no longer encountered in the aqueous phase in any oxidation state, since the counts per minute recorded are equal to background or within experimental error. On the other hand, it should be noted that this preliminary kinetic experiment is quite fast and it is not clear if Tc-99 has been reduced from Tc(VII) to Tc(IV) (and hence $TcO_4^-{}_{(aq)}$ converted to $TcO_{2(s)}$) or Tc(IV) complexed with carbonates in the aqueous phase and created soluble Tc(IV)-carbonato complexes, that subsequently sorbed onto the soil. The samples contained a ratio of Tc:HCO_3^- equal to 1:200, much higher than the 1:30 cited in literature (Eriksen et al., 1992), which would likely favor the formation of Tc(IV)-carbonate complexes under circumneutral conditions and prevent the precipitation of TcO_2. Future experiments with Hanford soil and pure minerals of interest will attempt to investigate this issue by performing XRD studies post reduction; TcO_2 phases should be identifiable through XRD studies, whereas the Tc(IV)-carbonate sorbed complex will not be identifiable.

During July, FIU encountered issues with abnormal oxygen readings and after several trial and error tests inside and outside of the glovebox, the O_2 sensor had to be sent back to Coy Lab for evaluation. Furthermore, the oxygen levels inside the glovebox were also due to the complete failure of the Pd catalyst located inside the chamber. The catalyst, which provides the surface for H_2 and O_2 reaction towards water molecules, was past its shelf life and had to be replaced. A new catalyst was purchased from Coy Lab and, upon receipt, was placed in the oven at 180°C overnight before introduction to the chamber.

In order to initiate the experiments with Fe(II)-bearing minerals of relevance to the Hanford Site, two different types of magnetite (Fe_3O_4) were purchased from Fisher: magnetite 325-mesh (micro-powder) and magnetite nano-powder, in order to investigate if different specific surface area of the same mineral plays an important role in Tc-99 reduction. Batch samples were prepared using 500 mg of each mineral type in 30 ml of Tc-99 solution, with an initial concentration 25μM (previously degassed as described before). The samples were introduced in the anaerobic chamber and were left to equilibrate for a period of a week, while pH and ORP were monitored. The initial pH of the degassed DI water was 7.5. The fluctuation of the pH values during the equilibration period is presented in Figure 2-24 and the fluctuation of ORP values in Figure 2-25.

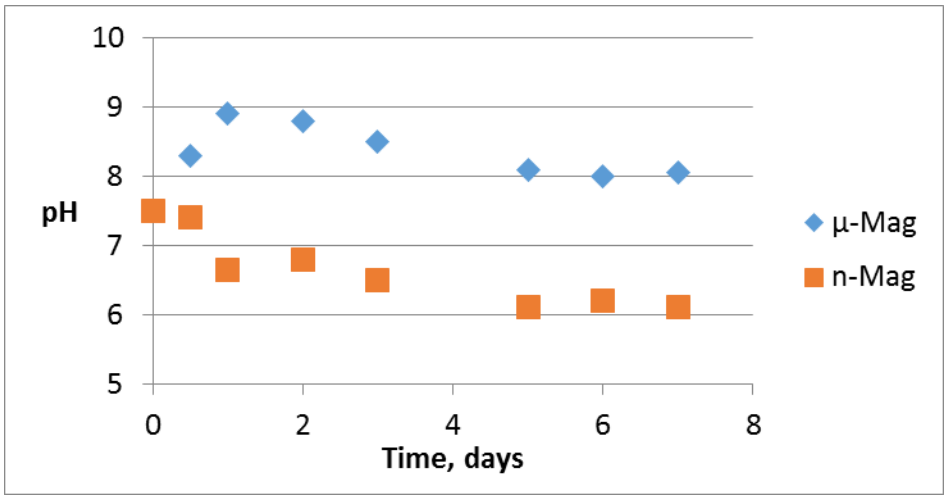

Figure 2-24. Variation of pH as a function of time at 98:2% N_2-H_2 atmosphere for micro-powder and nano-powder magnetite suspensions in Tc-99 solution, C_{init}=25μM.

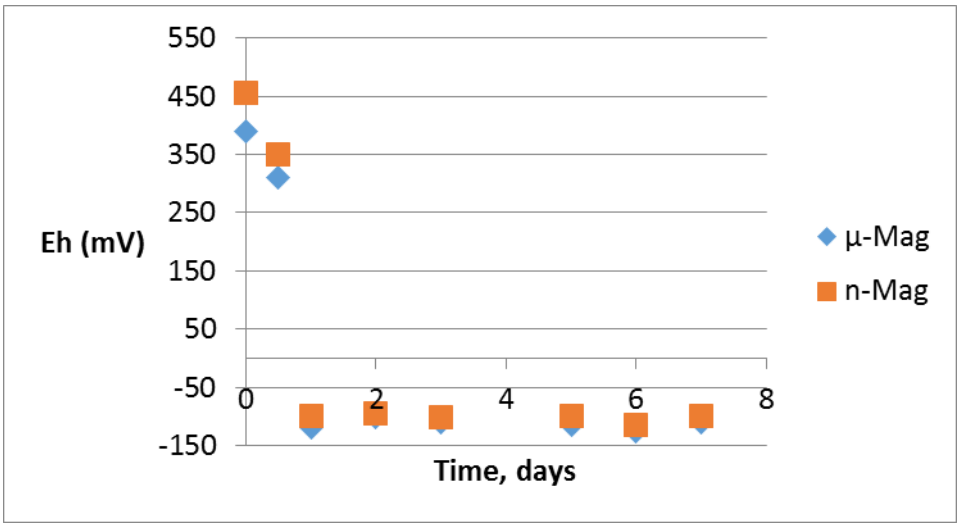

Figure 2-25. Variation of Eh as a function of time at 98:2% N_2-H_2 atmosphere for micro-powder and nano-powder magnetite suspensions in Tc-99 solution, C_{init}=25µM.

As it can be seen in Figures 2-24 and 2-25, more time is needed for pH stabilization compared to Eh values. It is noteworthy that after 24h inside the anaerobic chamber in an oxygen-depleted atmosphere, Eh values are still at oxidizing levels. The levels of equilibrations in the literature may vary depending on the substrate; nevertheless, samples in each case were equilibrated for several days: 3 days for magnetite suspensions in 3% H_2 atmosphere (Cui and Eriksen, 1996), 4 days for Fe(II) minerals sorbed on goethite (Peretyazhko et al., 2009) and 7 days for magnetite and mackinawite suspensions (Yalcintas et al., 2016). At this point, it should be noted that the first samples do not contain carbonate and they will serve as the baseline for the next experiments that will contain carbonate under identical conditions. After Day 7, sampling from the supernatant is performed every day to every two days for the determination of Tc-99 in the aqueous phase (in progress). This first step also aims to evaluate if the specific surface area plays a role in the electron transfer from Fe(II) minerals to Tc(VII), which will eventually lead to its reduction.

During the month of August, batch experiments were initiated and two duplicate samples of 300 mg of magnetite each (micro: d>44 µm and nano: 50<d<100 nm) were equilibrated with a solution of 25 µM of Tc (VII) for a final volume of 30 mL. Deionized water for the preparation of solutions was purged with nitrogen for 2h under vigorous stirring and then was placed in the anaerobic glovebox for equilibration under 98% N_2-2% H_2 atmosphere for 3 days. The initial pH of the solution was 7.5 and, upon mixing with magnetite, no further pH adjustment took place. pH for micro-magnetite stabilized at 8 and pH for nano-magnetite stabilized at 6. In Figure 2-26, the monitoring of Tc(VII)aq concentration is presented.

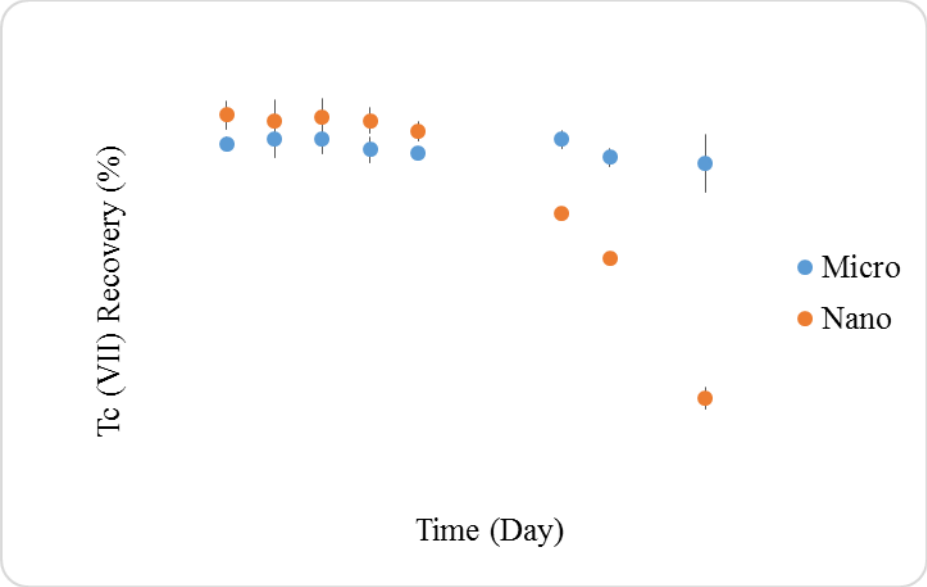

Figure 2-26. Tc(VII) recovery percentage detected in the aqueous phase as a function of time under anaerobic conditions.

In Table 2-10, the percentage of Tc-99 reduction as a function of time is presented. It is apparent that after 3 weeks of the experimental process, 33% of Tc is reduced in the presence of nano-magnetite, whereas in the case of micro-magnetite, there is negligible reduction. Sampling of the current samples will continue every 4 days for the nano-magnetite, given the fast reduction reaction of Tc(VII) to Tc(IV), and once a week for the micro magnetite every week, in order to observe a substantial reduction percentage while avoiding excessive sampling that would deplete the aqueous phase.

Table 2-10. Reduction of Tc (VII) in Difference Size Manganite over Time

Time (Days)	Micro-magnetite % Tc Reduction	Nano-magnetite % Tc Reduction
4	0.60	0.00
6	0.00	0.67
8	0.03	0.24
10	1.23	0.68
12	1.63	1.86
18	0.06	11.37
20	2.13	16.64
24	2.84	32.74

In order to further test the effect of a specific surface under the hypothesis that Tc reduction is a surface-mediated heterogeneous reduction, FIU prepared another set of samples of nano-magnetite particles where the pH was adjusted to 8. At the end of this experimental process, FIU aims to draw conclusions from the following comparisons:

1. Comparison of micro- and nano-magnetite ability and rate to reduce Tc(VII) to Tc(IV) at pH 8. Samples of micro- and nano-magnetite contain the same number of electron donors (ferrous iron) at the same pH, but they exhibit different specific surface areas.
2. Comparison of the ability of nano-magnetite to reduce Tc(VII) to Tc(IV) at different pH values (6 and 8) with the same number of electron donors and specific surface area available for the reduction of Tc under different pH values.

The new samples containing nano-sized magnetite were prepared under identical conditions compared to the previous ones and are currently equilibrating in the inert atmosphere of the anaerobic glovebox. Upon establishing equilibrium for the new nano-magnetite samples, batch experiments with soil samples, whose Fe content is at comparable levels to the pure mineral samples, will be prepared. This should conclude the baseline studies of Tc-99 interaction with magnetite in the absence of carbonate and then the batch experiments will be repeated in the presence of bicarbonate in order to assess if the presence of bicarbonate affects the phenomenon.

During the month of September, FIU continued monitoring the interaction of pertechnetate with micro- and nano- magnetite at pH 8 and 6, respectively. Furthermore, FIU initiated duplicate batch experiments with nano-size magnetite under identical experimental conditions (solid substrate nano-size magnetite 300mg, $[TcO_4^-{}_{init}]$= 25μM, final volume 30ml) at pH 8. The results are presented in Figure 2-27. The Eh in all samples did not fluctuate throughout the experiment significantly and was found to be -200±20mV.

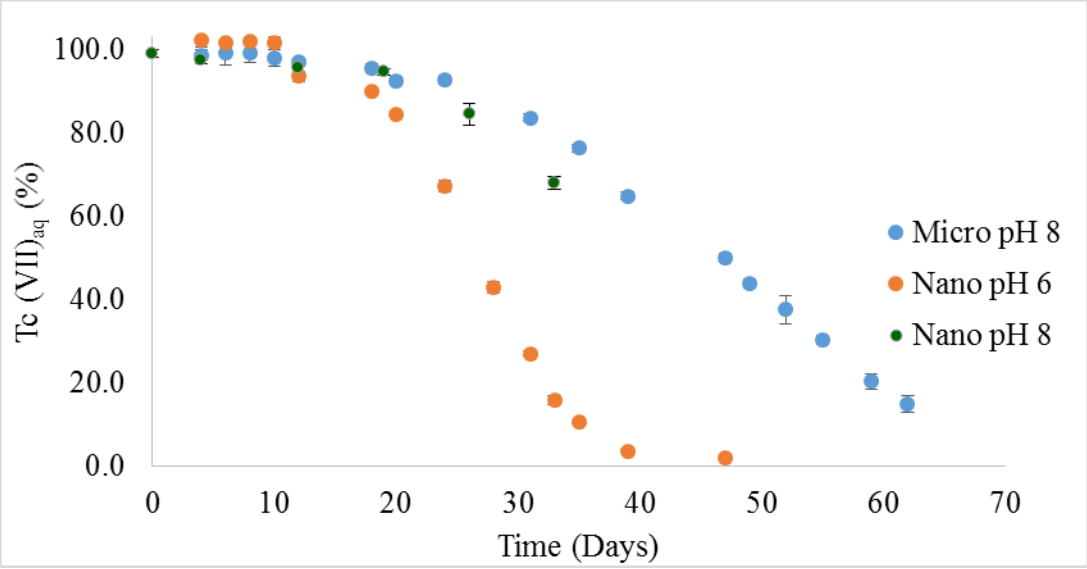

Figure 2-27. $Tc(VII)_{aq}$ percent concentration as a function of time under anaerobic conditions.

As can be seen from Figure 2-27, nano-size magnetite at pH 6 reduces pertechnetate 100% within 40 days. On the other hand, the preliminary results with nano-size magnetite at pH 8 indicate a much slower rate of reduction. In a similar fashion, after 62 days of contact between the pertechnetate solution and micro-size magnetite at pH 8, there is still no complete reduction (~15% of pertechnetate was detected in the solution). It is still early to identify whether reduction of pertechnetate by nano-size magnetite is faster compared to micro-size magnetite under the same conditions (pH 8); more experimental points are required in order to compare the reduction

rate between those two cases. In the case of nano-size magnetite at pH 6, the levels of ferrous iron were measured periodically throughout the experiments using the ferrozine method (Verschoor and Molot, 2013) and were equal to 5 mg/L; whereas, in the case of both micro- and nano-magnetite at pH 8, ferrous iron levels were below detection levels (<50 μg/L). The ferrous iron results for pH 8 imply that since pertechnetate reduction is taking place and practically no ferrous iron is detected in the aqueous phase, the reaction is due to the electron donation of the mineral (heterogeneous reaction). Interestingly, at pH 6, the levels of ferrous iron are significant and the role of $Fe(II)_{aq}$ is ambiguous: it is not clear if the faster reduction rate is facilitated by the presence of $Fe(II)_{aq}$, despite the fact that the $Fe(II)_{aq}$ concentration did not fluctuate as a function of time. To this end, FIU prepared additional control samples under identical conditions in the absence of solid mineral ($[TcO_4^-]_{init}$ = 25μM, $Fe(II)_{aq,init}$ 5ppm, pH 6 under anaerobic conditions) in order to monitor more closely the effect of $Fe(II)_{aq}$ in the pertechnetate reduction. The reduction of pertechnetate by Fe(II) in the aqueous phase, although thermodynamically feasible, has been reported to be kinetically hindered (Cui and Eriksen, 1996; Peretyazhko et al., 2008). Zachara (2007), also confirmed that $Fe(II)_{aq}$ may contribute, if present, to pertechnetate reduction at neutral and alkaline conditions (pH>7), but not in acidic conditions.

References:

Cui D, Eriksen T.T., 1996. Reduction of pertechnetate in solution by heterogeneous electron transfer from Fe(II)-containing Geological Material. Environmental Science and Tehcnology, 30, 2263-2269

Eriksen T.E., Ndalamba P., Bruno J., Caceci M., 1992. The solubility of $TcO_2 \cdot nH_2O$ in neutral to alkaline solutions under constant p_{CO2}. Radiochimica Acta, 58/59, 67-70

Verschoor M.J. Molot A.L. (2013). A comparison of three colorimetric methods of ferrous and total reactive iron measurement in freshwaters. *Limnology and Oceanography: Methods,* 11. 113-125.

Yalcintas E., Scheinost AC, Gaona X., Altmaier M. 2016. Systematic XAS study on the reduction and uptake of Tc by magnetite and mackinawite. Dalton Transactions, 45, 17874-17885

Peretyazhko T., Zachara JM, Heald SM, Jeon BH, Kukkadapu RK, Liu C., Moore D., Resch CT., 2009. Heterogeneous reduction of Tc(VII) by Fe(II) at the solid-water interface. Geochimica et Cosmochimica Acta, 72, 1521-1529

Zachara J.M., Heald S.M., Jeon B.H., Kukkadapu R.K., Liu C., McKinley J.P., Dohnalkova A.C., Moore D.A. (2007). Reduction of pertechnetate [Tc(VII)] by aqueous Fe(II) and the nature of solid phase redox products. *Geochimica et Cosmochimica Acta* 71, 2137-2157.

Task 2: Remediation Research and Technical Support for Savannah River Site

Task 2 Overview

The acidic nature of the historic waste solutions received by the F/H Area seepage basins caused the mobilization of metals and radionuclides, resulting in contaminated groundwater plumes. FIU is performing basic research for the identification of alternative alkaline solutions that can amend the pH and not exhibit significant limitations, including a base solution of dissolved silica and the application of humic substances. Another line of research is focusing on the evaluation of

microcosms mimicking the enhanced anaerobic reductive precipitation (EARP) remediation method previously tested at SRS F/H Area.

Task 2 Quarterly Progress

Subtask 2.1. Investigation on the Properties of Acid-Contaminated Sediment and its Effect on Contaminant Mobility

An abstract based on this research was accepted by the Waste Management 2018 Symposium for a presentation.

> **Abstract**: 18592
> **Title**: Investigation of the Properties of Acid-Contaminated Sediment Effects on Contaminant Mobility
> **Authors**: Awmna Rana (DOE Fellow), Vasileios Anagnostopoulos, Yelena Katsenovich, Miles Denham (SRNL)

During the month of July, FIU normalized the sorption results of the different acidified soil profiles as μg of U(VI) sorbed per soil mass (g), as well as per surface (mg of U(VI) / m^2 of each soil substrate). Results are presented in Table 2-11.

Table 2-11. Sorption capacity of different acidified profile soil substrates expressed as U(VI) uptake per mass and per surface area for pH values 4.5, 7 and 8 with relative standard deviation

Acidified profile	U(VI) sorbed pH 4.5		pH 7		pH 8	
	μg /g	mg/m^2	μg /g	mg/m^2	μg /g	mg/m^2
A (7 days)	275 ± 52	2.61 ± 0.66	950 ± 57	9.02 ± 1.5	725 ± 58	6.88 ± 1.2
B (30 days)	125 ± 50	1.87 ± 0.86	975 ± 20	14.6 ± 3.3	600 ± 55	8.96 ± 1.0
C (50 days)	0	0	500 ± 20	6.44 ± 2.5	450 ± 20	5.79 ± 1.3
Sat	275 ± 51	1.19 ± 0.25	1100 ± 75	4.76 ± 0.48	600 ± 18	1.15 ± 0.04
Background	450 ± 53	1.10 ± 0.13	1525 ± 30	3.72 ± 0.12		

The results for FAW-5 (plume core soil) normalized per mass and surface will be calculated once SRNL is able to provide results on the specific surface area and pore distribution.

It is evident from Table 2-11 that the acidified samples (acidified profile B) are the ones that exhibit the highest U(VI) uptake at circumneutral conditions when the sorption results are normalized as mg of U(VI) sorbed per area. However, the samples where secondary precipitates were allowed to form and precipitate (Sat) exhibited the lowest uptake. A comparison of the U(VI) uptake per mass reveals that samples A, B and Sat exhibit very similar results on uptake per mass. Sorption expressed in terms of radionuclide mass per substrate mass (μg U(VI)/g) may provide misleading results since all the samples contained the same amount of soil substrate; however, the specific surface area and the Fe content (as previously reported) were not the same.

In the month of July, FIU initiated the batch sorption experiments testing the "Sat" and the FAW-5 samples in different solid:liquid ratios, by keeping the initial uranium concentration and

the aqueous phase volume the same (C_{init}=500 μg L^{-1} and 10 mL, respectively) and altering the substrate mass (50-400 mg). Usually, when uptake is a surface phenomenon, there is a linear correlation between uptake and the substrate's mass (and consequently, surface area), whereas when there is little linear correlation, then other mechanisms contribute (e.g., chemical sorption) to the phenomenon (Anagnostopoulos, et al., 2012). All samples were equilibrated for 24h at pH 7 and the residual uranium concentration was determined by means of kinetic phosphorescence analysis (KPA). The sorption results of different solid:liquid ratios for the "Sat" soil samples are presented in Figure 2-28.

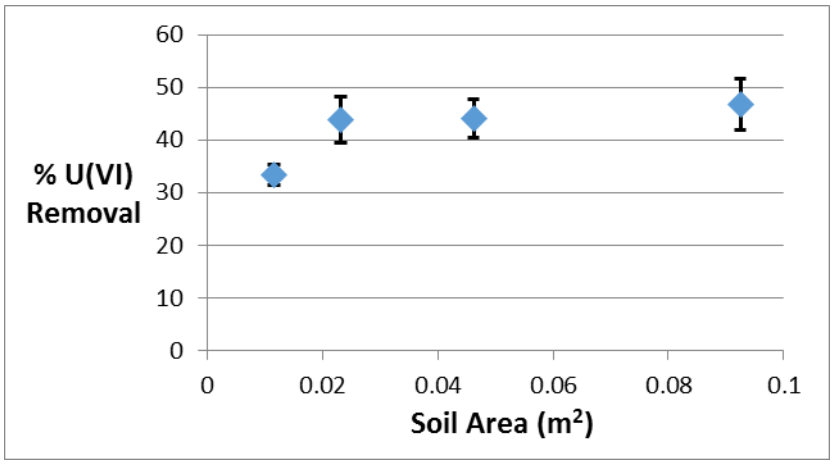

Figure 2-28. Percentage of uranium removal from the aqueous phase as a function of soil area for soil samples "Sat", pH 7, 24h equilibration time.

As it can be seen in Figure 2-28, an increase in the available area does not affect the uranium removal with the exception of the first experimental point. There does not seem to be a linear correlation between uranium removal and the substrate's surface area. Furthermore, an increase in the solid phase has been reported to bear an increase in removal, due to the increase of available surface active groups with a given amount of solute molecules (Akar et al., 2009; Anagnostopoulos et al., 2012). Nevertheless, in Figure 2-28, no increase in uranium removal was observed when increasing the soil mass, but uranium removal reached a plateau at ~45%. In literature, plateaus in solid:liquid ratio experiments have been explained as potential agglomerations of the soil particles during equilibration leading to a loss of the available surface area and, consequently, to a reduction of the available functional groups which interact with U(VI) species (Ucun et al., 2009; Anagnostopoulos et al., 2015). Nevertheless, in this case, the plateau is at ~45% U(VI) removal, so there is a~ 55% of U(VI) in the aqueous phase and saturation of the soil's active sites does not seem to be the cause. Additional experiments using different soil profiles under identical conditions are currently being performed in order to determine if a similar trend is observed.

Sorption of U(VI) was also found to be less at pH 8 compared to pH 7. This experimental finding could be explained by the difference in U(VI) aqueous speciation at pH 7 and pH 8. With the aid of speciation software Visual Minteq, Table 2-12 was compiled and contains the major uranyl species at different pH values.

Table 2-12 Major Uranyl Species at pH 7 and 8 using Visual Minteq

Species	% at pH 7	% at pH 8
$UO_2CO_3(OH)_3^-$	73	63
$UO_2(OH)_2$	3	-
UO_2CO_3 (aq)	10	2
UO_2OH^+	7	-
$(UO_2)_3(OH)_5^+$	5	-
$UO_2(OH)_2$	2	-
$UO_2(CO_3)_2^{2-}$	-	22
$UO2(CO_3)_3^{4-}$	-	12

As can be seen by Table 2-12, at pH 7, 73% of uranyl species are negatively charged; whereas at pH 8, 98% of the uranyl species are negatively charged. Similar studies have assumed that the most reactive component of the soil towards uranium is Fe (in goethite) according to the complexation reaction (Anagnostopoulos et al., 2017; Dong et al., 2012):

$$2 > FeOH^{-0.5} + UO_2^{2+} = (FeOH)_2\ UO_2^{+} \text{ at pH>4.0}$$

Given the fact that the background soil consists of ~95% quartz and quartz exhibits p*k* values ~4.5 (Leung et al., 2009; Liu et al., 2014), it is safe to assume that the net charge of the surface at both pH 7 and 8 is overall negative. Despite the fact that surface complexation is not dependent on electrostatic interactions, the existence of opposite charges between the surface and the aqueous species still facilitates the approach between active centers and radionuclides, which may end up binding by complexation. Hence, at pH 8, where all the aqueous uranium species are negatively charged, interaction between substrate sites and uranium may not be facilitated.

During the month of July, DOE Fellow Ms. Awmna Rana, under the supervision of Dr. Vasileios Anagnostopoulos, prepared a presentation summarizing all the experimental findings of this task and presented during the FIU Research Review to DOE Headquarters.

During the month of August, FIU concluded the solid:liquid ratio batch experiments using soil from the acidic groundwater plume from the SRS F/H Area (FAW-5). The volume of the aqueous phase was kept constant and equal to 10 ml and uranium initial concentration was 500 ppb. The soil mass was 50, 100, 200 and 400 mg and all experiments were performed in triplicate. Results are presented in Table 2-13. The pH was adjusted initially to 7 and was monitored for at least 4h after the initiation of the experiment and adjusted as needed. The residual uranium concentration in the supernatant was measured after 24 and 72h.

Table 2-13. Percent Uranium Removal from the Aqueous Phase

FAW-5 mass (mg)	% U(VI) Removal	
	Day 1	Day 3
50	34 ± 8	40 ± 5
100	64 ± 5	67 ± 4
200	72 ± 6	82 ± 4
400	84 ± 7	92 ± 2

Table 2-13 revealed no significant difference for the solid:liquid ratio uranium removal between day 1 and day 3 (confidence level: 95%), denoting that equilibrium is achieved within 24h. FIU reported similar results in the past, where equilibrium of uranium sorption on background soil from the F/H Area was achieved within 24h (Anagnostopoulos et al., 2017). As can be seen in Figure 2-29, there is a slight increase in uranium removal with soil mass increase, but there seems to be no linear correlation between the soil's mass and the uranium removal. This observation implies that sorption of uranium on FAW-5 soil is not a phenomenon dependent on the available sruface of the substrate for reaction with uranium in the aqueous phase.

Further kinetic experiments with FAW-5 soil will follow during the month of September and the solid:liquid ratio batch experiments will be normalized as U(VI) sorption per surface area and compared with previous results with "Sat" acidic soil created in the lab.

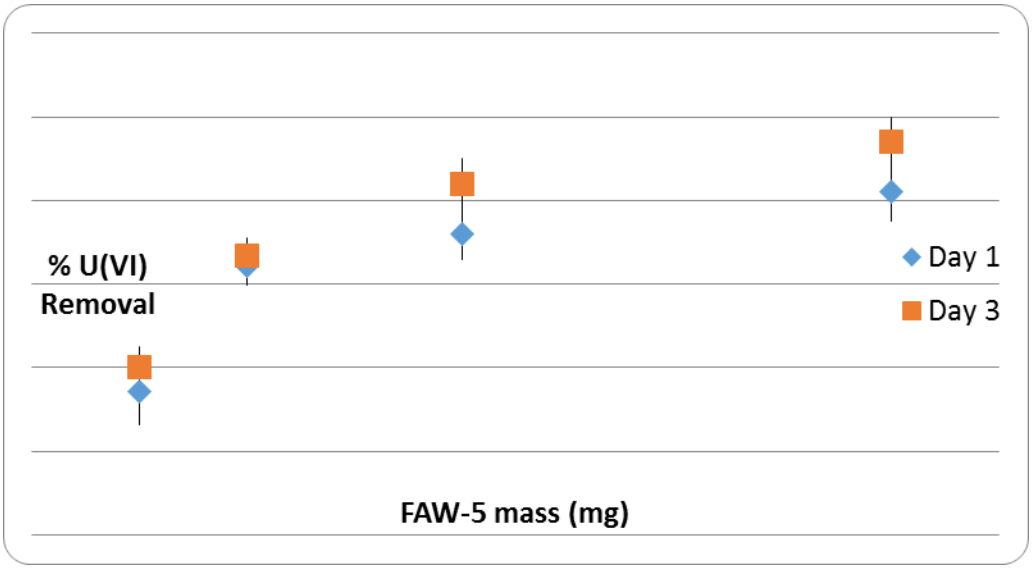

Figure 2-29. U(VI) removal (%) from the aqueous phase as a function of soil mass after 24 and 72h of contact.

During the month of September, FIU worked on the Year End Report for this subtask as well as the Project Technical Plan for next performance year. In addition, FIU defined a carryover scope for this subtask that will include several experiments to conclude FIU's studies on uranium interactions with acidified soil.

Furthermore, DOE Fellow Awmna Rana prepared a poster presentation summarizing all the experimental results for the subtask. The poster (Figure 2-30) was titled "Effect of Acidic Plume on Soil's Properties and Capacity to Retain Uranium at the Savannah River Site" and was presented at Emory STEM Research and Career Symposium by Ms. Rana. Ms. Rana was awarded the Emory STEM Research and Career Symposium Travel Award.

FIU also initiated experiments investigating the solid:liquid ratio for "Sat", as well as batch kinetic experiments using FAW-5 and "Sat" soil, which will be completed during the month of October. The solid:liquid ratio experiments have been initiated during Performance Year 7 and their continuation is needed in order to compare the performance of several different soil profiles. These experiments will be performed as carryover scope.

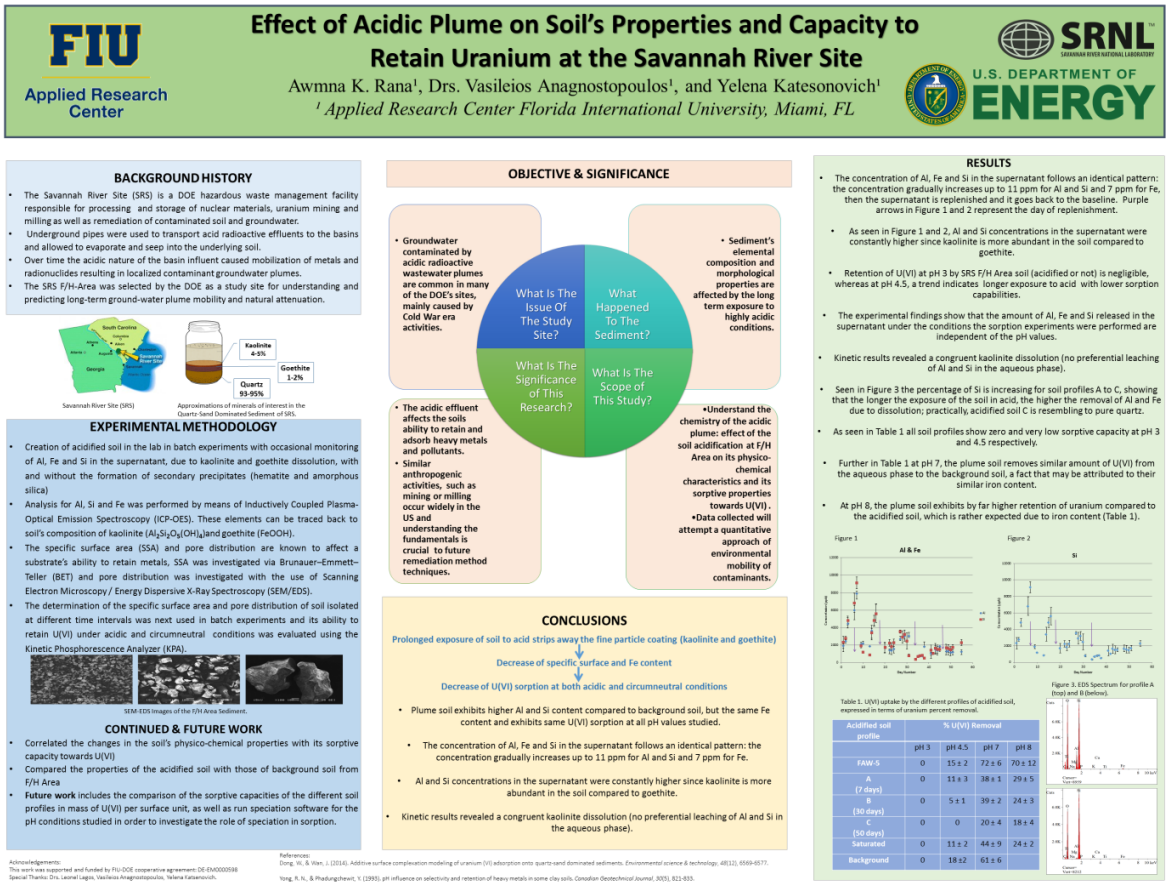

Figure 2-30. Effect of Acidic Plume on Soil's Properties and Capacity to Retain Uranium at the Savannah River Site by A. Rana, V. Anagnostopoulos, Y. Katsenovich, Emory STEM Research and Career Symposium, Atlanta, GA, 2018

During the month of October, FIU performed kinetic experiments with Sat and FAW-5 (plume soil) soil profiles. 400 mg of each soil profile were brought in contact with 20ml of uranium solution, Cinit = 500µg L^{-1}, pH 7. Samples were placed on a platform shaker at 110rpm and periodically aliquots were isolated and diluted with 1% HNO_3 and stored at 4ºC till further analysis. Uranium residual concentration in the supernatant was determined by Kinetic Phosphorescence Analysis. Kinetic results are presented in Figure 31.

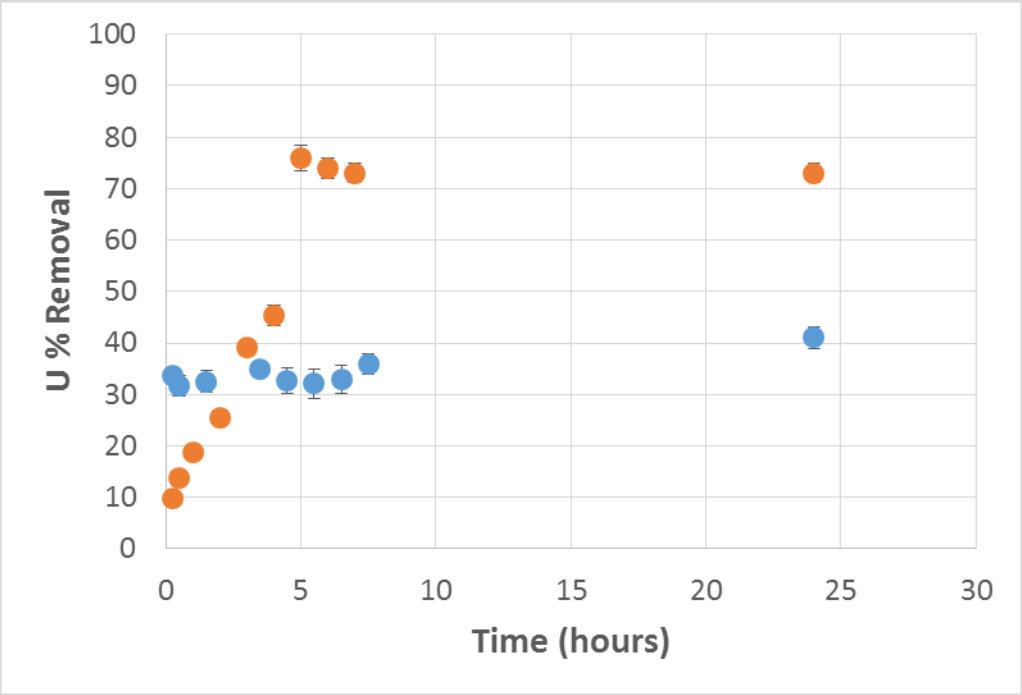

Figure 31. Uranium percent removal by Sat acidic profile (blue dots) and FAW-5 plume soil (orange dots) as a function of time

As it can be seen in Figure 31, the uptake of uranium by Sat soil profile is rapid and equilibrium has been established within the first 15 minutes, whereas for plume soil 5 hours are needed for the establishment of the equilibrium. The uptake at equilibrium was ~32% for Sat soil profile and ~63% for plume soil, which is in agreement with our previous equilibrium experiments performed at 24 and 48h intervals.

References

Akar T., Kaynak Z., Ulusoy S., Yuvaci D., Ozsari G., Akar S.T. Enhanced biosorption of nickel(II) ions by silica-gel-immobilized waste biomass: biosorption characteristics in batch and dynamic flow mode, *J Hazard Mater* (2009) 163, 1134–1141.

Anagnostopoulos VA, Koutsoukos P, Symeopoulos BD. Removal of U(VI) from Aquatic Systems, Using Winery By-Products as Biosorbents: Equilibrium, Kinetic, and Speciation Studies. *Water Air Soil Pollut* (2015), 226, 107

Anagnostopoulos VA, Manariotis ID, Karapanagioti HK, Chrysikopoulos CV. Removal of mercury from aqueous solutions by malt spent rootlets. *Chem Eng J*, 2012, **213**, 135-141

Anagnostopoulos VA, Katsenovich Y. Denham M. Sodium silicate treatment for the attenuation of U(VI) by iron-bearing sediments in acidic groundwater plumes, *J Chem Technol Biotechnol*, 2017, **92**, 1919-1927

Dong W, Tokunaga TK, Davis JA and Wan J, Uranium(VI) adsorption and surface complexation modeling onto background sediments from the F-Area Savannah River Site. *Environ Sci Technol*, 2012, **46,** 1565–1571.

Liu X., Cheng J., Lu X., Wang R., Surface acidity of quartz: understanding the crystallographic control. *Phys. Chem. Chem. Phys.*, 2014, **16**, 26909-26916

Leung K., Nielsen I. M. B., and Criscenti L. J., Elucidating the bimodal acid-base behavior of the water-silica interface from first principles, *J. Am. Chem. Soc.*, 2009, **131**, 18358-18365.

Ong S., Zhao X., and Eisenthal K. B., Polarization of water molecules at a charged interface: second harmonic studies of the silica/water interface, *Chem. Phys. Lett.*, 1992, **191**, 327-335.

Ucun, H., Aksakal, O., & Yildiz, E. (2009). Copper(II) and zinc(II) biosorption on *Pinussylvestris L. J Hazard Mater*, *161*, 1040–1045

Subtask 2.2: The Synergistic Effect of Humic Acid and Colloidal Silica on the Removal of Uranium (VI)

An abstract based on this research was accepted by the Waste Management 2018 Symposium for a poster presentation.

> **Abstract**: 18581
> **Title**: Study of Synergetic Interactions between Uranium, Humic Acid, Silica Colloids and SRS Sediments
> **Authors**: Ravi Krishna Prasanth Gudavalli, Alexis Smoot, Yelena Katsenovich, Miles Denham (SRNL)

Previously, FIU completed the KPA analysis of triplicate samples containing 3.5 mM of silica, 400 mg of sediment and 30 ppm uranium for batches pH 6-8. In order to evaluate to effect of HA on uranium removal, control HA-free triplicate samples of batches containing 3.5 mM of silica, 400 mg of sediment and 30 ppm uranium at pH 5 -7 were prepared by mixing known amounts of various constituents, except uranium, as shown in Table 2-14 - Table 2-16. Uranium was added prior to the pH adjustment and specific amounts of deionized water were added with the addition of acid/base so that the final volume totaled approximately 20 ml. The pH of the samples was adjusted with a stock solution of 0.1M HCl and 0.1M NaOH to the desired pH and the samples were then placed on a platform shaker. The pH of the samples was measured periodically and readjusted if there was a change in pH. Table 2-17 - Table 2-19 shows the data for the daily change of pH for each batch sample.

Table 2-14. Overall pH Adjustments for pH 5 Batch Samples

pH 5 Adjusted Set		Constituents						
		SiO_2	Sediments	Uranium, U (VI)	Volume of acid/ base	DIW, H_2O	pH	
		mL	mg	mL	mL	mL	Initial pH	Final pH
Batch No. 1	1.1	2.10	0.00	0.50	1.25	16.00	2.25	5.02
	1.2				1.95	16.00	2.24	5.05
	1.3				2.50	16.00	2.26	5.06
Batch No. 4	4.1	2.10	400.00	0.50	2.05	16.00	2.26	5.05
	4.2				1.80	16.00	2.27	5.06
	4.3				2.20	16.00	2.25	4.97
Batch No. 7	7.1	0	400.00	0.50	1.90	18.10	2.36	4.97
	7.2				1.82	18.10	2.34	4.97
	7.3				1.92	18.10	2.34	4.98

Table 2-15. Overall pH Adjustments for pH 6

pH 6 Adjusted Set		Constituents						
		SiO2	Sediments	Uranium, U (VI)	Volume of acid/ base	DIW, H2O	Initial pH	Final pH
		ml	mg	Ml	ml	ml	log(H)	log(H)
Batch No. 1	1.1	2.10	0.00	0.50	2.47	14.00	1.46	5.98
	1.2				1.82	14.00	1.51	6.04
	1.3				1.82	14.00	1.51	5.95
Batch No. 4	4.1	2.10	400.00	0.50	2.29	14.00	1.55	5.97
	4.2				1.89	14.00	1.57	5.95
	4.3				1.79	14.00	1.55	5.97
Batch No. 7	7.1	0	400.00	0.50	1.82	16.00	1.56	6.10
	7.2				1.80	16.00	1.19	6.05
	7.3				1.51	16.00	1.01	6.01

Table 2-16. Overall pH Adjustments for pH 7

pH 7 Adjusted Set		Constituents						
		SiO2	Sediments	Uranium, U (VI)	Volume of acid/ base	DIW, H2O	Initial pH	Final pH
		ml	Mg	Ml	ml	ml	log(H)	log(H)
Batch No. 1	1.1	2.10	0.00	0.50	2.56	15.00	1.50	7.05
	1.2				1.93	15.00	1.50	7.07
	1.3				1.87	15.00	1.59	6.98
Batch No. 4	4.1	2.10	400.00	0.50	1.88	15.00	1.47	6.90
	4.2				1.97	15.00	1.46	6.95
	4.3				1.84	15.00	1.46	7.04
Batch No. 7	7.1	0	400.00	0.50	2.45	17.00	1.47	7.03
	7.2				1.86	17.00	1.60	7.08
	7.3				1.72	16.50	1.75	7.06

Table 2-17. Daily Change of pH 5 Batch Samples

Sample #		pH 5						
		Day 1	Day 2	Day 3	Day 4	Day 5	Day 6	Day 7
Batch No. 1	1.1	5.05	5.03	4.96	5.04	5.03	4.97	5.02
	1.2	4.98	5.04	4.98	4.95	4.95	5.04	5.05
	1.3	5.05	5.06	4.99	4.97	4.96	5.06	5.06
Batch No. 4	4.1	5.01	4.98	5.01	4.97	4.96	5.02	5.05
	4.2	5.03	4.97	5.02	4.97	4.97	5.06	5.06
	4.3	4.99	5.02	4.95	5.02	5.02	4.95	4.97
Batch No. 7	7.1	5.02	5.04	4.96	4.95	4.99	4.96	4.97
	7.2	4.98	4.97	5.01	1.96	4.98	4.95	4.97
	7.3	4.96	5.04	4.98	4.96	4.98	4.95	4.98

Table 2-18. Daily Change of pH 6 Batches

Sample #		pH 6						
		Day 1	Day 2	Day 3	Day 4	Day 5	Day 6	Day 7
Batch No. 1	1.1	1.46	6.21	5.96	5.90	5.94	5.87	5.98
	1.2	1.51	6.22	6.02	6.00	6.06	5.87	6.04
	1.3	1.51	6.14	6.01	5.95	5.96	5.85	5.95
Batch No. 4	4.1	1.55	6.24	6.01	6.03	5.94	5.84	5.97
	4.2	1.57	6.24	6.07	5.99	5.97	5.83	5.95
	4.3	1.55	6.24	6.09	6.06	6.06	5.96	5.97
Batch No. 7	7.1	1.56	5.95	5.98	5.96	5.97	6.07	6.10
	7.2	1.19	6.07	5.77	5.86	5.87	6.00	6.05
	7.3	1.01	5.96	5.85	6.02	6.03	6.10	6.01

Table 2-19. Daily Change of pH 7 Batches

Sample #		pH 7						
		Day 1	Day 2	Day 3	Day 4	Day 5	Day 6	Day 7
Batch No. 1	1.1	1.50	7.09	7.08	7.03	7.08	7.04	7.05
	1.2	1.50	7.06	7.06	7.09	7.01	7.08	7.07
	1.3	1.59	6.93	6.96	6.90	6.95	7.09	6.98
Batch No. 4	4.1	1.47	7.03	6.92	6.99	6.90	7.01	6.90
	4.2	1.46	6.94	7.08	6.95	6.98	6.99	6.95
	4.3	1.46	6.95	6.99	7.00	7.00	7.00	7.04
Batch No. 7	7.1	1.47	6.94	7.10	7.10	6.92	7.00	7.03
	7.2	1.60	6.92	6.97	7.06	7.06	7.07	7.08
	7.3	1.75	7.01	6.94	6.96	7.03	7.05	7.06

FIU completed the analysis of batch samples containing humic acid (HA); Figure 2-32 and Figure 2-33 show the uranium removal data for the unfiltered and filtered samples for batches 2, 3, 5 and 6. The removal of uranium increased with an increase in pH for both filtered and unfiltered samples.

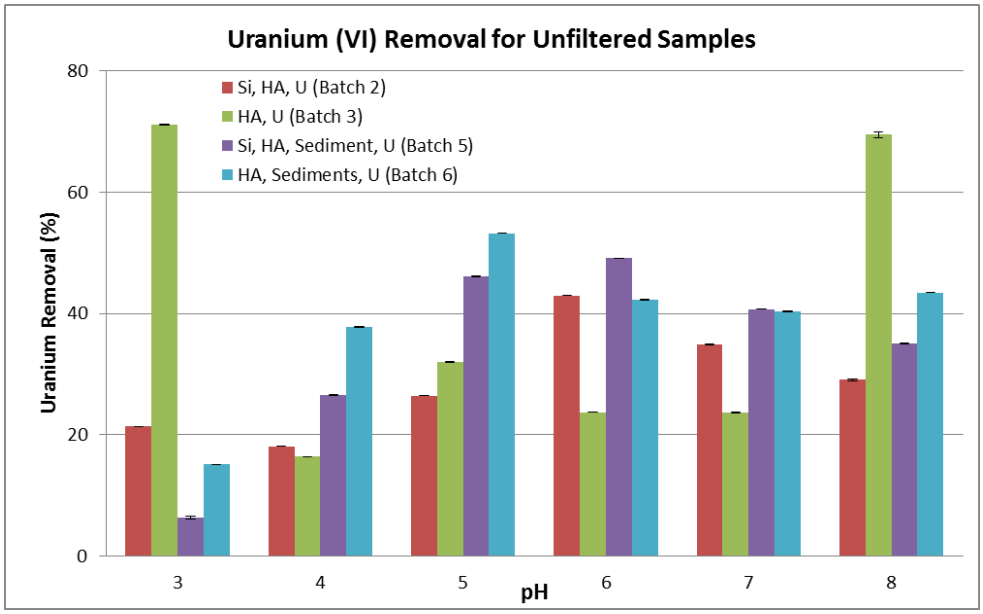

Figure 2-32. Unfiltered uranium removal samples.

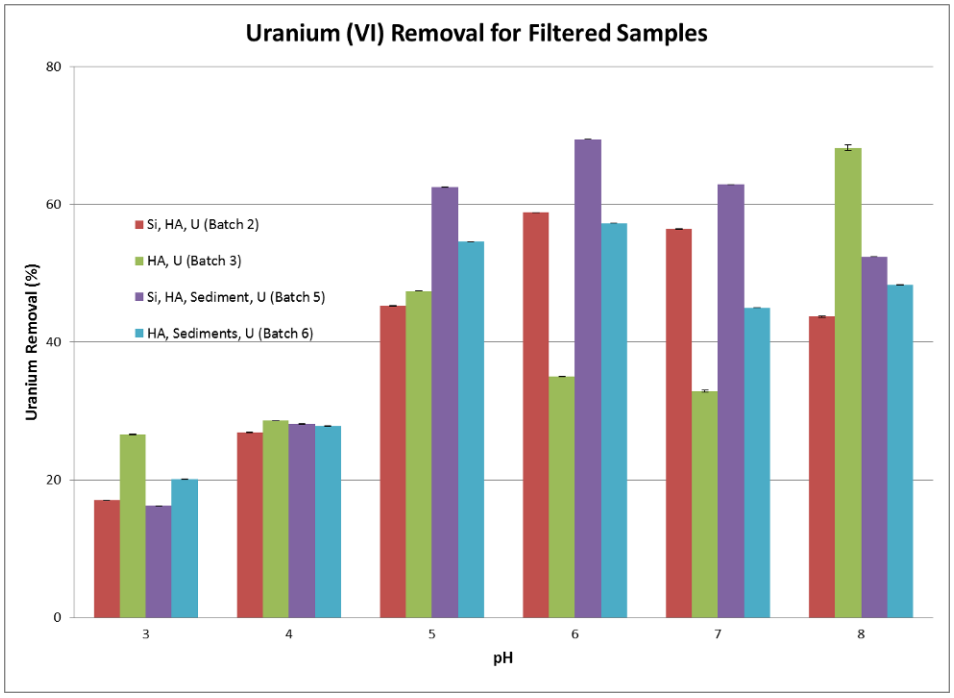

Figure 2-33. Filtered uranium removal samples.

The study conducted during FIU Performance Year 7 highlighted the need to determine the sorption of uranium in the absence of humic acid in order to establish the baseline removal of uranium. Thus, the carryover scope will include batch experiments to estimate uranium removal in the absence of humic acid. The following batch systems will be evaluated at each pH condition between 5 and 8 in the absence of humic acid and with a 30 ppm uranium concentration to determine the removal of U(VI) from the aqueous solution:

- Si (3.5 mM) + U(VI)
- Sediments + U(VI)
- Sediments + Si (3.5 mM) + U(VI)

Subtask 2.3: Humic Acid Batch Sorption and Column Experiments with SRS Soil

Humic Acid Batch Sorption Experiments

During the month of July, it was continued uranium sorption kinetic experiment onto SRS sediments coated with Huma-K (20 ppm) at pH 4 for a time period up to 7 days (Figure 2-34). The results showed that sediments amended with Huma-K significantly increased the removal of uranium (68%) compared to plain sediments (11%). After seven days, the kinetics of uranium sorption onto sediments amended with Huma-K had not reached equilibrium; therefore, the period of sample collection was extended to 10-14 days. In addition, a new set of samples was prepared to study the kinetics of uranium sorption using higher concentrations of Huma-K treated sediments. Initially, 20 mL of Huma-K solution with a fixed concentration of 100 ppm at pH 4 was brought into contact with 200 mg of SRS soil for five days. After five days, the samples were centrifuged and the supernatant was replaced by a solution with ionic strength 0.01M $NaCLO_4^-$ at pH 4. The samples were equilibrated on a platform shaker for three days prior to the addition of uranium (0.5 ppm). The samples were vortex mixed, placed on a platform shaker, and centrifuged. The supernatant was analyzed by KPA for uranium content.

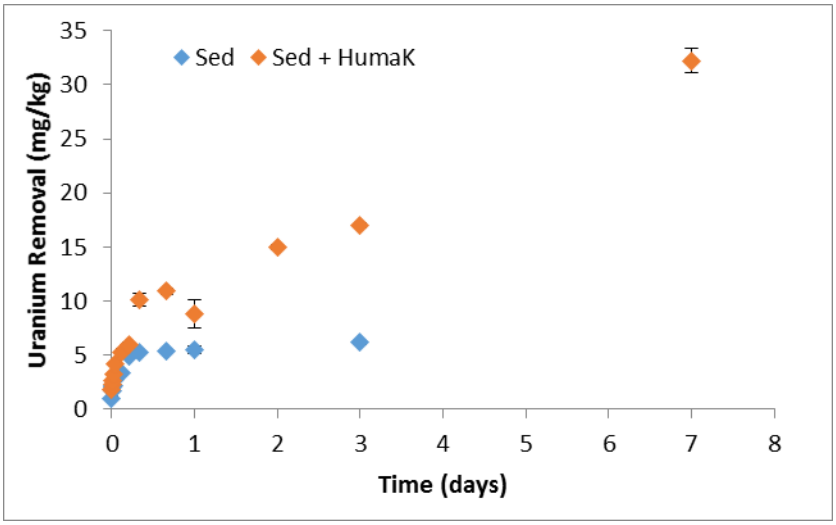

Figure 2-34. Kinetics of uranium sorption onto SRS sediments at pH 4.

During the month of August, the kinetic experiments investigating sorption of uranium onto SRS sediments amended with Huma-K at pH 4 for different periods of time was completed (Figure 2-35). Some previous kinetics studies performed by Tinnacher et al. (2013) suggested that the presence of organic matter in sediments can either slow down or increase the kinetic sorption rate depending on the concentration. The results of our experiments indicate that uranium sorption onto SRS sediments can be either slower or faster in the presence of Huma-K compared to plain sediments. At a concentration of 20 ppm of Huma-K, the characteristic time for uranium sorption to SRS sediment (52.2 h) was significantly increased relative to the corresponding plain sediment system (2.06 h). This indicates that uranium sorption is slowed down in the presence of

low Huma-K concentration. In contrast, at a concentration of 100 ppm of Huma-K, a significant decrease in the characteristic time for uranium sorption (0.98 h) was observed, meaning that uranium sorption kinetics become significantly faster. In addition, SRS sediments with a low content of Huma-K showed an increase in removal of uranium (60%) compared to a higher content of Huma-K (30%) and plain sediment (10%). The percent removal of uranium was calculated by using Eq. (1):

$$R(\%) = \frac{(C_{in} - C_{fin})}{C_{in}} * 100 \qquad [1]$$

where C_{in} is the initial spiked uranium concentration (0.5 ppm) and C_{fin} is the final concentration of uranium left in solution at day 14.

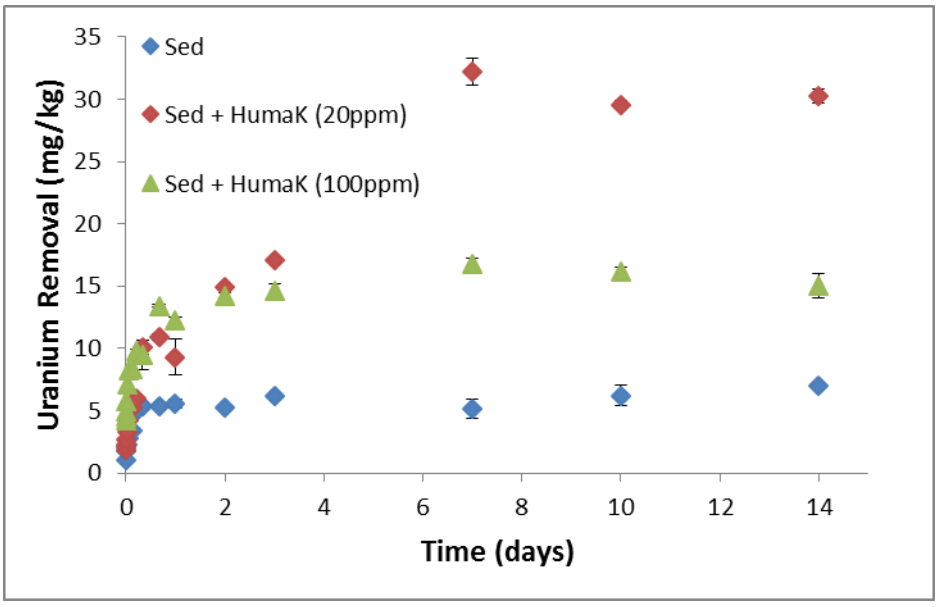

Figure 2-35. Kinetics of uranium sorption at pH 4.

During the month of September, FIU completed an isotherm batch experiment for the sorption of uranium onto SRS sediment. The experiment was conducted by bringing 200 mg of SRS soil into contact with deionized water spiked with uranium (C_i = 25 – 1000 ppb) at pH 4 and constant ionic strength (0.01M $NaCLO_4^-$). The samples were vortex mixed, placed on a platform shaker for seven days and centrifuged. In addition, FIU initiated an isotherm batch experiment for the sorption of uranium onto SRS sediments amended with Huma-K. Initially, 20 mL of Huma-K solution with a fixed concentration (20 ppm) at pH 4 was brought into contact with 200 mg of SRS soil for five days. After five days, the samples were centrifuged and the supernatant was replaced by deionized water spiked with uranium (C_i = 25 – 1000 ppb) at pH 4 and ionic strength 0.01M $NaCLO_4^-$. The samples were vortex mixed, placed on a platform shaker, and centrifuged. FIU also worked on the Project Technical Plan for FIU Performance Year 8 as well as the Year End Report.

Humic Acid Column Experiments

FIU analyzed a set of samples collected during the column experiment via TOC analyzer and compared the concentration of humate with samples analyzed via UV-Vis pre- and post-centrifugation (Table 2-20). Pre-centrifuged samples showed a much higher concentration of humate than post-centrifuged samples as well as for TOC analysis. Even though there was a significant difference in the concentration of humate from post-centrifuged samples to TOC analysis initially, this difference reduced and was within the statistical error once post-centrifuged humate concentration was used from sample 21 onwards. After analyzing the data, humate mass and total recovery was calculated. When 862 mg of humate was injected into the column, 634 mg was recovered; the total amount of humate retained in the column was calculated to be 228 mg, resulting in 857 mg of humate per kg of soil. Figures 2-36 and 2-37 show the changes in pH and the concentration of humate with pore volume (PV). The concentration of humate increased with volume and reached a maximum concentration of about 7100 ppm. When the concentration of effluent reached approximately 20 ppm, 100 ppb uranium was injected into the column. Similar to the humate concentration, the pH increased with volume and reached a maximum of 8.0 and equilibrated around pH 7. The peak in the concentration of humate was due to stopping the flow to inject uranium; the concentration of humate decreased further and reached a steady state after a total of 6 PV.

Table 2-20 Concentration of Sample Before and After Centrifugation and from TOC Analysis

Sample ID	Concentration of modified humic acid (ppm)		
	Pre-centrifuged	Post-centrifuged	TOC Analysis
8	4255.96	3709.09	4033.37
9	7273.20	6368.18	5830.84
10	8178.27	7407.73	7122.69
11	8816.36	8109.20	6967.78
12	9123.86	8352.27	6903.48
13	9051.70	8635.11	7163.61
14	9551.36	8795.34	5906.83
15	8882.39	8410.23	5827.92
16	6895.57	6081.93	4246.73
17	7462.61	3678.98	2582.82
18	6588.07	1843.98	1596.10
19	5544.20	1177.27	1085.80
20	3878.18	845.34	770.43

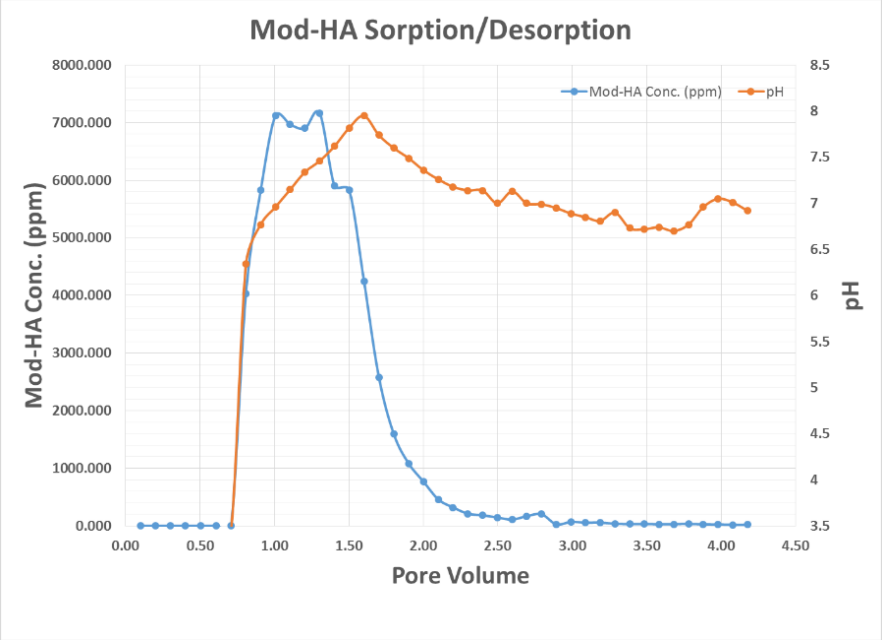

Figure 2-36. Humate breakthrough during sorption and desorption and pH.

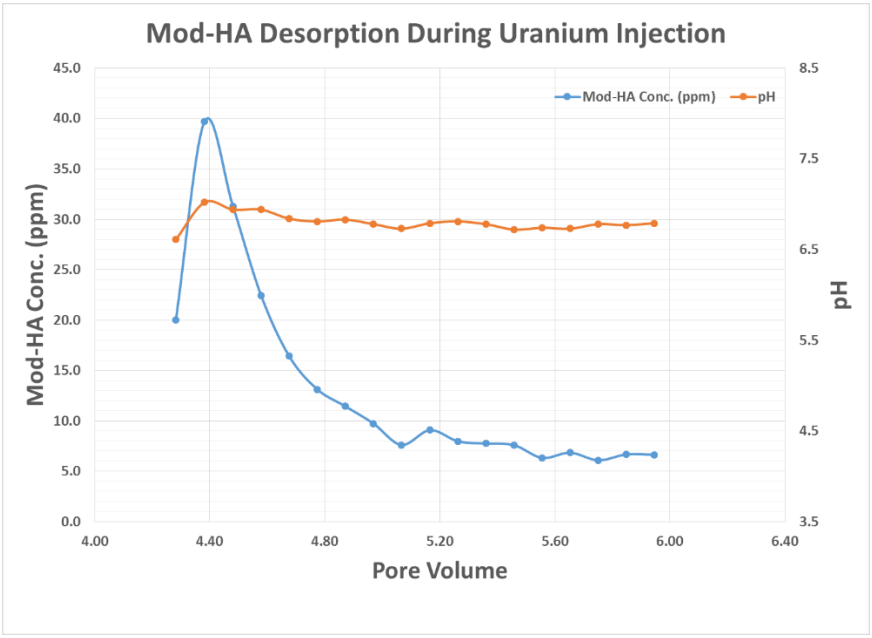

Figure 2-37. Humate breakthrough during sorption and desorption and pH during uranium injection.

FIU next analyzed samples containing uranium that were collected during the column experiment via KPA. Two pore volumes (2 PV) of 100 ppb (20.05 µg) uranium solution at pH 3.5 was injected into the column followed by 2 PV of artificial ground water (AGW) solution at pH 3.5, 4.5 and 5.5, respectively. A total of 81 samples were collected in 5 minute intervals. Several samples were analyzed via KPA and it was observed that the concentration of uranium in the samples was below the detection limit; hence, the samples were subsequently spiked with 100 µL of 100 ppb uranium and re-measured for uranium content. The spike-corrected concentrations were used to estimate the uranium retention in the column; analysis showed that

only 0.59 µg of uranium was recovered, resulting in a 97% retention of uranium in the column. Table 2-21 shows the retention data for the modified humic acid (mod-HA) and uranium. Figure 2-38 shows the change in uranium concentration and pH during the uranium sorption desorption process of the experiment. During uranium injection into the column, the concentration of uranium in the effluent solution was inversely proportional to pH (Figure 2-39); however, during the injection of uranium-free AGW solutions at pH 3.5, 4.5 and 5.5, the uranium concentration in the effluent solution were directly proportional to the change in the pH value (Figure 2-40).

Table 2-21. Sorption and Desorption of Mod-HA and Uranium

Sediment weight (g)	Mod-HA sorption/desorption					Uranium sorption/desorption				
	pH		Modified Humic Acid			pH		Uranium		
	Initial	Final	Injected (mg)	Retained (mg)	Retained (mg/kg)	Initial	Final	Injected (µg)	Recovered (µg)	Retained (µg/kg)
266.42	4.28	6.92	862.22	228.47	857.57	6.92	5.42	20.05	0.59	73.04

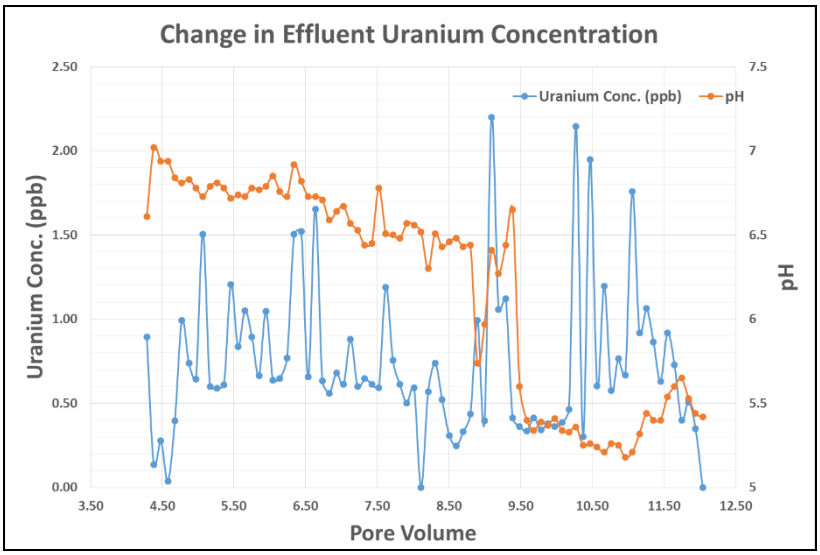

Figure 2-38. Change in uranium concentration and pH during the uranium sorption desorption process.

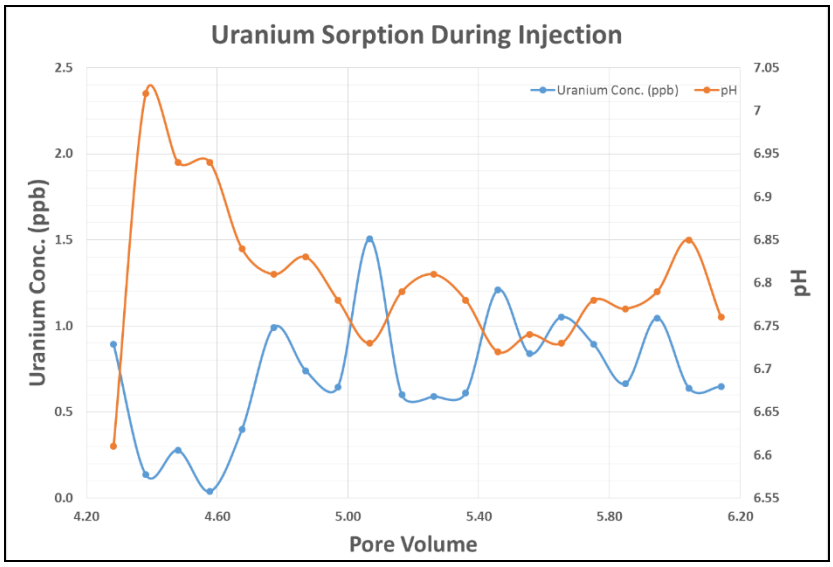

Figure 2-39. Changes in uranium concentration and pH during injection of uranium at pH 3.5.

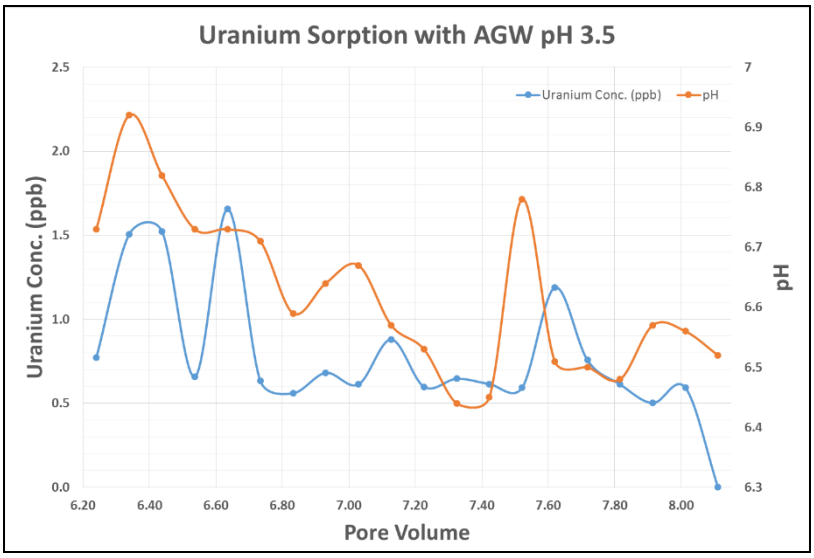

Figure 2-40. Change in uranium concentration and pH during injection of AGW at pH 3.5.

As part of the investigation that FIU is conducting on the relationship between modified humic acid and the mobility of uranium, a rhenium tracer test was conducted to determine the parameters for a flow-through column experiment containing SRS sediment. The parameters found to be: residence time of 52.6 minutes, pore volume of 0.104L, and peclet number of 9. After completing the rhenium tracer test, a flow-through column experiment utilizing modified humic acid and uranium was conducted. Data from the column experiment concluded that out of 862.22 mg of modified humic acid injected into the column, 857.57 mg was retained. As 20.05 µg of uranium was injected, the pH of the column decreased, causing desorption of modified humic acid. From the 20.05 µg of uranium injected, only 0.59 µg of uranium was recovered, resulting in 97% of retention in the column.

Finally, the two columns that were used to investigate the effect of Huma-K and mod-HA on uranium mobility were dismantled and cleaned in order to setup new columns. SRS sediment (300 g) was dried at 35^{o}C for 24 hours and systematically packed into the column. The control experiments will be performed by saturating the column with D.I. water followed by an injection of artificial ground water (AGW) which mimics SRS water characteristics. AGW is added to adjust the overall pH of the column to approximately 3.5. After the column pH has reached equilibrium pH, a uranium solution will be injected into the column and samples will collected for uranium analysis via KPA and for pH measurements. Results obtained during the control column experiments will be compared with results obtained during previous experiments to estimate the effect of Huma-K and mod-HA on uranium mobility.

This subtask will have a carryover scope that includes a uranium sorption column experiment as a control to quantify the effect of modified humate and Huma-K on uranium mobility. The control column experiment will be conducted using SRS sediment and at pH conditions relevant to conditions observed during the completed modified humate and Huma-K injection experiment.

Task 3: Surface Water Modeling of Tims Branch

Task 3 Overview

This task will perform modeling of surface water, and solute/sediment transport specifically for mercury and tin in Tims Branch at the Savannah River Site (SRS). This site has been impacted by 60 years of anthropogenic events associated with discharges from process and laboratory facilities. Tims Branch provides a unique opportunity to study complex systems science in a full-scale ecosystem that has experienced controlled step changes in boundary conditions. The task effort includes developing and testing a full ecosystem model for a relatively well defined system in which all of the local mercury inputs were effectively eliminated via two remediation actions (2000 and 2007). Further, discharge of inorganic tin (as small micro-particles and nanoparticles) was initiated in 2007 as a step function with high quality records on the quantity and timing of the release. The principal objectives are to apply geographical information systems and stream/ecosystem modeling tools to the Tims Branch system to examine the response of the system to historical discharges and environmental management remediation actions.

Task 3 Quarterly Progress

Subtask 3.1. Modeling of Surface Water and Sediment Transport in the Tims Branch Ecosystem

The overall objective of this subtask is to develop an integrated surface water, infiltration loss, and contaminant transport model to investigate the fate and transport of contaminants such as mercury and tin in Tims Branch at SRS. The MIKE SHE/MIKE 11 model being developed for Tims Branch can be used as a tool to better understand the effect of extreme weather on flow in Tims Branch. The results of the hydrology model will be used to assess the fate and transport of remedial by-products, such as tin dioxide or other existing solutes (e.g. uranium, nickel, other metals and radionuclides), that may have direct or indirect impact on the environment in SRS. The outcome of such a model can determine spatial and temporal distribution of suspended particles or contaminants in the area when storms or heavy rainfalls occur.

The work during this reporting period included:

- Literature review on MIKE SHE sensitivity analysis. The results of the model (shown in the Table 2-22) are consistent with previous sensitivity analysis studies.

Table 2-22. MIKE SHE Sensitivity Analysis

Parameter	Value	Number of Simulations	Total Simulation Time (hrs)	Results
Detention Storage (mm)	0.0, 2.5 (± 5%, ±10%, ±15%, ±20%)	10	80	Insensitive
Surface-Subsurface Leakage (sec^{-1})	0.0, 0.0001 (± 5%, ±10%, ±15%, ±20%)	10	80	Insensitive
Initial Water Depth (m)	From previous simulation	22	176	Highly Sensitive
Separated Flow Area	Yes/No	2	16	Highly Sensitive

- Various methods of rainfall analysis are also under review to identify a method that can be used to represent the rainfall intensity in the SRS area.
- Literature review on MIKE SHE calibration methods. Methods that have been considered for calibration include:
    - Selecting five storm events based on a method implemented by Rogers et al. (1985).
    - Using two-year timeseries of daily stream flow measured by a USGS stage gauge downstream of Tims Branch based on Xevi et al. (1997).
    - The methods described by Wijesekara (2013) in his dissertation entitled "An integrated modeling system to simulate the impact of land-use changes on hydrological processes in the Elbow River watershed in Southern Alberta [Ph.D.: University of Calgary]" as well as another one of his publications (Wijesekara, 2014).
- Literature review on MIKE SHE uncertainty analysis and measurement. This review will be used to develop background and introduction sections for the planned publication.
- Simulated timeseries of flow velocity and depth are being created for each MIKE SHE simulation.
- A compressive literature review is being completed to support a future publication on hydrology of the streams and outfalls at SRS.
- MIKE 11 activities included:
    - Previous model evaluation for A-014 outfall
    - Preliminary model development for Tims Branch
    - Topography modification

- Cross section preparation (measured during the last field work on June 2017)
- Tims Branch stream network delineation
- Selecting boundary conditions
- Review of the stream model to eliminate the associated errors with recent model modifications with boundaries and topography.

References:

Ahmed, F., 2010, Numerical modeling of the Rideau valley watershed: Natural hazards, v. 55, no. 1, p. 63-84.

Ahmed, F, 2014, Calibration of hydrologic model in a data-limited watershed: Tay Basin, Canada: Journal of Civil Engineering (IEB), v. 42, no. 1, p. 1-37.

Bosson, E., Sassner, M., Sabel, U., and Gustafsson, L.-G., 2010, Modelling of present and future hydrology and solute transport at Forsmark. SR-Site Biosphere: Swedish Nuclear Fuel and Waste Management Co., Stockholm (Sweden).

Larsen, M. A., Refsgaard, J. C., Jensen, K. H., Butts, M. B., Stisen, S., and Mollerup, M., 2016, Calibration of a distributed hydrology and land surface model using energy flux measurements: Agricultural and Forest Meteorology, v. 217, p. 74-88.

Rogers, C., Beven, K., Morris, E., and Anderson, M., 1985, Sensitivity analysis, calibration and predictive uncertainty of the Institute of Hydrology Distributed Model: Journal of Hydrology, v. 81, p. 179-191.

Tu, V. T., and Tingsanchali, T., Flood hazard and risk assessment of Hoang Long River basin, Vietnam2010.

Vázquez, R., Feyen, L., Feyen, J., and Refsgaard, J., 2002, Effect of grid size on effective parameters and model performance of the MIKE-SHE code: Hydrological processes, v. 16, no. 2, p. 355-372.

Wijesekara, G., Farjad, B., Gupta, A., Qiao, Y., Delaney, P., and Marceau, D., 2014, A Comprehensive Land-Use/Hydrological Modeling System for Scenario Simulations in the Elbow River Watershed, Alberta, Canada: Environmental Management, v. 53, no. 2, p. 357-381.

Xevi, E., Christiaens, K., Espino, A., Sewnandan, W., Mallants, D., Sorensen, H., and Feyen, J., 1997, Calibration, Validation and Sensitivity Analysis of the MIKE-SHE Model Using the Neuenkirchen Catchment as Case Study: Water Resources Management, v. 11, no. 3, p. 219-242.

Subtask 3.2. Application of GIS Technologies for Hydrological Modeling Support

The data collected during FIU ARC's visit to SRS in June 2017 is currently being integrated into the SRS geodatabase. The raw data coordinate data of the sample locations will be imported into ArcGIS for conversion to a point shapefile, which will then be merged with the other locations formerly sampled in August 2016. The cross section profile measurements will also be imported using ArcGIS and MIKE HYDRO tools for implementation in the MIKE 11 model of the main

Tims Branch stream which will be developed during FIU Performance Year 8. The use of GIS tools will remain a continuous integrated component of the hydrological model development. Over the next few months, GIS will be used for cross section delineation and for preparing maps and charts of the study area that depict model results.

Subtask 3.3. Biota, Biofilm, Water and Sediment Sampling in Tims Branch

DOE Fellow Ron Hariprashad completed his summer internship at SREL based on scope developed in collaboration with SREL and SRNL researchers, which involved the collection of field data as well as water and biofilm samples from Tims Branch. Mr. Hariprashad presented details of his internship during the DOE-FIU Cooperative Agreement Research Review held via video teleconference on July 18, 2017.

Permitting for the installation of a dedicated monitoring station in Tims Branch just below Steed Pond was approved and the ISCO sampler was successfully installed by Mr. Hariprashad with the aid of SREL's research professional, Paul Stankus. The unit is expected to provide estimates of discharge rates that can be used to direct sampling events. The unit also has a turbidity sensor that can provide estimates of sediment loading. Once the station is operational, stream samples representing base flow and episodic precipitation events will be collected for extensive characterization. The data from this device will be periodically downloaded by SREL personnel and shared with FIU to support hydrological model calibration.

The field data collected during the internship is being tabulated and converted to GIS and MIKE compatible formats. Water samples were analyzed for heavy metals via ICP-MS at SREL and biofilm samples were analyzed via XRF analysis at the SRNL laboratories. The results are currently under review. SREL researchers are also considering digesting a small fraction of the biofilm samples and analyzing them with a low-level alpha/beta counter to see if there are elevated radionuclide concentrations at levels unable to be detected using traditional counting methods. Results can be compared with earlier work from samples collected at that location to examine U and Ni movement, both baseline and during storm events.

The cross-section profiles collected along the main Tims Branch stream are being implemented in the MIKE 11 model to delineate the stream network using ArcGIS and MIKE Hydro tools. This data will assist in calibration of the hydrological models being developed by FIU.

Task 5 Quarterly Progress

Column and sequential batch experiments at 0.1 and 5 M ionic strength (IS) were finalized during the July – September quarter. Solid samples from sequential batch and column experiments were washed, dried, and sent to National Petrographics for thin sectioning and polishing for microscopy. Solids recovered from the columns were also subjected to a leaching. Preliminary results for the batch and column experiments are presented below.

DOE Fellow Frances Zengotita presented a poster entitled "The role of *Chromohalobacter* on the transport of lanthanides and cesium in the dolomite mineral system" at the LANL summer intern competition on August 9, 2017. In addition, postdoc Hilary Emerson presented a poster entitled "The role of ionic strength on sorption of neodymium on dolomite" at the Fall American Chemical Society meeting on August 23, 2017.

Preliminary batch and column results

Batch kinetics

Results are presented below for 0.01, 0.1, 0.5, 1.0, 2.0, and 5.0 M ionic strength (0.003 M $NaHCO_3$ + NaCl) (Figure 2-41). It should be noted that 3.0 M ionic strength data has not yet been analyzed. These data show that removal of Nd increases with ionic strength. The current working hypothesis is that either (1) removal increases with ionic strength due to increased mineral dissolution leading to greater re-precipitation and incorporation of Nd with increasing ionic strength or (2) a change in aqueous speciation with increasing ionic strength due to changes in aqueous activity lead to increased adsorption. The latter hypothesis has been highlighted in previous work on different solid phases as discussed in previous monthly reports.

Sequential batch

Sequential batch experiments were conducted with 15 sequential additions of 40 mL of 20 ppb Nd solutions at 0.1 or 5.0 M ionic strength (3 mM $NaHCO_3$ + NaCl) with 0.2 grams of dolomite. After approximately 5 days, the solutions were removed and replaced with a fresh stock solution. The five day contact time was chosen because equilibrium was reached by 48 hours in batch kinetics experiments (Figure 2-41). These data show that approximately an order of magnitude more Nd is removed at higher ionic strength and is consistent with previous kinetics (Figure 2-42). Based on these aqueous phase measurements by ICP-MS, the loading of Nd on these samples is 34 and 58 µg/g for 0.1 and 5.0 M ionic strength, respectively. Further, two wash steps were employed with pH adjusted 18 MΩ*cm H_2O which removed a negligible amount of Nd (<0.02% of total Nd on the solid) prior to drying of solids at 30°C for preparation for microscopy.

Miniature columns

Results are presented for variable ionic strength (0.1 and 5.0 M via 0.003 M $NaHCO_3$ + 20 ppb Nd + NaCl) solutions injected into one gram mini columns packed with dolomite mineral at 1.5 mL/hr. More than 11.5 L of solution (>40,000 pore volumes) was injected into the columns over a period of nearly a year. These data are distinctly different from the batch experiments because there is not a significant difference in breakthrough as compared to the variable ionic strengths. Therefore, the first hypothesis presented in the description of the batch experiments can be excluded as similar Nd speciation should be present in the aqueous phase whether it is a batch or column experiment.

The difference between the column and batch experimental results is likely due to (1) a lack of equilibrium being reached within the columns with respect to adsorption of Nd or (2) a lack of re-precipitation and incorporation processes taking place within the column as compared to batch experiments. However, because the variable ionic strength batch experiments are significantly different after 15 minutes of contact time (Figure 2-41), the first hypothesis can be effectively discarded. An equilibrium, one-dimensional, constant dispersivity model is presented in Figure 2-44 and shows the significant differences in breakthrough that would be observed for the 0.1 and 5.0 M K_d values observed at 24 hours in batch experiments. The model dispersivity was estimated based on a Br^- tracer breakthrough curve conducted as part of DOE Fellow Zengotita's internship.

Therefore, it is most likely that the column and batch experiments are different due to the effects of re-precipitation and incorporation of Nd which would likely not occur with the constant flow and refresh in the column experiments. Further, as described in the July monthly report, samples are under preparation for microscopy to observe potential precipitate formation and incorporation of Nd with respect to depth in the particles via electron microprobe analysis.

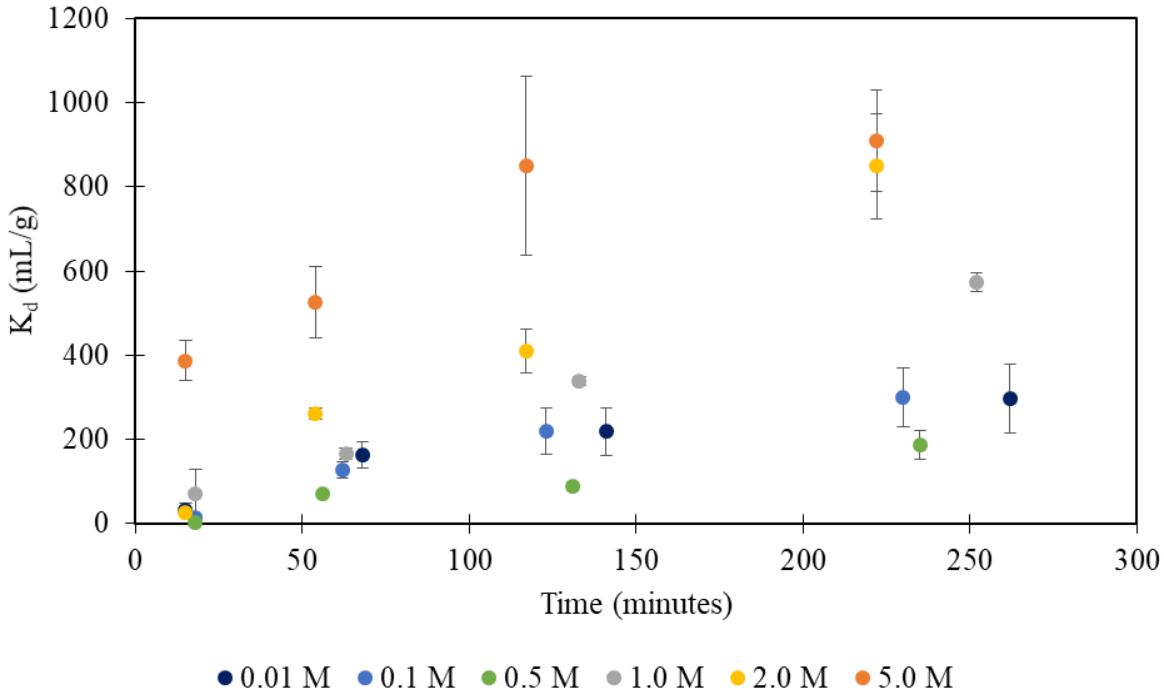

Figure 2-41. Results for batch kinetics experiments for 20 ppb Nd sorption to 5 g/L dolomite suspensions at variable ionic strength (0.003 M NaHCO3 + NaCl). Note: error bars are based on triplicate samples.

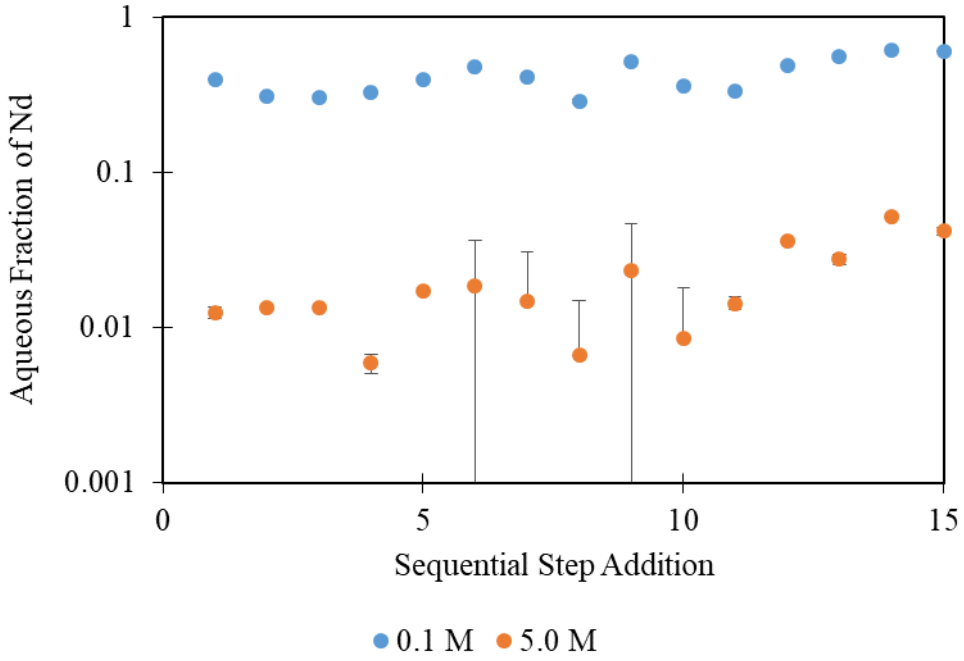

Figure 3-42. Results for sequential addition of 20 ppb Nd at 0.1 or 5 M ionic strength (0.003 M NaHCO3 + NaCl) to 1.25 g/L suspensions of dolomite. Note: each sequential addition equilibrated for at least five days to reach equilibrium based on kinetics and error bars are based on error of triplicate analysis by ICP-MS.

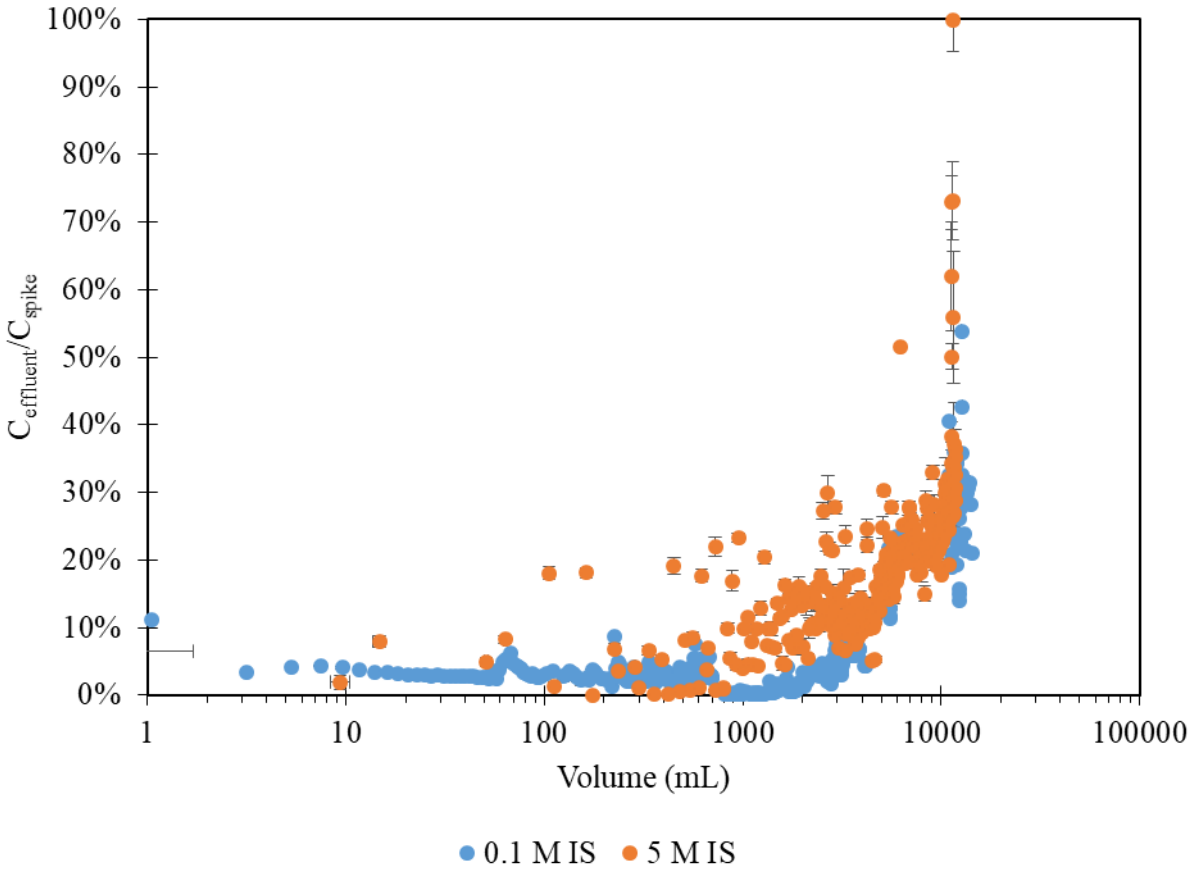

Figure 2-43. Nd breakthrough in effluent for 0.1 and 5.0 M ionic strength input through dolomite mini columns with an influent Nd concentration of 20 ppb and 1.5 mL/hr flow rate. Note: error is based on triplicate measurement by ICP-MS.

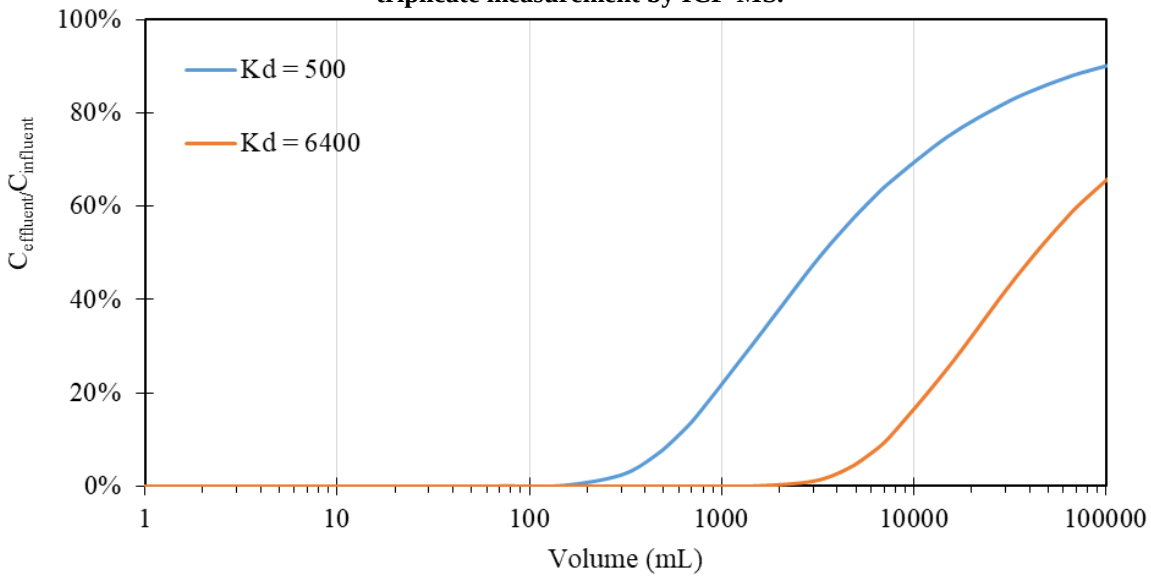

Figure 2-44. Predicted Nd breakthrough for a 1-D, constant dispersivity model with an influent Nd concentration of 20 ppb, Kd = 500 and 6400 mL/g estimated for 0.1 and 5.0 M ionic strength, respectively, based on batch experimental results.

Analysis of samples polished by National Petrographics was begun in September. These data will be presented in the October monthly report as analysis is still ongoing via both SEM EDS. In addition, the project technical plan scope was finalized with Los Alamos National Laboratory collaborators and work on draft publications and the Year End Report continued. FIU Performance Year 8 will focus on the interactions of actinides and lanthanides with relevant ligands and minerals for the WIPP.

Upcoming efforts include analysis of the batch and column solids for samples sent to National Petrographics for polishing in July 2017. A publication of the work performed during FIU Performance Year 7 is targeted for November 2017.

Milestones and Deliverables

The milestones and deliverables for Project 2 for FIU Performance Year 7 are shown on the following table. FIU completed a set of batch experiments for uranium removal by Huma-K sorbed on SRS sediments (milestone 2016-P2-M6). FIU has reforecast the technical report deliverable on the surface water modeling of Tims Branch (Project 2, Task 3) from August 17, 2017, and will now be submitting it with the Year End Report to allow for the inclusion of additional results derived from the laboratory analyses of samples collected from Tims Branch at SRS during DOE Fellow Ron Hariprashad's summer 2017 internship at the Savannah River Ecology Laboratory (SREL). FIU has communicated all project research progress and solicited agreement to any changes to the planned schedule during regularly scheduled teleconferences with FIU's research collaborators at SRNL and SREL as well as SRS contacts and DOE HQ. Milestones and deliverables reforecast to be completed as carryover scope with the last increment of FIU Performance Year 7 funding from DOE are also shown below.

FIU Performance Year 7 Milestones and Deliverables for Project 2

Task	Milestone/ Deliverable	Description	Due Date	Status	OSTI
Project	2016-P2-M1	Submit three draft papers to Waste Management 2017 Symposium	11/4/16	Complete	
Task 1: Hanford Site	2016-P2-M2	Submit abstract to ACS Spring Conference (Subtask 1.1)	11/30/16	Complete	
	2016-P2-M5	Complete training on LSC analytical technique and trial-and-error experiments for separations and determination of Tc(IV) and Tc(VII) (Subtask 1.4)	1/27/17	Complete	
	2016-P2-M9	Complete batch experiments on the biodissolution of Na-autunite (Subtask 1.2)	3/20/17	Complete	
	Deliverable	Technical report on the results of columns monitoring using geochemical and SIP analyses (Subtask 1.3)	1/30/17	Complete	
Task 2: SRS	2016-P2-M4	Complete the creation of acid-impacted soil samples through conditioning of SRS F/H Area soil	12/15/16	Complete	

		with acidified water in columns (Subtask 2.1)			
	Deliverable	Technical report on the Investigation on the Properties of Acid-Contaminated Sediment and its Effect on Contaminant Mobility (Subtask 2.1)	2/13/17	Complete	
	2016-P2-M6	Complete batch experiments of uranium removal by Huma-K sorbed on SRS sediments (Subtask 2.3)	2/15/17	Complete	
	2016-P2-M7	Complete a set of column experiments using modified humic acid (Subtask 2.3)	2/28/17	Complete	
	Deliverable	Technical report on the synergy between colloidal Si and HA on the removal of U(VI) (Subtask 2.2)	3/31/17	Reforecast to 12/15/17	
	Deliverable	Technical report on the Investigation of the Removal of Uranium by Huma-K Sorbed on SRS Sediments via Batch Experiments (Subtask 2.3)	4/3/17	Reforecast	
Task 3: Tims Branch	2016-P2-M3	Complete development of MIKE 11 stream flow model for A-014 outfall (Subtask 3.1)	12/8/16	Complete	
	2016-P2-M8	Complete calibration of MIKE SHE and MIKE 11 models (Subtask 3.1)	3/1/17	Complete	
	2016-P2-M10	Complete coupling of MIKE SHE and MIKE 11 models (Subtask 3.1)	5/5/17	Reforecast to FIU Performance Year 8	
	Deliverable	Technical report on the surface water modeling of Tims Branch (Task 3)	6/15/17	Reforecast to YER	
Task 5: WIPP	Deliverable	Technical report on the effect of ionic strength on the sorption of neodymium to dolomite (Task 5)	5/12/17	Complete	

Work Plan for Next Quarter

Project-wide:

- Draft the Year End Report (YER) for FIU Performance Year 7.
- Draft the Project Technical Plan (PTP) for FIU Performance Year 8.

Task 1: Remediation Research and Technical Support for the Hanford Site

Subtask 1.1 – Remediation Research with Ammonia Gas for Uranium

- Analyze solids treated with ammonia gas via SEM and prepare in epoxy for EMPA.
- Finalize experimental data in the presence of minerals including statistical comparison of results for each treatment.
- Develop publication for DOE Fellow Silvina Di Pietro's summer 2016 internship investigating mineral dissolution kinetics with basic treatment.
- Finalize publication comparing treatment of batch samples with NaOH, NH_4OH and NH_3 gas on mineral dissolution/precipitation and uranium removal.
- Finalize low Si/Al experimental data.

Subtask 1.2. Investigation on Microbial-Meta-Autunite Interactions - Effect of Bicarbonate and Calcium Ions

- Complete the carryover scope for this task.

Subtask 1.3. Investigation of Electrical Geophysical Response to Microbial Activity in the Saturated and Unsaturated Environments

- Complete U(VI) analysis of porewater samples collected during the fall of 2016.
- Prepare new samples and conduct SEM/EDS analysis for columns 1 and 2. Prepare samples and conduct SEM/EDS analysis for columns 5 and 6.
- Conduct speciation modeling to predict the formation of solid phases.
- Initiate preparations for new columns experiments for FIU Year 8.

Subtask 1.4: Contaminant Fate and Transport under Reducing Conditions

- Conclude bicarbonate-free experiments of pertechnetate reduction.
- Initiate pertechnetate reduction experiments at pH 8 in the presence of bicarbonates.
- Conclude dissolution experiments of TcO_2 in low bicarbonates concentration (5 mM) and initiate at high bicarbonate concentration (50 mM).

Task 2: Remediation Research and Technical Support for Savannah River Site

Subtask 2.1. FIU's Support for Groundwater Remediation at SRS F/H –Area

- Complete the carryover scope for this subtask.

Subtask 2.2 – The Synergistic Effect of Humic Acid and Colloidal Silica on the Removal of Uranium (VI)

- Prepare technical report on synergy between colloidal silica and HA on the removal of uranium.
- Submit a draft paper to Waste Management Symposia 2018.

Subtask 2.3. Humic Acid Batch Sorption and Column Experiments with SRS Soil

- Finalize isotherm batch experiment for the sorption of uranium onto SRS sediments amended with Huma-K.

- Conduct batch desorption experiments of uranium from SRS sediment with and without amended Huma-K at pH 4.
- Perform a column experiment to estimate uranium removal due to sorption onto the soil; this experiment will act as a control column test.

Task 3: Surface Water Modeling of Tims Branch

Subtask.3.1. Modeling of surface water and sediment transport in the Tims Branch ecosystem

- Continue sensitivity analysis with various parameters such as detention storage, reference evapotranspiration, vegetation dynamics, etc., and perform simulations, graphing the results to compare the effect of the various parameters on overland flow.
- Assist DOE Fellows with completion of their summer internship reports, master's thesis proposal (including literature review, preliminary data collection, etc.) and review of a poster to be presented at the annual DOE Fellows Exhibition/Competition as part of the DOE Fellows program.

Subtask 3.2. Application of GIS technologies for hydrological modeling support

- Complete the integration of the sampling location and water quality data collected during FIU ARC's visit to SRS in June 2017 into the existing geodatabase and generate shapefiles that can be used in the MIKE SHE and MIKE 11 models.
- Import the cross section profile measurements using ArcGIS and MIKE HYDRO tools for implementation in the MIKE 11 model of the main Tims Branch stream which will be developed during FIU Performance Year 8.
- Use GIS for cross section delineation and for preparing maps and charts of the study area that depict model results.

Subtask 3.3. Biota, biofilm, water and sediment sampling in Tims Branch

- Assemble and test the HOBO RX3000 Remote Monitoring System purchased by FIU in a nearby stream and use to train DOE Fellow students prior to its deployment at SRS. This instrument is a water level data logger which has a web-based configuration so that timeseries data is stored and managed via the internet in the HOBOlink service cloud. HOBOlink allows the user to access current and historical data and manage and control the configuration of sensors, logging rates, alarm notifications and relay activations.
- Begin discussions with collaborators at SRNL and SREL in preparation for a fieldtrip in January 2018 to deploy one or two HOBO units in Tims Branch. Discussions will include time and budget availability for FIU staff and students to travel to SRS, availability of SRNL/SREL collaborators, required SRS site permitting, etc.
- Follow up with SREL on data derived from the ISCO installation over the summer.

Task 5: Remediation Research and Technical Support for WIPP

- Finalize and submit a publication on sorption and incorporation of Nd at variable ionic strengths
- Model breakthrough results from column experiments

- Conduct mini column experiments investigating transport of Nd complexed with relevant ligands
- Initiate a publication based on DOE Fellow Frances Zengotita's summer internship results

Project 3
Waste and D&D Engineering & Technology Development

Project Manager: Dr. Leonel E. Lagos

Project Description

This project focuses on delivering solutions under the decontamination and decommissioning (D&D) and waste areas in support of DOE EM. This work is also relevant to D&D activities being carried out at other DOE sites such as Oak Ridge, Savannah River, Hanford, Idaho and Portsmouth. The following tasks are included in FIU Performance Year 7:

Task No	Task
Task 1: Waste Information Management System (WIMS)	
Subtask 1.1	Maintain WIMS – database management, application maintenance, and performance tuning
Subtask 1. 2	Incorporate new data files with existing sites into WIMS
Task 2: D&D Support to DOE EM for Technology Innovation, Development, Evaluation and Deployment	
Subtask 2.1	D&D Technology Demonstration & Development and Technical Support to SRS's 235-F Facility Decommissioning
Subtask 2.2	Technology Demonstration and Evaluation
Subtask 2.3	Support to DOE EM-4.11 and the D&D Community
Task 3: D&D Knowledge Management Information Tool	
Subtask 3.1	Outreach and Training (D&D Community Support)
Subtask 3.2	Mobile Native Applications Development
Subtask 3.3	Data Mining and Visualization
Subtask 3.4	Social Media Integration
Subtask 3.5	IT Administration and Support

Task 1: Waste Information Management System (WIMS)

Task 1 Overview

This task provides direct support to DOE EM for the management, development, and maintenance of a Waste Information Management System (WIMS). WIMS was developed to receive and organize the DOE waste forecast data from across the DOE complex and to automatically generate waste forecast data tables, disposition maps, GIS maps, transportation details, and other custom reports. WIMS is successfully deployed and can be accessed from the web address http://www.emwims.org. The waste forecast information is updated at least annually. WIMS has been designed to be extremely flexible for future additions and is being enhanced on a regular basis.

Task 1 Quarterly Progress

The Waste Information Management System (WIMS) was developed to receive and organize the DOE waste forecast data from across the DOE complex and to automatically generate waste forecast data tables, disposition maps, GIS maps, transportation details, and other custom reports. WIMS is successfully deployed and can be accessed from the web address http://www.emwims.org. The 2017 waste data set was integrated into WIMS and made available on the website on May 10, 2017. During this reporting period, FIU performed database management, application maintenance, and performance tuning to the online WIMS in order to ensure a consistent high level of database and website performance.

An abstract based on this research was accepted by the Waste Management 2018 Symposium for a poster presentation:

> **Abstract**: 18302
> **Title**: Waste Information Management System with 2017-18 Waste Streams
> **Authors**: Himanshu Upadhyay, Walter Quintero, Leonel Lagos, Peggy Shoffner

FIU also began development of the related conference paper.

Task 2: D&D Support to DOE EM for Technology Innovation, Development, Evaluation and Deployment

Task 2 Overview

This task provides direct support to DOE EM for D&D technology innovation, development, evaluation and deployment. For FIU Performance Year 7, FIU will assist DOE EM-4.11 in meeting the D&D needs and technical challenges around the DOE complex. FIU will expand the research in technology demonstration and evaluation by developing a phased approach for the demonstration, evaluation, and deployment of D&D technologies. One area of focus will be working with the Savannah River Site to identify and demonstrate innovative technologies in support of the SRS 235-F project. FIU will further support the EM's International Program and the EM-4.11 D&D program by participating in D&D workshops, conferences, and serving as subject matter experts.

Task 2 Quarterly Progress

Subtask 2.1.1: Adaptation of Intumescent Coatings

The objective of this research task is to improve the operational performance of fixatives to mitigate the release of radioisotopes during fire and/or extreme heat conditions. FIU has performed a series of tests to subject test coupons of intumescent coatings (IC) to increasing temperatures using a muffle furnace along with adhesion and impact testing of these test coupons on various types of substrates, both before and after exposure to extreme heat conditions. FIU used the ASTM D3359 standard protocol during the adhesion testing in order to quantify the ability of two selected intumescent coatings (FX and FD) to adhere to stainless steel substrates under various conditions. The results will serve as the basis for future testing efforts designed to determine the impacts of fixatives/intumescent coatings on the airborne release fraction (ARF) and respirable fraction (RF) coefficients in the source term formula used to calculate a facility's safety basis.

The following abstract (submitted by SRNL) has been accepted by the Waste Management 2018 Symposium for presentation. The abstract is based on the collaborative research being performed on fixatives/intumescent coatings:

> **Abstract**: 18556
> **Title**: Environmental and Radiological Readiness of Fixatives and Intumescent Coatings for D&D Applications
> **Authors**: Aaron Washington[1], James Nicholson[1], Joseph Sinicrope[2], Peggy Shoffner[2], Leonel Lagos[2], Mike Serrato[1] ([1]SRNL; [2]FIU)

During this reporting period, FIU worked on developing the technical report for this subtask, which will be combined with the technical report on subtask 2.2.2 for the testing and demonstration of the application of intumescent coatings in a hot cell test bed under nonradioactive conditions.

Subtask 2.1.3: Robotic Technologies for D&D Applications

As part of this subtask during FIU Performance Year 6, FIU performed research to identify robotic technology systems applicable to the challenges and needs of the SRS 235-F Facility. Research utilized the Robotic Database in D&D KM-IT to search and identify potential robotic technologies and compiled a spreadsheet of all of the available robotic technologies in the database. During FIU Performance Year 7, FIU is coordinating with SRNL to leverage the research already completed to assist in identifying cross-cutting applications of robotic technologies being developed at FIU in the high-level waste research area that could potentially be used in support of D&D activities.

Based on initial observations and finding from Phase II of the Incombustible Fixatives Test Plan, a potential requirement for a remote dry film thickness gauge capability has been identified. Determining the precise thickness of fixatives applied in restricted spaces and confirming they are within specified parameters throughout the area has proven exceptionally challenging. It is possible that one of ARC's remote / robotic platforms could be modified and paired with a dry film thickness gauge to validate the thickness of the fixative application throughout the radioactive space.

Activities during this reporting period for this task have included:

- developing a conceptual design for the inspection tool, and
- evaluating deployable coating thickness sensors.

FIU also briefly investigated different communication methods between microcontrollers and sensors, searching for a better alternative for tether construction. For this task, FIU is planning to use a controller area network (CAN bus) in the tether design.

The conceptual design is based on an existing wall climbing platform currently being developed at FIU. The existing technology, shown in Figure 3-1, has the potential to be successfully deployed to measure thickness of fixative coatings. These type of coatings are applied to stabilize radioactive contamination during D&D activities of hot cells.

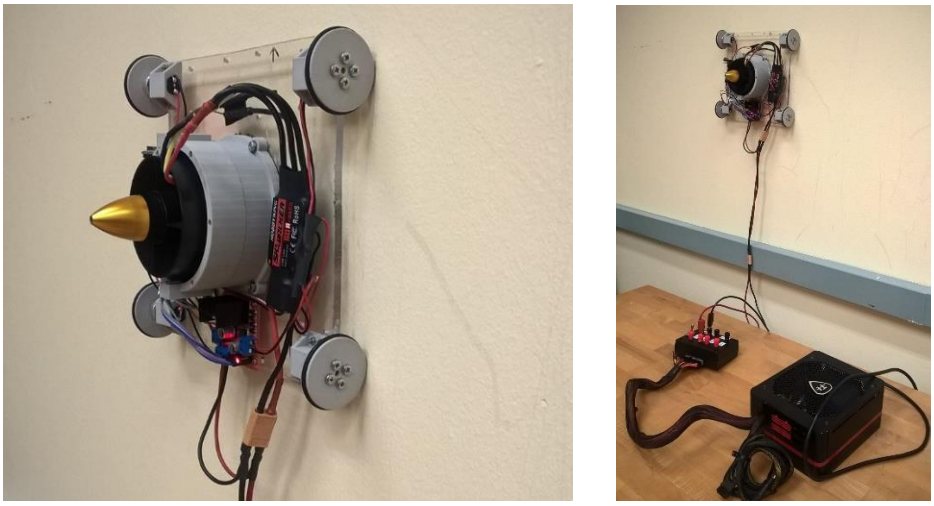

Figure 3-1. FIU wall crawler technology.

The conceptual design shown in Figure 3-2 is an articulate wall crawler developed to climb walls and ceilings as well as transition between floor-and-wall, wall-and-wall, and wall-and-ceiling. The tool will also be capable of mapping the inside of the hot cell, overcoming obstacles, and potentially carrying additional instrumentation.

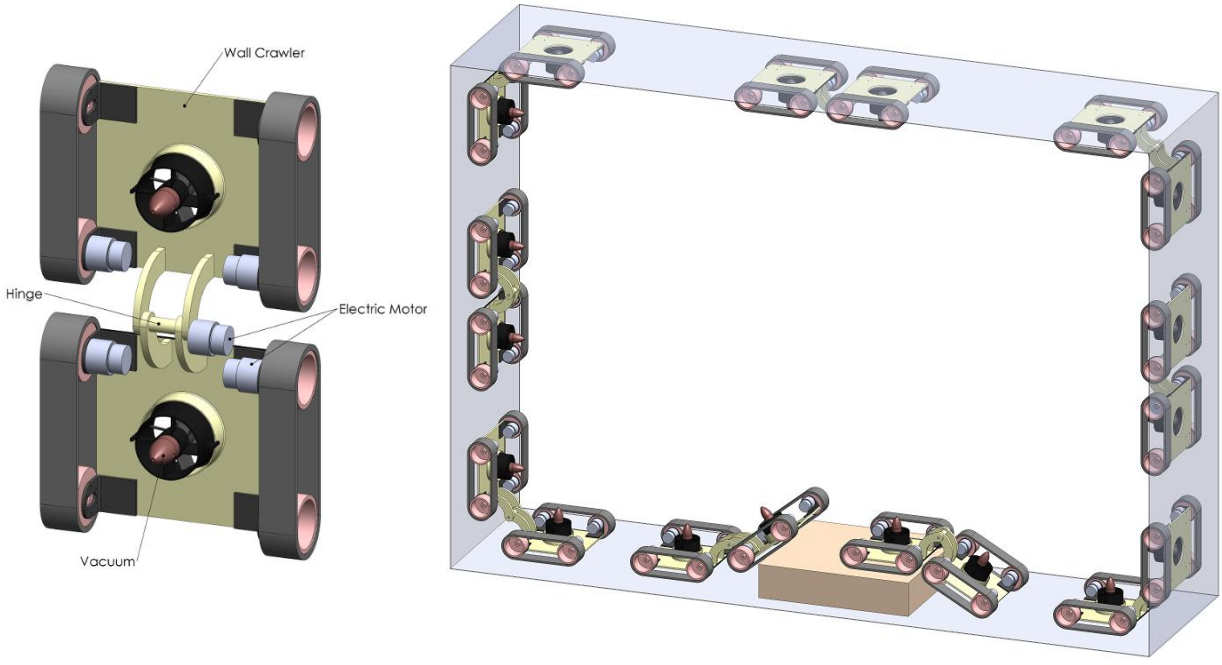

Figure 3-2. Wall crawler conceptual design.

Figure 3-3 shows the sensor currently being used at FIU to measure coating thickness. The device is a fully electronic coating thickness gauge that uses magnetic and eddy current principles on both ferrous and non-ferrous metals.

Figure 3-3. PosiTector 6000 coating thickness gage.

The current electronic coating thickness gauge is accurate and versatile. However, in the current package and size, it will be difficult to deploy. The typical fixative thickness is around 1/8th of an inch, and the team is researching alternative sensors suitable for integration and deployment.

Task 2.2: Technology Demonstration and Evaluation

The primary objective of this task is to standardize and implement proven processes to refine and better synchronize DOE-EM technology needs, requirements, testing, evaluation, and acquisition by implementing a three-phased technology test and evaluation model. The development of uniformly accepted testing protocols and performance metrics is an essential component for testing and evaluating D&D technologies.

Subtask 2.2.1: Uniform Testing Protocols and Performance Metrics for D&D

An abstract based on this research was accepted for an oral presentation by the Waste Management 2018 Symposium. FIU began development of the related conference paper.

> **Abstract**: 18315
> **Title**: International Standards Development and Its Role in Transitioning D&D Technologies to Deployment
> **Authors**: Joseph Sinicrope, Peggy Shoffner, James Nicholson (SRNL), Rick Demmer (INL), Leonel Lagos

The development of uniformly accepted testing protocols and performance metrics is an essential component for testing and evaluating D&D technologies. During FIU Performance Year 6, an FIU representative obtained official membership on ASTM International's E10 Committee on Nuclear Technologies and Applications and was selected to lead the ASTM International E10.03

Subcommittee. In this position, FIU oversaw the development of two new draft standard specifications for removable/strippable coatings and permanent coatings/fixatives.

On July 24, 2017, ASTM International's E10 Committee on Nuclear Technology and Applications published the two new international standard specifications for fixative technologies that aim to immobilize radioactive contamination, minimize worker exposure, and protect uncontaminated areas against the spread of radioactive contamination during the decommissioning of nuclear facilities. FIU has been working with the ASTM International subcommittee on the development, review, revision, and ultimate approval of these standards as part of the D&D effort.

The first specification, Specification for Strippable & Removable Coatings to Mitigate Spread of Radioactive Contamination (E 3104-17), establishes performance specifications for a coating that is intended to be removable during subsequent decontamination operations. The second specification, Specification for Permanent Coatings Used to Mitigate Spread of Radioactive Contamination (E 3105-17) is for coatings that are intended to be permanent, non-removable, long-term material for fixing contamination in place during decommissioning.

The E10 Committee, through the E10.03 Subcommittee on Radiological Protection for Decontamination and Decommissioning of Nuclear Facilities and Components, has moved forward with creating consensus based standards for D&D technologies that are not only aligned with technical specifications, but also account for the safety, regulatory, and operational requirements encountered during D&D activities. The intent is to promulgate relevant, uniform testing protocols that can be leveraged across the nuclear environmental management community, and support decision makers and end users with common references in the selection and employment of those standards and associated technologies.

Figure 3-4. From left: Joseph Sinicrope (FIU ARC / Chairman, E10.03 Subcommittee), Connor Nicholson (SRNL), Brent Peters (SRNL), Ed Walker (Chairman, E10 Committee on Nuclear Technology and Applications).

FIU and ASTM have widely publicized the availability of the two new international standard specifications for fixative technologies. ASTM issued an online news release and the new standards were publicized in the September/October issue (both online and print copy) of the ASTM Standardization News publication (Figure 3-5) and is available at: https://www.astm.org/standardization-news/?q=update/coatings-help-prevent-radioactive-contamination-decommissioning. In addition, FIU published an article on this topic on D&D KM-IT and the ARC website, and issued announcements on ARC's Facebook, Twitter, and LinkedIn social media. FIU also supported the development and revision of an article for publication in the EM Update newsletter.

FIU initiated planning for the next ASTM International E10.03 Subcommittee meeting scheduled for January 21-23, 2018, in New Orleans, LA. The focus of this meeting will be on initiating the development of standardized testing protocols for: 1) Determining the Decontamination Factor (DF) of strippable coatings on various substrates; 2) Determining a fixative's ability to immobilize radioactive contamination and measuring its impacts on Airborne Release Fractions (ARF) and Respirable Fractions (RF) in the Source Term Formula. Both of these objectives are directly aligned with the incombustible fixatives initiative, and address SRNL's and FIU's collaborative research efforts on providing empirical data to support updating the DOE-HDBK-3010. It is also an excellent venue for capturing and archiving lessons learned / best practices in a systematic manner.

News / Magazines & Newsletters

ASTM Standardization News

Coatings Help Prevent Radioactive Contamination in Decommissioning

ASTM International's committee on nuclear technology and applications (E10) has created new specifications for coatings that help prevent the release of radioactive particles when nuclear facilities are being decommissioned.

The specifications aim to immobilize radioactive contamination, minimize worker exposure, and protect uncontaminated areas against the spread of radioactive contamination.

The first specification is for a coating intended to be removed during subsequent decontamination operations: Specification for Strippable and Removable Coatings to Mitigate Spread of Radioactive Contamination (E3104).

The second specification is for a coating intended to be a permanent, non-removable, long-term material for fixing contamination in place during decommissioning: Specification for Permanent Coatings Used to Mitigate Spread of Radioactive Contamination (E3105).

The coatings are applied to surfaces commonly found in nuclear facilities and aim to reduce:

- Migration of the contamination into or along buildings, equipment, and other surfaces;
- Resuspension of contamination in the air; and,
- The spread of contamination as a result of external forces such as pedestrian traffic and fire.

"These standards, and the subsequent testing protocols being developed by our committee, can potentially assist in updating directives and guidance documents, such as U.S. Department of Energy handbooks on airborne release fractions and respirable fractions for nonreactor nuclear facilities," says Joseph Sinicrope of Florida International University's Applied Research Center. Sinicrope also serves as chairman of ASTM International's subcommittee on radiological protection for decontamination and decommissioning of nuclear facilities and components (E10.03).

Figure 3-5. ASTM News publication on new fixative standards (Sept/Oct 2017 edition).

Subtask 2.2.2: Technology Demonstration under Nonradioactive Conditions at FIU

Leveraging the research being performed on intumescent coatings as part of subtask 2.1.1 and including close coordination with DOE EM, SRNL, and SRS, FIU is conducting a cold demonstration / test and evaluation of applying intumescent coatings in a full-scale SRS 235-F hot cell mock-up at the FIU Hot Cell Test Bed during FIU Performance Year 7.

The test objectives outlined in the final test plan (*Adapting Intumescent Coatings as Fire Resilient Fixatives in Support of SRS 235-F D&D Activities Phase II: Construction of SRS 235-F Hot Cell Test Bed and Application Demonstration*) include: 1) constructing a to-scale SRS 235-F Hot Cell Test Bed on site at ARC that mirrors the operating environment encountered in an adjoining corner and middle hot cell configuration at the SRS 235-F facility and 2) evaluating the mechanics and processes associated with applying the selected intumescent coatings in the hot cell configurations using: a) the approved tools as identified in the 235-F Risk Reduction Tooling List, Rev 0, dated 26 January 2015; and b) alternative application methods, such as airless sprayers, recommended by the IC manufacturer.

Phase I of the test plan was completed on May 25, 2017 with the final construction of the SRS 235-F Hot Cell Test Bed. Phase II of the test plan commenced on May 31, 2017 and was completed in early October. Testing to date has included:

- Application of the intumescent coating using the site approved tools, specifically the extension pole and a roller brush.
- Monitoring of curing time.
- Observation and recording of ability of all required tools and materials to fit through the bag in/bag out port and pass-through port.
- Evaluation of volume/surface area of intumescent coating required to cover all surfaces to minimum thickness needed.
- A small scale test to evaluate the effectiveness of using a simple slow-pour method of applying an intumescent coating to the floor of the hot cell test bed.
- A larger scale (5'x5') test to further evaluate the effectiveness of using a simple slow-pour method of applying an intumescent coating to the floor of the hot cell test bed.
- Fire testing on a test coupon (18"x18") after using the slow pour method of applying the intumescent coating.
- Testing a handheld sprayer as a possible option for applying the IC fixative to vertical / wall surfaces.

With 95% of the assayed contamination residing on the floor of the SRS 235F facility hot cells, and given the composition and characteristics of the intumescent coatings, FIU performed a small scale test of slowly pouring the IC onto a 1' x 1' area within the hot cell testbed. This method showed significant promise in reducing worker time and potential for disturbing residual contamination during the application of intumescent coating on horizontal / floor surfaces in hot cells. The IC cured within 24-hours of application with a heat index of around 100ºF. Consequently, FIU moved forward with a full-scale test and evaluation of the technique.

Figure 3-6. Small scale test of a slow pour technique using intumescent coatings (left) and preparing for full-scale demo of slow pour application method for horizontal / floor surfaces in hot cell (right).

FIU used the following tools to support the slow pour application method of the IC onto a horizontal surface (i.e., floor of hot cell mockup):

- Container – 2.5-quart-size plastic bucket to hold/transport the IC
- Gripper - used to maneuver a 2.5-quart-size plastic container of IC
- Custom wooden T-shaped extension tool - used to spread the IC. To develop this tool, FIU connected a 13" wooden head to the approved extension handle on the SRS tooling list.

Figure 3-7. Tools used for slow pour method to apply IC to hot cell floor.

FIU poured the IC into a 2.5 quart plastic container outside the hot cell, filling the container with 1 to 1.25 quarts of IC to keep the weight between 2 to 3 pounds to minimize worker fatigue. The container and tools were then passed through the bag in/bag out port. Maneuvering the 2.5-qt container to various locations within the hot cell by manipulating the gripper from the glove-ports was relatively easy and allowed for targeted pouring of the IC. After marking the hot cell

border at 1/8” above the floor, FIU poured the IC from the container at a height of about 1 to 3” above the floor to minimize any potential for splatter or disturbance of any residual contamination that may be present in a radioactive environment. FIU then spread and smoothed the IC across the floor area using the wooden T-shaped tool, using the 1/8” markings along the perimeter of the hot cell as a thickness guide. The custom wooden T-shaped extension tool allowed access to all locations within the hot cell test bed from the glove-ports and easily reached the corners. An area of 5’ x 5’ was coated to 1/8” thickness in approximately 15 minutes once the tools and IC were in the hot cell. Total curing time after the slow pour application was 48 hours under hot and humid weather conditions (temperatures 75°-97° F and humidity 45%-93%).

The slow pour method for the floor/horizontal surfaces proved very effective during application, significantly reducing time and effort while greatly facilitating application to the requisite thickness level. With an estimated 95% of the contamination residing on the hot cell floors at the SRS 235-F facility and given the composition and characteristics of the IC being tested, the slow pour method may be a viable application method for horizontal surfaces that would expedite application and minimize disturbance of any residual contamination.

Figure 3-8. Slow pour method to apply IC to hot cell floor.

After the small-scale slow pour application on a 18”x18” test coupon and subsequent curing, FIU performed fire testing on the coupon. This testing yielded positive results with minimal to no flame propagation or smoke and demonstrated excellent thermal insulation from the IC.

Figure 3-9. Fire testing a 18”x18” wooden test coupon after applying IC to 1/8” thickness using a slow pour method.

Testing of the handheld sprayer showed some initial success as a possible option for applying the IC fixative to vertical/wall surfaces. The sprayer is self-contained, relatively lightweight, battery operated, easily fits through the bag in/bag out and passthrough ports, and appears to be compatible with the viscosity of the FD intumescent coating. FIU conducted a series of comparison tests between roller vs sprayer application. The roller method of application averaged less than 14 mils of thickness per application on a vertical surface and approximately 12 total applications are needed to reach the requisite 1/8” coating thickness. With a 24-48 hour curing period between applications, this option does not appear like a viable for field deployment. On the other hand, the results with the hand held sprayer were much more promising in terms of labor, time, and number of applications.

FIU used a cordless GRAYCO UltraMax Handheld Airless Paint Sprayer at a setting 10 to apply the IC to a 36” x 40” vertical (wall) surface of the hot cell test bed to a 1/8” coating thickness. Approximately 2 quarts of product were consumed. Including time needed to refill the sprayer, the total application time with the sprayer was 5 minutes.

Figure 3-10. Airless sprayer (left) and manual film thickness gauge (right).

FIU is developing the technical report with all of the testing results and will submit the draft to DOE and SRNL by October 31.

Task 3: D&D Knowledge Management Information Tool (KM-IT)

Task 3 Overview

The D&D Knowledge Management Information Tool (KM-IT) is a web-based system developed to maintain and preserve the D&D knowledge base. The system was developed by Florida International University's Applied Research Center (FIU-ARC) with the support of the D&D community, including DOE-EM (EM-4.11 & EM-5.12), the former ALARA centers at Hanford and Savannah River, and with the active collaboration and support of the DOE's Energy Facility Contractors Group (EFCOG). The D&D KM-IT is a D&D community driven system tailored to serve the technical issues faced by the D&D workforce across the DOE Complex. D&D KM-IT can be accessed from web address http://www.dndkm.org.

Task 3 Quarterly Progress

An abstract based on this research was accepted for a poster presentation by the Waste Management 2018 Symposium:

> **Abstract**: 18300
> **Title**: KM-IT Mobile Platform for D&D
> **Authors**: Himanshu Upadhyay, Walter Quintero, Leonel Lagos, Peggy Shoffner, John De Gregory (DOE EM)

DOE Fellows are supporting D&D KM-IT by reviewing the information in the vendor and technology modules and researching new vendors and technologies for adding to the system. As of September 30, 2017 the system included a total of 954 vendors and 1,337 technologies (including 521 robotic technologies). In addition, there were 988 registered users and 103 subject matter specialists.

FIU maintains the KM-IT cyber security infrastructure on an ongoing basis based on the guidelines provided by DOE EM IT and NIST. The KM-IT system and infrastructure undergoes audits by internal and external auditors on a periodic basis. During this reporting period, FIU worked to implement solutions to the application, servers, and infrastructure based on two separate security audits performed in May.

FIU also completed the initial development of a pilot native mobile application using the D&D Fixatives Module for the Android platform (milestone 2016-P3-M3.4). A native application is an app that is developed for use on a specific platform and which is downloaded onto a mobile device in order to be accessed. As such, the native app does not need an internet connection to be used. The pilot native mobile app is being designed and developed to run on Android 7.1 (Nougat). From the welcome screen for the app, the user can choose to perform a keyword search or a criteria search. The keyword search will search for fixative products according to the search word entered. If no keyword is entered and the search button is clicked, it will return all fixative products. The criteria search allows the user to build a multi-tier criteria search by adding the desired criteria and sub-criteria allowing for targeted results.

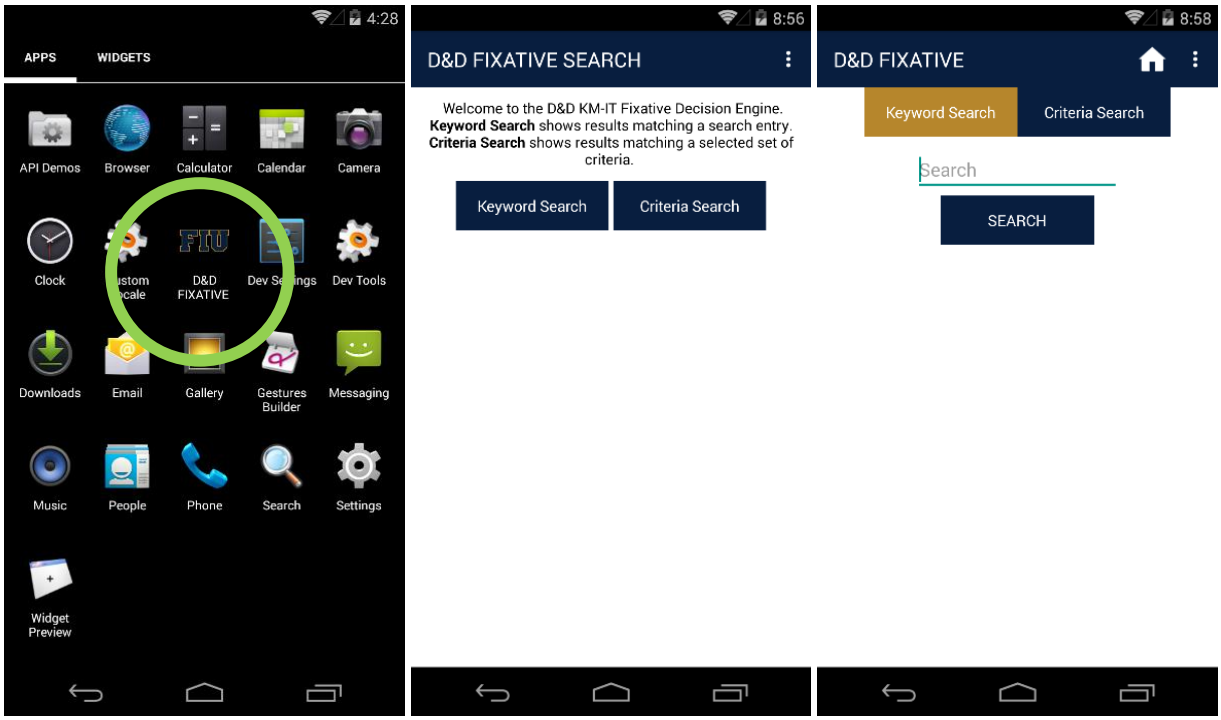

Figure 3-11. D&D fixative module mobile app on Android, search main page, and keyword search page.

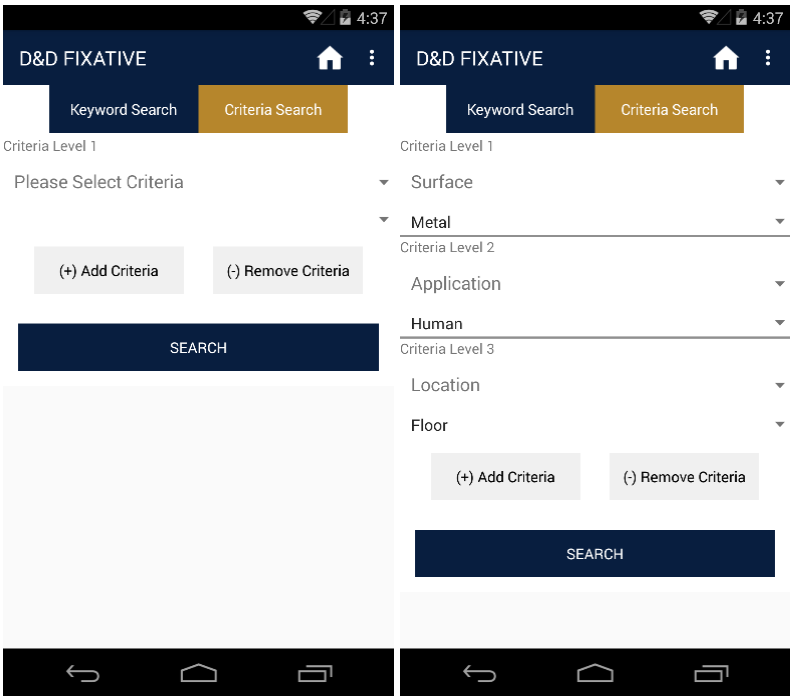

Figure 3-12. D&D fixative module mobile app criteria search pages.

The search results view displays the names of the fixative products that meet the search query. The user can click on any of the product names to view the details of the fixative product. The user can get further product or vendor data by clicking on the corresponding buttons on the fixative product detail view. Throughout the mobile app, the user can click on a phone number to dial it or launch their phone browser by clicking on an URL.

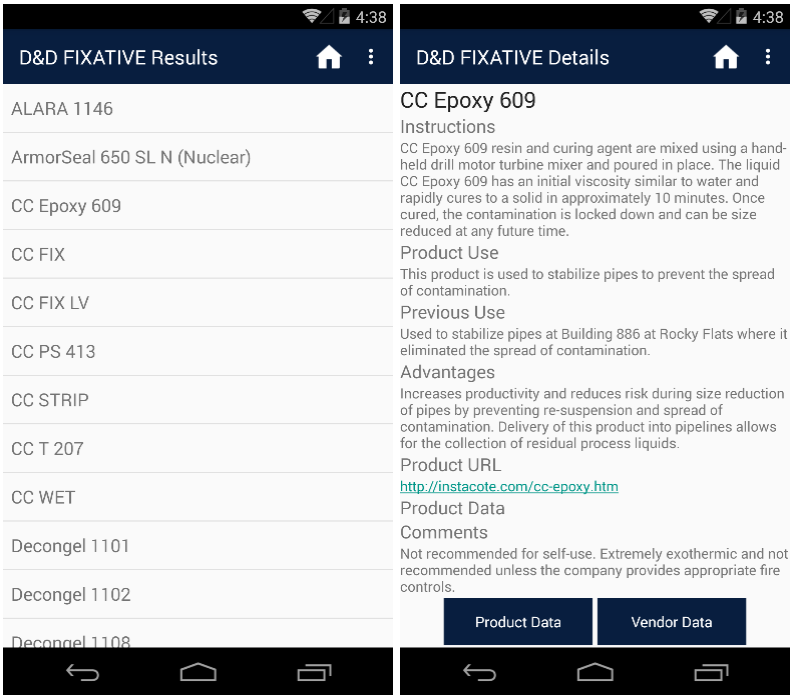

Figure 3-13. D&D fixative module mobile app search results and fixative details.

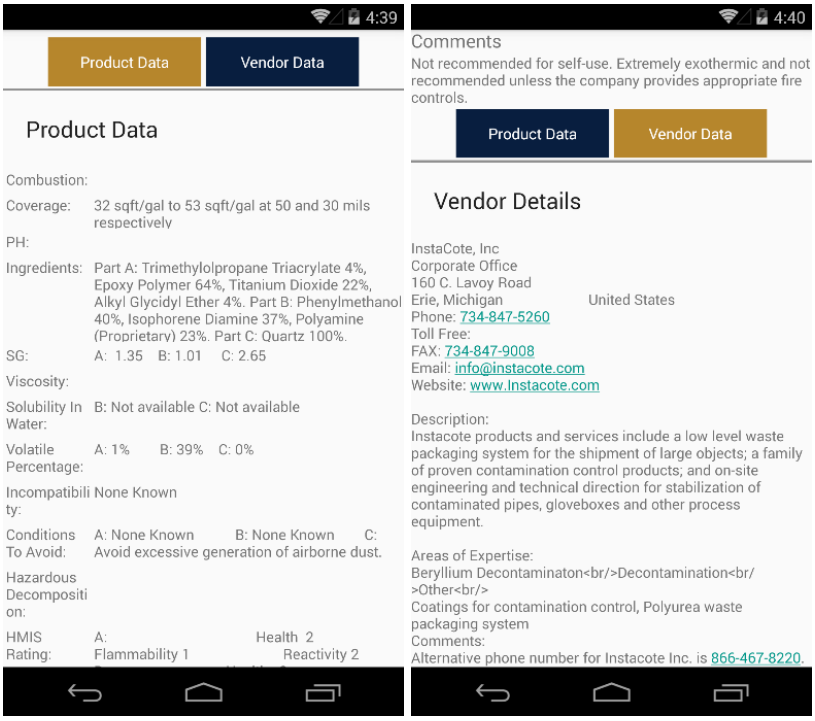

Figure 3-14. D&D fixative module mobile app product data and vendor details.

The mobile app also includes a description of D&D KM-IT and contact information for FIU ARC as well as a help page and disclaimer page.

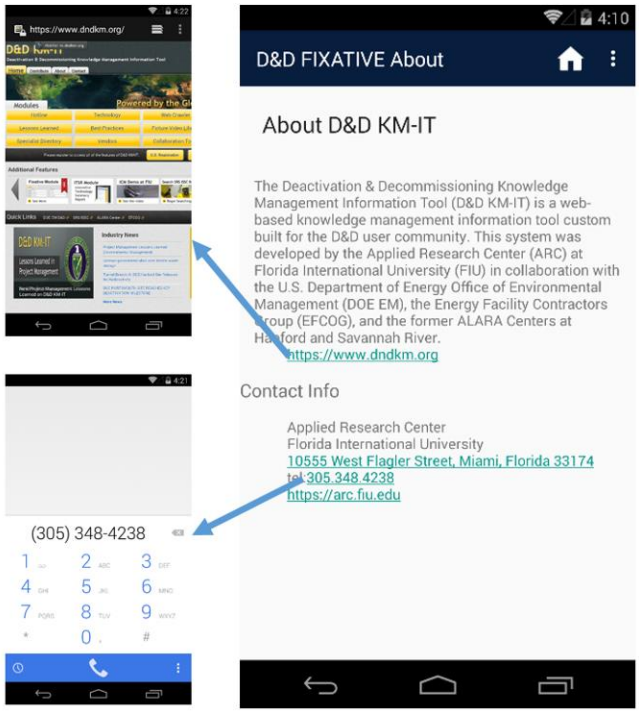

Figure 3-15. D&D fixative module mobile app about D&D KM-IT page.

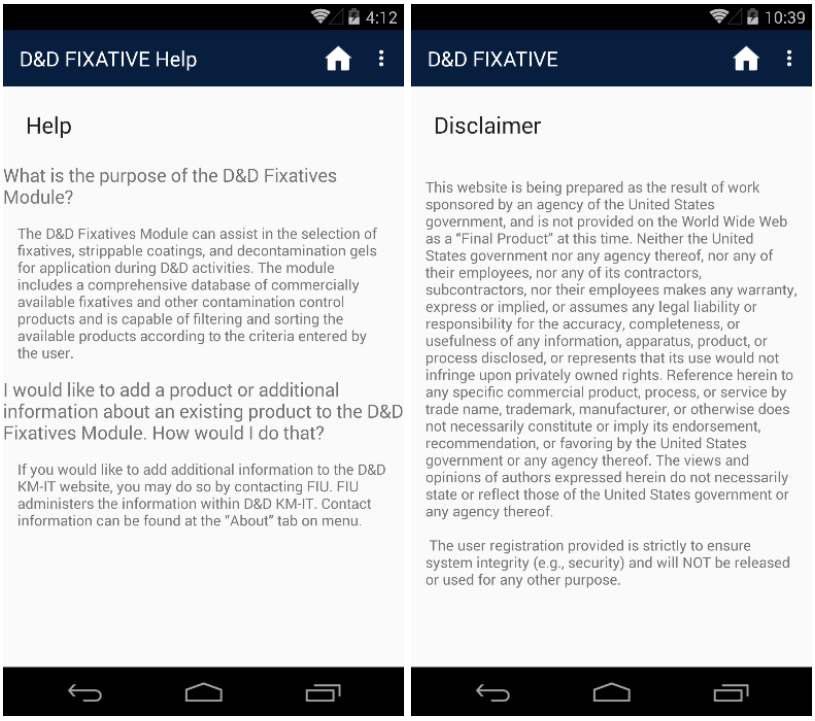

Figure 3-16. D&D fixative module mobile app help and disclaimer pages.

A Representational State Transfer (REST) web service was built to support the Android mobile app. REST is an architectural style that specifies constraints, such as the uniform interface, that is applied to a web service**.** It provides desirable properties, such as performance, scalability, and modifiability. REST relies heavily on JSON (JavaScript Object Notation), a minimal, readable format for structuring data. It is used primarily to transmit data between a server and web application, as an alternative to XML.

The following technologies were used in the development of the D&D KM-IT Fixative Android Native Mobile App:

- Microsoft Visual Studio 2015
- Xamarin
- REST Web Services
- JSON
- Microsoft SQL Server
- Android
- Postman

FIU provided a demonstration of the pilot native mobile app on the fixative module to DOE on August 10, 2017 via Adobe Connect and then provided a broader presentation on the potential for applying native mobile apps to a wide variety of DOE EM challenges on August 24, 2017.

FIU also worked on developing additional security features to protect all of the systems against possible cyber attacks and infections once the mobile applications are made available to the public. In a computer network, a de-militarized zone (DMZ) is a special local network configuration designed to improve security by segregating computers on each side of a firewall.

A DMZ divides or splits such a network into at least two parts by taking one or more devices inside the firewall and moving them to the outside, or to a separate subnet network, that does not allow a compromised or hacked server into a local area network (LAN). This configuration better protects the inside servers and domains from possible attacks by the outside and vice versa. These DMZs help to manage and protect systems from hackers and malware that an outfacing public or web server could be exposed to but not allow the local corporate servers to be directly in the line of fire of cyber threats. To further describe a network DMZ, it establishes a new subnet from the firewall where certain computer services run one or more computers or network devices. That DMZ system on the outside subnet adds an extra layer of protection for computers behind the firewall of the main LAN as all incoming requests are routed away from the corporate computers. True DMZs also restrict computers behind the firewall from communicating directly with the DMZ devices. Multi-level DMZs with several layers of firewall support can be set up to support larger corporate networks for more in depth cyber protection. A typical setup for a DMZ is shown in the following figure.

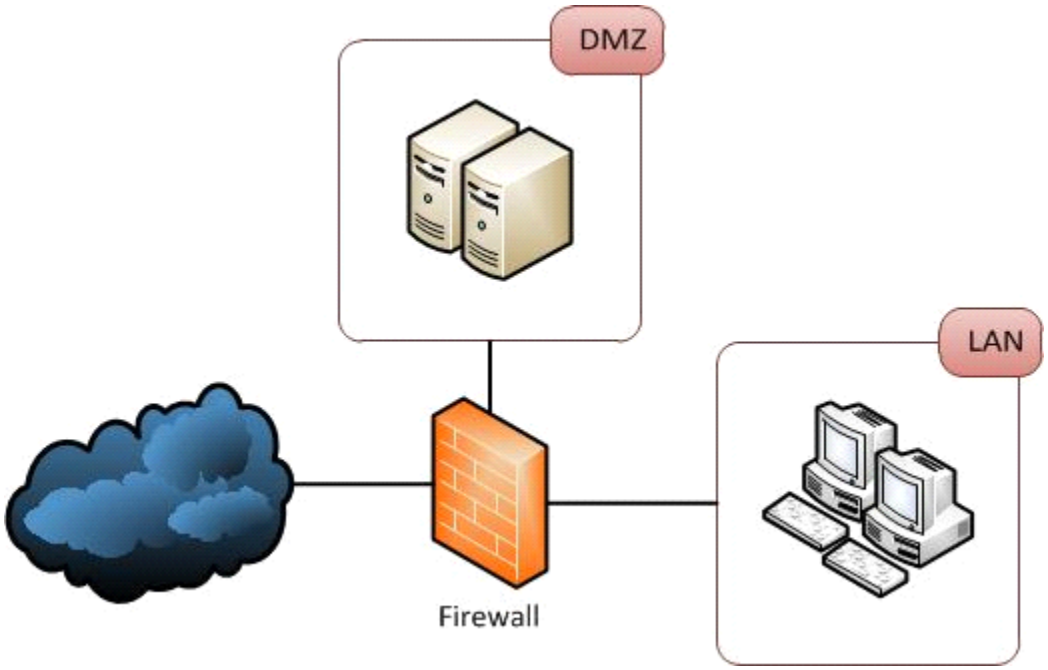

Figure 3-17. Typical de-militarized zone (DMZ) computer network setup.

ARC has developed Fixative Rest Services that will be consumed by the native mobile android application once deployed onto the Google Marketplace. This communication will occur over HTTP and will need to be secured in a DMZ zone. FIU has designed the DMZ network to host the Fixative Rest Services such that it can be accessed from outside the FIU network. A mobile server to host the Fixative Rest Services and the fixative database is under procurement. Deployment of the fixative mobile server in a DMZ will increase the security of the API and the host along with the database used to store the fixative information.

FIU is also coordinating through the DOE to transfer a series of legacy technology video files that FIU converted from VHS to digital for posting to the DOE EM YouTube channel to make them assessable to the EM community. During September, FIU completed uploading 25 video files, a total of approximately 860 MB, to the established “EM Videos” folder on Kiteworks for

DOE review prior to posting to YouTube. In addition, FIU received confirmation of approval from DOE EM that the strategy for leveraging social media via adding Like/Share/Pin style buttons on KM-IT can be implemented. FIU will begin executing this addition on KM-IT.

Milestones and Deliverables

The milestones and deliverables for Project 3 for FIU Performance Year 7 are shown in the following table. Milestone 2016-P3-M2.3 was completed with the participation in the ASTM E10 committee meeting to coordinate developing standardized testing protocols and performance metrics for D&D technologies (subtask 2.2.1). A deliverable for a second infographic was completed with a postcard style infographic on the DOE-FIU Cooperative Agreement and the DOE Fellows program. Milestone 2016- P3-M3.4 was completed on August 3, 2017 with the completion of the initial development of a pilot native mobile application using the D&D Fixatives Module for the Android platform. Milestones and deliverables reforecast to be completed as carryover scope with the last increment of FIU Performance Year 7 funding from DOE are also shown below.

FIU Performance Year 7 Milestones and Deliverables for Project 3

Task	Milestone/ Deliverable	Description	Due Date	Status	OSTI
Task 1: WIMS	2016-P3-M1.1	Import 2017 data set for waste forecast and transportation data	Within 60 days after receipt of data from DOE	Complete	
	2016-P3-M1.2	Draft paper submitted to WM17 conference	11/04/16	Complete	
Task 2: D&D	Deliverable	Draft Test Plan for IC Demo / Test & Evaluation at FIU (subtask 2.2.2)	1/6/17	Complete	OSTI
	2016-P3-M2.1	Participate in ASTM E10 committee meeting to coordinate developing standardized testing protocols and performance metrics for D&D technologies (subtask 2.2.1)	2/28/17	Complete	
	2016-P3-M2.2	Complete demonstration / test and evaluation of IC on FIU hot cell test bed (subtask 2.2.2)	4/28/17	Complete	
	Deliverable	Decision brief to DOE EM on recommended D&D technologies to test for FIU Performance Year 8 using the 3-phased model	4/28/17**	Complete	
	Deliverable	Draft summary report of robotic technologies for D&D (subtask 2.1.3)	5/31/17	Reforecast to 12/15/17	OSTI
	Deliverable	Draft progress report on the adaptation of IC to enhance fire resiliency (subtask 2.1.1)	6/30/17	Reforecast - to be included in technical report for IC test/ evaluation	OSTI
	2016-P3-M2.3	Participate in ASTM E10 committee meeting to coordinate developing standardized testing protocols and performance metrics for D&D technologies (subtask 2.2.1)	7/31/17	Complete	
	Deliverable	Draft progress report on the identification of IC	7/31/17	Reforecast	OSTI

		applications to other DOE EM problem sets (subtask 2.1.2)		to FIU Performance Year 8	
	Deliverable	Draft technical reports for demonstrated technologies	30-days after evaluation/ demo	Reforecast to 10/30/17	OSTI
	Deliverable	Draft Tech Fact Sheet for technology evaluations/ demonstrations	30-days after evaluation/ demo	Reforecast to 10/30/17	
Task 3: D&D KM-IT	2016-P3-M3.1	Waste Management Symposium Draft Paper	11/4/16	Complete	
	Deliverable	D&D KM-IT Workshop to DOE EM staff at HQ	2/28/17	Not scheduled**	
	Deliverable	Preliminary Metrics Progress Report on Outreach and Training Activities	3/10/17	Complete	
	Deliverable	Unclassified summary report on the status and findings of the KM-IT audits	3/24/17 Reforecast 5/31/17	Complete	
	2016-P3-M3.2	Four Wikipedia integration edits/articles	3/31/17 Reforecast to 6/30/17	Complete	
	Deliverable	First D&D KM-IT Workshop to D&D community /DOE Site	3/31/17	Complete	
	Deliverable	First infographic to DOE for review	3/31/17	Complete	
	2016-P3-M3.3	Deploy pilot video onto YouTube platform	4/28/17	Complete	
	2016-P3-M3.4	Development of pilot native mobile application for D&D Fixatives Module	5/31/17 Reforecast to 8/4/17	Complete	
	Deliverable	Second infographic to DOE for review	7/31/17	Complete	
	Deliverable	D&D KM-IT Web Analysis Report	Quarterly	Complete	
	Deliverable	Draft Tech Fact Sheet for new modules or capabilities of D&D KM-IT	30-days after deployment of new module or capability	Complete	

***Completion of this deliverable depended on scheduling and availability of DOE EM staff*

Work Plan for Next Quarter

Project-wide:

- Complete the Year End Report (YER) for FIU Performance Year 7.

Task 1: Waste Information Management System

- Perform database management, application maintenance, and performance tuning to WIMS.
- Submit draft paper on this research task to Waste Management 2018 Symposia.

Task 2: D&D Support

- Complete development of the draft technical report for the cold demonstration / test & evaluation of intumescent coatings at FIU which will include the results of testing on the adaptation of IC to enhance fire resiliency
- Continue leading the working group in for ASTM International's E10 Committee on Nuclear Technologies and Applications and Subcommittee E10.03 - Radiological Protection for Decontamination and Decommissioning of Nuclear Facilities and Components to support the initiative of developing and promulgating uniform testing protocols and performance metrics for D&D technologies across the stakeholder community.
- Draft summary report of robotic technologies for D&D.
- Submit draft paper on this research task to Waste Management 2018 Symposia.

Task 3: D&D Knowledge Management Information Tool

- Complete work on the developed Android native mobile app (Fixatives) to allow users to download the app onto their mobile devices for beta testing.
- Perform outreach and training, community support, data mining and content management, and administration and support for the D&D KM-IT system, database, and network.
- Submit draft paper on this research task to Waste Management 2018 Symposia.

Project 4
DOE-FIU Science & Technology Workforce Development Initiative

Project Manager: Dr. Leonel E. Lagos

Project Description

The DOE-FIU Science and Technology Workforce Development Initiative has been designed to build upon the existing DOE/FIU relationship by creating a "pipeline" of minority engineers specifically trained and mentored to enter the Department of Energy workforce in technical areas of need. This innovative program was designed to help address DOE's future workforce needs by partnering with academic, government and DOE contractor organizations to mentor future minority scientists and engineers in the research, development, and deployment of new technologies, addressing DOE's environmental cleanup challenges.

Project Overview

The main objective of the program is to provide interested students with a unique opportunity to integrate course work, Department of Energy (DOE) field work, and applied research work at ARC into a well-structured academic program. Students completing this research program would complete the M.S. or Ph.D. degree and immediately be available for transitioning into the DOE EM's workforce via federal programs such as the Pathways Program or by getting directly hired by DOE contractors, other federal agencies, and/or STEM private industry.

Project Quarterly Progress

FIU STEM (science, technology, engineering, and math) students are actively supporting the research efforts under the DOE-FIU Cooperative Agreement during FIU Performance Year 7. The following DOE Fellows are supporting the research under Projects 1-3:

Project 1: Max Edrei (graduate, M.S., mechanical engineering), Sebastian Zanlongo (graduate, Ph.D., computer science), Clarice Davila (undergraduate, mechanical engineering) Michael DiBono (undergraduate, mechanical engineering), Manuel Losada (undergraduate, electrical engineering), Anibal Morales (undergraduate, electrical engineering), and Joseph Coverston (graduate, M.S., mechanical engineering).

Project 2: Alejandro Garcia (graduate, M.S. geoscience), Alejandro Hernandez (undergraduate, chemistry), Alexis Smoot (undergraduate, environmental engineering), Awmna Kalsoom Rana (undergraduate, chemistry), Christine Wipfli (undergraduate, environmental engineering), Hansell Gonzalez (graduate, Ph.D., chemistry), Silvina Di Pietro (graduate, Ph.D., chemistry), Sarah Solomon (undergraduate, environmental engineering), Mohammed Albassam (undergraduate, environmental engineering), Frances Zengotita (undergraduate, chemistry and health), Juan Morales (graduate, M.S., public health), Ripley Raubenolt (undergraduate, environmental engineering), Ron Hariprashad (undergraduate, environmental engineering).

Project 3: Jesse Viera (undergraduate, mechanical engineering), Alexander Piedra (undergraduate, mechanical engineering), and Andres Cremisini (undergraduate, computer science).

Fellows continue their support to the DOE-FIU Cooperative Agreement by actively engaging in EM applied research and supporting ARC staff in the development and completion of the various tasks. The program director continues to work with DOE sites and HQ to fully engage DOE Fellows with research outside ARC where Fellows provide direct support to mentors at DOE sites, DOE-HQ, and DOE contractors. All Fellows also participated in a weekly meeting conducted by the program director, a conference line has been established to enable DOE Fellows conducting internship to join to weekly meeting and update program director on their internship. During each of these meetings, one DOE Fellow presents the work they performed during their summer internship and/or EM research work they are performing at ARC.

DOE Fellows participated and presented their research accomplishments during FIU's Research Review with DOE-HQ and the national labs on July 18, 2017, as a part of technical projects 1, 2 and 3 as well as during the workforce development project 4. Below is the list of presentations given by DOE Fellows under the various projects:

Project 1

- **Sebastian Zanlongo** (VTC from Sandia) - Anomaly Detection and Task Planning via Neural Networks and Hierarchical Task Networks
- **Michael Di Bono** (via phone from University of Texas-Austin) - Simulation of Mobile Platform, Vaultbot, using Robotic Operating System (ROS) and Gazebo

Project 2

- **Frances Zengotita** from (VTC from LANL at Univ of New Mexico location) - Role of Chromohalobacter on the Potential Transport of Lanthanides and Cesium in a Dolomite Mineral System
- **Ron Hariprashad** (VTC from SRNL) - In-Situ Data Collection, Sampling, and Water Quality Monitoring in Tim's Branch Watershed

Project 3

- **Alexander Piedra** (VTC from SRNL) - High Density Polyurethane Foam for Radiation Shielding & D&D Applications

Project 4

- **Juan Morales & Mohammed Albassam** (VTC from HQ) - Surface/Ground Water Interface and Radioactive Contaminant Ecological Risk Assessment Using EPA Method in the (F-Area)-Savannah River Site (SRS) Aiken, SC.
- **Hansell Gonzalez** (VTC from FIU) - Unrefined Humic Substances as a Potential Low-Cost Remediation Method for Acidic Groundwater Contaminated with Uranium
- **Silvina Di Pietro** (VTC from FIU) - Ammonia Gas Treatment for Uranium Immobilization at the DOE Hanford Site
- **Awmna Rana** (VTC from FIU) - Effect of Acidic Plume on Soil's Properties & Capacity to Retain Uranium at SRS
- **Maxmiliano Edrie** (VTC from FIU) - CFD Evaluation of Mixing Processes for High-Level Waste

This summer, twelve (12) DOE Fellows completed 10-week internships across the DOE Complex and at two universities. The DOE Fellows engaged in research projects at DOE Headquarters in Maryland, DOE national laboratories (Savannah River Nat. Lab and Sandia Nat. Lab), Savannah River Ecology Lab, the Waste Isolation Pilot Plant, University of Texas-Austin Nuclear and Applied Robotics Group, and San Jose State University.

DOE-EM coordinated a presentation session for all of their summer interns to share their internship experience on August 3, 2017. A total of six (6) DOE Fellows participated in this event and presented information based on their summer internship.

SRNL Interns
- Sarah Solomon
- Ripley Raubenolt
- Alexander Piedra

HQ Interns
- Juan Morales
- Mohammed Albassam
- Christine Wipfli

Upon returning to FIU in August, the DOE Fellows began to develop their technical reports based on their summer 2017 internships. Table 4-1 shows the summer 2017 internships and the technical report titles.

Table 4-1. Summer 2017 Internships

DOE Fellow(s)	Site	Mentor(s)	Report Title
Juan Morales and Mohammed Albassam	DOE-HQ	Skip Chamberlain	Groundwater/Surface Water Interface and Radioactive Contaminant Ecological Risk Assessment at SRS F-Area
Christine Wipfli	DOE HQ	Robert Seifert	Supporting DOE EM 4.31, Office of Regulatory Compliance
Sebastian Zanlongo	Sandia National Lab	Scott Gladwell	Anomaly Detection and Task Planning via Neural Networks and Hierarchical Task Networks
Andres Cremisini	Sandia National Lab	Kristopher Klingler Jon Bradley	Coding a Weather Model
Sarah Solomon and Ripley Raubenolt	SRNL	Mike Paller Brian Looney	Mercury Speciation via Diffusive Gradients in Thin-Film Technology
Alexander Piedra	SRNL	Aaron Washington Connor Nicholson	TBD
Ron Hariprashad	SRNL/SREL	John Seaman Brian Looney	In-Situ Data Collection, Sampling, and Water Quality Monitoring in Tims Branch Watershed, Savannah River Site, SC
Michael Di Bono	University of Texas-Austin	Mitch Pryor	Simulation of a Mobile Robotic Platform in Gazebo and RViz using ROS

Frances Zengotita	WIPP	Don Reed Tim Dittrich Julie Swanson	The Role of Chromohalobacter on Transport of Lanthanides and Cesium in the Dolomite Mineral System
Alejandro Hernandez*	San Jose State University	David Robertson Annalise Van Wyngarden	n/a

**This internship is separate from and not funded by the DOE-FIU Cooperative Agreement.*

Highlights from the internship assignments are included below.

DOE FELLOW: Andres Cremisini
LOCATION: Sandia National Laboratory
MENTORS: Kristopher Klinger

This summer Andres helped developed a weather model for a large system currently in development at Sandia National Labs under the mentorship of Kristopher Klingler, Bill Prentice and Jon Bradley. The work entailed researching statistical methods primarily for wind modeling and identifying efficient algorithms to implement these methods, packaging the algorithms into a software library and integrating this library into the larger system. Andres states that the work was challenging and very fun.

Figure 4-1. DOE Fellows Sebastian Zanlongo and Andres Cremisini interning at Sandia.

DOE FELLOW: Michael DiBono
LOCATION: University of Texas-Austin
MENTORS: Mitch Pryor

Michael DiBono conducted his summer internship at the Applied Robotics Group at the University of Texas at Austin. Michael's research work was on the simulation of their mobile platform, Vaultbot, using Robotic Operating System (ROS) and Gazebo. The Vaultbot was developed for the inspection and radiation surveying of the Canyon Air Exhaust tunnel (CAEX) at the DOE Savannah River Site. The Vaultbot has a LIDAR attached to the front for mapping and navigation, along with two industrial manipulators (arms) mounted to the top for inspection.

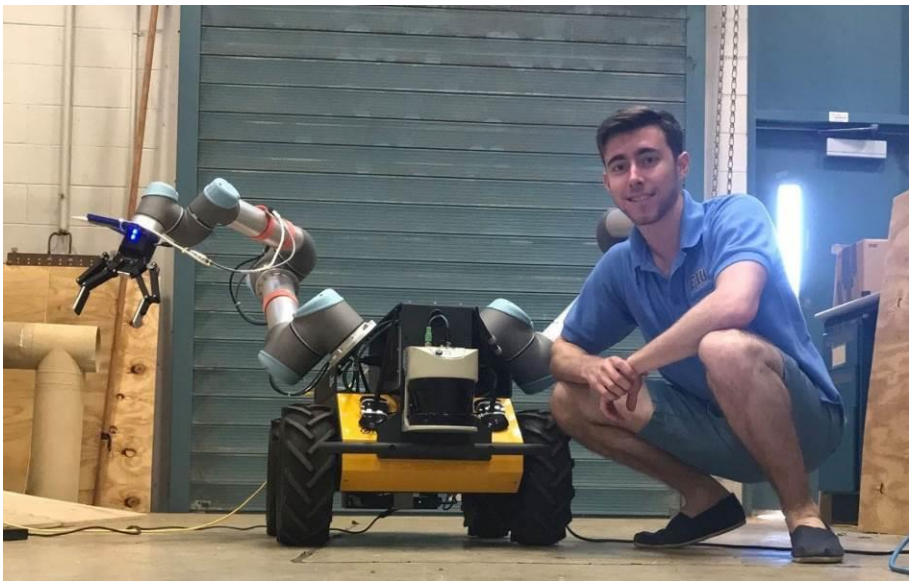

Figure 4-2. DOE Fellow Michael DiBono pictured with the robotic system developed for inspection and radiation surveying of CAEX.

DOE FELLOW: Frances Zengotita
LOCATION: WIPP
MENTORS: Don Reed, Tim Dittrich

Frances Zengotita interned at Los Alamos National Laboratory Carlsbad Field Office and investigated how a salt-resistant microbe may be affecting the mobility of contaminants at the Waste Isolation Pilot Plant (WIPP), a deep geologic repository for permanent disposal of transuranic radioactive waste that is a byproduct of the nation's nuclear defense program. Dr. Hilary Emerson at ARC worked with Frances Zengotita to quantify both the mobility of the contaminants in the presence of microbes and the remobilization potential by microbes after sorption to subsurface minerals.

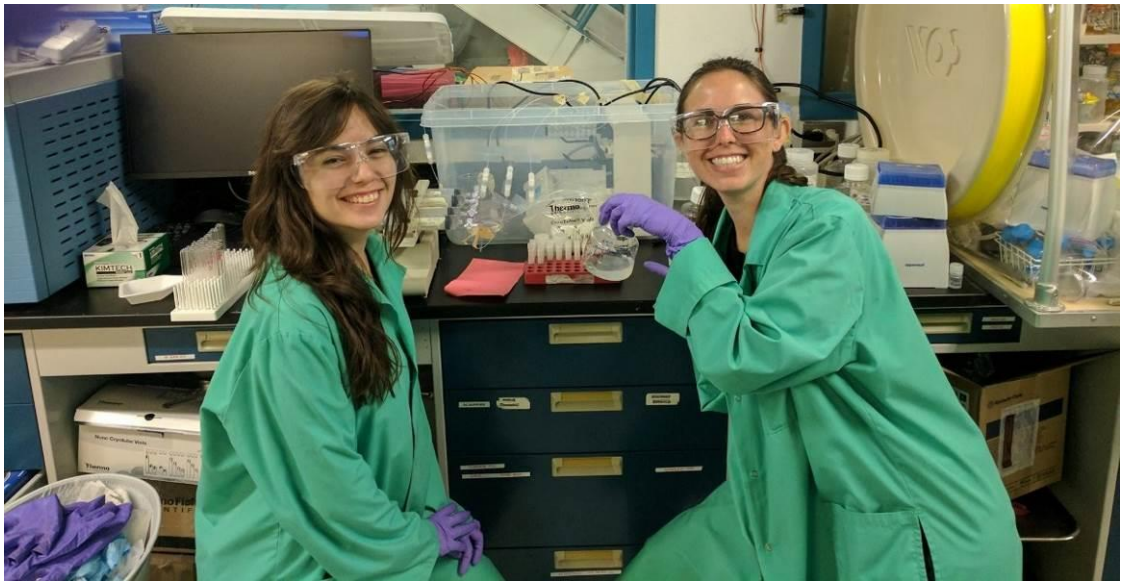

Figure 4-3. Frances Zengotita at WIPP with ARC mentor Dr. Emerson.

DOE FELLOW: **Ron Hariprashad**
LOCATION: **SREL/SRNL**
MENTORS: **John Seaman (SREL), Brian Looney (SRNL)**

Ron Hariprashad conducted an internship at Savannah River Site where he conducted fieldwork in Tims Branch with assistance from Dr. John Seaman and his research team at the Savannah River Ecology Lab (SREL). The aim was to collect cross-section measurements along the main Tims Branch stream, as well as *in situ* water quality and flow data to assist in calibration of the hydrological models being developed by ARC. Water and biofilm samples were also collected for chemical analysis of radiological and other contaminants of concern, and to monitor the chemical by-product of a tin-based DOE EM implemented remediation technology.

Figure 4-4. DOE Fellow Ron Hariprashad collecting flow data along the Tims Branch stream at SRS with ARC mentor Dr. Mahmoudi.

DOE FELLOW: **Christine Wipfli**
LOCATION: **DOE Headquarters**
MENTOR: **Robert Seifert**

Christine Wipfli (DOE Fellow Class of 2014) spent her DOE Fellow internship at the Department of Energy's Office of Environmental Management, Office of Regulatory Compliance in Germantown, Maryland, under the mentorship of Mr. Robert Seifert, the Office Director. Christine spent her internship supporting various environmental compliance projects pertaining to the National Environmental Policy Act (NEPA), along with The Resource Conservation and Recovery Act (RCRA) and the Comprehensive Environmental Response, Compensation, and Liability Act (CERCLA). Christine also supported a National Dialogue effort which is an initiative with the Environmental Protection Agency (EPA) and local governments. This is Christine's second internship at DOE EM headquarters, her first was completed two summers ago with the Office of Soil and Groundwater (now the Office of Subsurface Closure).

Figure 4-5. DOE Fellow Christine Wipfli during her internship at DOE HQ.

DOE FELLOW: **Alexander Piedra**
LOCATION: **SRNL/SREL**
MENTORS: **John Seaman (SREL) and Brian Looney (SRNL)**

DOE Fellow, Mr. Alexander Piedra, completed his 10-week internship at SRNL under the mentorship of Dr. Aaron Washington and Dr. Connor Nicholson. During his internship, he participated in two tasks; the first was to help establish the testing protocols and personnel safety paperwork for the radiologically hot 235-F demonstration of incombustible fixatives. This task entails coordination with F-area personnel, document generation, and testing setup development for the demonstration-level deployment. The second task involved fabrication and testing of radiological shielding foams to be used for small-scale contaminated environments such as gloveboxes. For this task, Alexander worked alongside SRNL researchers in the lab to generate samples and test them with low level radiation sources.

Figure 4-6. DOE Fellow Alexander Piedra during his internship at SRNL/SREL.

DOE FELLOW: **Sebastian Zanlongo**
LOCATION: **Sandia National Lab**
MENTORS: **Kristopher Klingler, Bill Prentice and Jon Bradley**

This summer, DOE Fellow Sebastian Zanlongo participated in a 10-week internship at Sandia National Laboratory under the mentorship of Kristopher Klingler, Bill Prentice and Jon Bradley. He participated in the development of a weather model for a large system currently in development. The work entails researching statistical methods primarily for wind modeling and identifying efficient algorithms to implement these methods, packaging the algorithms into a software library and integrating this library into the larger system. Sebastian described the experience with "The work is challenging and very fun."

Figure 4-7. DOE Fellow Sebastian Zanlongo during his internship at Sandia.

DOE FELLOW: **Alejandro Hernandez**
LOCATION: **San Jose State University**
MENTORS: **David Robertson and Annalise Van Wyngarden**

This internship was separate from and not funded by the DOE-FIU Cooperative Agreement.

DOE Fellow, Mr. Alejandro Hernandez, was awarded one of the twelve national fellowships for the National Nuclear Chemistry School, funded by the Department of Energy and sponsored by the American Chemical Society. During this six-week program at San José State University, Alejandro attended lectures by prominent nuclear scientists on the fundamentals and applications of nuclear science (e.g., nuclear medicine, environmental radiochemistry, energy production, etc.), performed hands-on experiments on state-of-the-art instrumentation routinely used in the nuclear field, as well as visited national lab facilities, including the National Ignition Facility at Lawrence Livermore National Lab and Lawrence Berkeley National Lab. The summer school program was founded as an educational outreach and workforce development activity to promote expertise in nuclear science and to provide trained personnel to meet national needs in nuclear research.

Figure 4-8. DOE Fellow Alejandro Hernandez during his internship at Sandia.

New DOE Fellows Manuel Losada and Anibal Morales started their fellowship and were assigned an ARC mentor to work with on DOE EM related projects. Prior to engaging in research related tasks, they completed the following health and safety trainings required by FIU's environmental health and safety (EH&S):

- Laboratory Hazard Awareness
- HazCom: In Sync with GHS
- Fire Safety
- Environmental Awareness Part 1 & 2
- Small Spills and Leaks
- EPA Hazardous Waste Awareness & Handling
- Personal Protective Equipment
- Safe Use of Fume Hood
- Compressed Gas Safety Awareness

Sixteen (16) DOE Fellows prepared and submitted abstracts for the student poster session at the 2018 Waste Management Conference based on their summer internship and ARC research being conducted in close collaboration with national laboratories and DOE site. The titles of the abstracts submitted are as follows:

- Alejandro Garcia - Evaluating the Effects of Microbes on the Spectral Induced Polarization Response in Hanford Sediment
- Alejandro Hernandez - Interaction of Technetium-99 with Fe(II)-performed minerals in the presence of bicarbonates under reducing conditions
- Awmna Rana - Effect of Acidic Plume on Soil Properties and Capacity to Retain Uranium at the Savannah River Site

- Christine Wipfli - Investigating the Remobilization of Technetium-99 in the Presences of Bicarbonates at the Hanford Site
- Clarice Davila - Erosion/Corrosion Detection in Carbon Steel Pipes Using Ultrasonic Sensors
- Frances Zengotita - Role of Chromohalobacter on the potential transport of lanthanides and cesium in a dolomite mineral system
- Hansell Gonzalez - Study of an Unrefined Humate Solution as a Possible Remediation Method for Groundwater Contamination
- Joseph Coverston - Development of an Experimental Pipeline Flushing Guideline for the Transport of High Level Waste
- Juan Morales - Ecological Role in Health Physics by Monitoring the Effective Dose Rates of Radionuclides in Lepomis Auritus Fish Species, Savannah River Site- (FASB), Aiken, S.C.
- Michael DiBono - Simulation of a Mobile Robotic Platform in Gazebo and RVIZ using ROS
- Mohammed Albassam - Understanding the Groundwater / Surface-Water Interface Phenomenon and the Contaminants of the (F-Area)-Savannah River Site (SRS) Aiken, SC
- Ripley Raubenolt - Investigating the Effects of Sorbed Humic Acid on the Mobility of Uranium
- Ron Hariprashad - Accumulation and Distribution of Tin in Soil and Biofilm Samples in Tims Branch on the Savannah River Site, Aiken, S.C.
- Sarah Solomon - Autunite Dissolution in the Presence of Shewanella Oneidensis MR1
- Sebastian Zanlongo - Informative Path Planning for Leak Detection
- Silvina Di Pietro - Effects of Alkaline Treatment and Redox Conditions on Mineral Dissolution for Hanford Sediments

In addition, a professional abstract was accepted by the Waste Management 2018 Symposium for an oral presentation:

> **Abstract:** 18636
> **Title:** International Training to Promote Successful Decommissioning and Environmental Remediation Projects
> **Authors:** Karen P. Smith, Lisa Durham, Lawrence Boing (Argonne National Lab); Leonel E. Lagos (FIU); Horst Monken-Fernandez, Patrick O'Sullivan (IAEA)

Three DOE Fellows are scheduled to complete the Workforce Development Program and graduate FIU in December 2017, including Alexis Smoot, Max Edrei, and Jesse Viera. FIU is extremely proud of the accomplishments of these remarkable students and wish to highlight their many successes. A DOE Fellow Spotlight is included below for Alexis and the next couple of monthly reports will include a Spotlight on Max and Jesse.

DOE Fellow Spotlight
Alexis Smoot (Environmental Engineering)

Alexis Smoot will successfully complete the DOE-FIU Science and Technology Workforce Development Program in December 2017 and graduate with a Bachelor's of Science in Environmental Engineering from Florida International University (FIU). She is actively pursuing career opportunities at DOE EM, other government agencies, and the national research laboratories as well as industry environmental companies and consultants. Alexis has special interests and abilities in environmental remediation, energy efficiency, and sustainable and renewable energy technologies.

> *Alexis possesses that ideal blend of intellect, leadership, and interpersonal skills that would benefit any organization in our industry. Her involvement and leadership on a broad spectrum of activities across the University have made her a true standout among her peers.* – Joe Sinicrope, ARC Research Scientist

Alexis has supported the research at FIU ARC under the mentorship of Dr. Yelena Katsenovich and Dr. Ravi Gudavalli by investigating the synergistic interactions between uranium ions, humic acid and colloidal silica under oxidized conditions using sediments collected from the SRS F/H Area. This study will assist the site in understanding the potential for colloid-facilitated transport of uranium in the SRS subsurface.

In the summer of 2016, Alexis spent 10 weeks interning at DOE-EM Headquarters in Germantown, MD, under the mentorship of Mr. Grover "Skip" Chamberlain. During the internship, Alexis developed a high-level quantitative sustainability analysis which compared active and passive remediation technologies at the Hanford and Mound sites by considering 10 metrics for the environmental, social, and economic aspects of sustainability.

Alexis Smoot was recognized with the FIU Honors College Annual Research Award for her achievements and has also been featured in various university publications. She has presented her research at regional, national and international conferences including:

- Feb 2016 - Life Science South Florida Undergraduate Research Symposium
- Oct 2016 - FIU McNair Scholars Research Conference
- Mar 2017 - Florida International University Conference of Undergraduate Research
- Mar 2017 - Waste Management Symposia
- Apr 2017 - National Conference of Undergraduate Research

Alexis has also served on the executive board as president of the Society of Women Engineers section at FIU, and actively participated in the American Academy of Environmental Engineers and Scientists (AAEES) and the Eco Engineering Club.

The fall recruitment efforts for new DOE Fellows were initiated on August 28, 2017 and ran through September 29. Recruitment campaigns were conducted by placing recruitment tables at the College of Engineering and at the main FIU campus in the computer science building. A large group of students showed interest in the program and a signup sheet was used to collect student information. The deadline for FIU students to submit applications for DOE Fellowship was September 29, 2017. Thirty-one (31) applications were received and reviewed by ARC researchers and staff. Sixteen (16) FIU students were selected for interviews to be conducted in October.

FIU initiated coordination and preparations for the DOE Fellows Induction Ceremony scheduled for November 8, 2017. FIU staff and DOE Fellows are taking the lead in making all preparations for this event. It is expected that colleagues/collaborators from DOE EM HQ, DOE national labs, other federal agencies, industry, and alumni from the DOE Fellows program, as well as FIU faculty and staff will participate in this event.

In addition, DOE Fellows began preparation of posters based on their DOE EM research as a part of summer internships as well as the research being conducted at FIU ARC throughout the year for the DOE Fellows Poster Competition scheduled for November 7, 2017. A total of 16 posters are anticipated for presentation during this event.

The DOE Fellows who participated in a summer 2017 internships are preparing and presenting an oral presentation at the weekly DOE Fellows meetings. The schedule for these presentations is provided below.

Table 4-2. Research Presentation Schedule for DOE Fellow Meetings

DOE Fellow	Internship Location	Date
Michael Di Bono	University of Texas-Austin	9/29/17
Juan Morales and Mohammed Albassam	DOE-HQ	10/11/17
Sarah Solomon and Ripley Raubenolt	SRNL	10/18/17
Ron Hariprashad	SRNL/SREL	10/25/17
Sebastian Zanlongo	Sandia National Lab	11/1/17
Frances Zengotita	WIPP	11/15/17
Christine Wipfli	DOE HQ	11/22/17

FIU continued working with DOE Fellows interested in federal jobs. FIU supports our Fellows with identifying federal entry-level career opportunities within DOE and other federal agencies on USA Jobs and forward those vacancy announcements to the DOE Fellows. FIU also continues to identify those DOE Fellows who are preparing to transition from academia to the workforce within the next year for conducting focused mentoring sessions with those Fellows on resume preparation and the USA Jobs application process.

During this month, the Fellows continued their research in the DOE EM applied research projects under the cooperative agreement and research topics identified as part of their summer internships at DOE sites, national labs, and/or DOE HQ. Each DOE Fellow is assigned to DOE EM research projects as well as ARC mentors. A list of the current Fellows, their classification, areas of study, ARC mentor, and assigned project task is provided below.

Table 4-3. Project Support by DOE Fellows

Name	Classification	Major	ARC Mentor	Project Support
Alejandro Garcia	Graduate - B.S.	Geoscience	Dr. Yelena Katsenovich	Influence of microbial activity on corresponding electrical geophysical response after ammonia injections in the vadose zone
Alejandro Hernandez	Undergrad - M.S.	Chemistry	Dr. Vasileios Anagnostopoulos	Contaminant Fate & Transport Under Reducing Conditions
Alexander Piedra	Undergrad - B.S.	Mechanical Engr.	Mr. Joseph Sinicrope	Database of Robotic Technologies for D&D
Alexis Smoot	Undergrad - B.S.	Environmental Engr.	Dr. Ravi Gudavalli	Synergistic Effects of Silica & Humic Acid on U(VI) Removal
Andres Cremisini	Undergrad - B.S.	Computer Science	Dr. Himanshu Upadhyay	D&D KM-IT
Anibal Morales	Undergrad - B.S.	Electrical Engr.	Mr. Anthony Abrahao	Development of Inspection Tools for DST Primary Tanks
Awmna Kalsoom Rana	Undergrad - B.S.	Chemistry	Dr. Vasileios Anagnostopoulos	Investigation on the Properties of Acid-Contaminated Sediment and its Effect on Contaminant Mobility
Christine Wipfli	Undergrad - B.S.	Environmental Engr.	Dr. Vasileios Anagnostopoulos	Groundwater Remediation at SRS F/H Area
Clarice Davila	Undergrad - B.S	Mechanical Engr.	Dr. Aparna Aravalli	Investigation Using an Infrared Temperature Sensor to Determine the Inside Wall Temperature of DSTs
Frances Zengotita	Undergrad - B.S.	Chemistry & Health	Dr. Hilary Emerson	Absorption of Neodymium into the Dolomite Mineral
Hansell Gonzalez	Graduate - Ph.D.	Chemistry	Dr. Yelena Katsenovich	Sorption Properties of Humate Injected into the Subsurface System
Jesse Viera	Undergrad - B.S.	Mechanical Engr.	Mr. Joseph Sinicrope	Incombustible Fixatives
Joseph Coverston	Graduate – M.S.	Mechanical Engr.	Dr. Reza Abassi Baharanchi	Computational Fluid Dynamics Modeling of HLW Processes in Waste Tanks
Juan Morales	Graduate – M.S.	Public Health	Ms. Angelique Lawrence	Development of Flow and Contaminant Transport Models for SRS
Maximiliano Edrei	Graduate – M.S.	Mechanical Engr.	Dr. Dwayne McDaniel	Computational Fluid Dynamics Modeling of a Non-Newtonian Fluid Undergoing Sparging for

Name	Classification	Major	ARC Mentor	Project Support
				Estimating PJM Mixing Times
Michael DiBono	Undergrad - B.S.	Mechanical Engr.	Mr. Anthony Abrahao	Development of Inspection Tools for DST Primary Tanks
Mohammed Albassam	Graduate – M.S.	Environmental Engr.	Dr. Noosha Mahmoudi	Environmental Remediation and Surface Water Modeling of Tims Branch Watershed at SRS
Ripley Raubenolt	Undergrad - B.S.	Environmental Engr.	Dr. Ravi Gudavalli	Modeling of the Migration and Distribution of Natural Organic Matter Injected into Subsurface Systems
Ron Hariprashad	Undergrad - B.S.	Environmental Engr.	Dr. Noosha Mahmoudi	Surface Water Modeling of Tims Branch
Sarah Solomon	Undergrad - B.S.	Environmental Engr.	Dr. Yelena Katsenovich	Investigation on Microbial-Meta-Autunite Interactions - Effect of Bicarbonate and Calcium Ions
Sebastian Zanlongo	Graduate - Ph.D.	Computer Science	Dr. Dwayne McDaniel	Cooperative Controls for Robotic Systems
Silvina Di Pietro	Graduate - Ph.D.	Chemistry	Dr. Hilary Emerson	Evaluation of Ammonia for Uranium Treatment

Milestones and Deliverables

The milestones and deliverables for Project 4 for FIU Performance Year 7 are shown in the following table. No milestones or deliverables were due during this reporting period.

FIU Performance Year 7 Milestones and Deliverables for Project 4

Milestone/ Deliverable	Description	Due Date	Status	OSTI
2016-P4-M1	Draft Summer Internships Reports	10/14/16	Complete	
Deliverable	Deliver Summer 2016 interns reports to DOE	10/31/16	Complete	OSTI
Deliverable	List of identified/recruited DOE Fellow (Class of 2016)	10/31/16	Complete	
2016-P4-M2	Selection of new DOE Fellows – Fall 2016	10/31/16	Complete	
2016-P4-M3	Conduct Induction Ceremony – Class of 2016	11/04/16	Complete	
2016-P4-M4	Submit student poster abstracts to WM17 Symposium	1/16/17	Complete	
Deliverable	Update Technical Fact Sheet	30 days after end of project	On Target	

Work Plan for Next Quarter

- Complete the Year End Report (YER) for FIU Performance Year 7.
- Continue research by DOE Fellows in the DOE-EM applied research projects under the cooperative agreement and research topics identified as part of their summer internships.

- Finalize and submit DOE Fellow internship reports for summer 2017 at DOE sites, national laboratories, DOE-HQ, and DOE contractors.
- Complete selection of new DOE Fellows for the fall recruitment period and submit list of selected DOE Fellows to DOE.
- Complete preparation and coordination for the DOE Fellows Poster Exhibition & Competition and host event on November 2, 2017.
- Complete preparation and coordination for the DOE Fellows Induction Ceremony for the Class of 2017 and host event on November 3, 2017.